THEORETICAL INVESTIGATION OF AUSTRALIAN DESIGNED REINFORCED CONCRETE FRAMES SUBJECTED TO EARTHQUAKE LOADING

By Anthony K.M. Wong

March 1999

Department of Civil and Environmental Engineering
The University of Adelaide

CONTENTS

ABSTRACT

Research into the behaviour of structures under seismic/earthquake loading was accelerated following the 1989 Newcastle earthquake and the 1990 Kobe earthquake. Two main points are to be learned from these two events: (1) an area of moderate reactivity can be caught unprepared by an unexpected earthquake and (2) there is a need not only to improved the behaviour of newly designed structures but also to understand how an existing typically "Australian designed" structure will behave under earthquake loading.

The new Australian Loading code AS1170.4 - Minimum Designed Loads on Structures Part 4 - introduced new design methods to bring Australia in line with the design methods used around the world. In areas of low seismicity, structures tend to be governed by gravity and/or wind loads and this type of structures would exhibit little ductility thus will perform poorly under earthquake loading. The research presented is concentrated on the behaviour of reinforced concrete frame structures designed in accordance with AS3600 - concrete structures code. There are three types of moment resisting frames (1) normal moment resisting frame, (2) intermediate moment resisting frame and (3) special moment resisting frame. The normal moment resisting frame was chosen to be investigated because it represented the majority of the existing structures of this type. Furthermore, no special provision in terms of detailing of the reinforcement was made to make allowance for seismic loading with normal moment resisting frame.

A non-linear computer model of a reinforced beam-column joint was produced using the computer analysis program called "Ruaumoko" which allowed the modelling of joint stiffness and strength degradation. A hysteresis rule was chosen by comparing analytical results using the model to the experimental results of 1/2 scale quasi-static joint tests carried out at the University of Melbourne. After calibrating the initial stiffness and the yield level to the Melbourne tests results, the model was used to predict the behaviour of a full scale equivalent of the 1/5 scale reinforced concrete frame dynamically tested at the University of

Adelaide. The results obtained were compared to the experimental results from Adelaide and comments were made with regards to the performance of the computer model.

A computer model of a multi-storey multi-bay prototype structure was created by using the same calibrated beam-column joint model developed earlier and the mode of failure for this prototype structure was identified. A discussion on the Response Modification Factor (R_f) given in AS1170.4 for a normal moment resisting was made and comments were given as to whether the value given in AS1170.4 was conservative. In conclusion, suggestions to areas in need of further research were recommended.

This work contains no material which has been accepted for the award of any other degree or diploma in any university or other tertiary institution and, to the best of my knowledge and belief, contains no material previously published or written by another person, except where references have been made in text.

I give consent to this copy of my thesis, when deposited in the University Library, being available for loan or photocopying.

Date: 16/3/99

ACKNOWLEDGMENT

The author would like to thank Dr. Michael Griffith, Senior Lecturer and Head of the Department of Civil and Environmental Engineering for his guidance and patience in supervising this research; Rouska, my wife for her constant support, help and advice; Greg Klopp for his expertise in many areas; Stephen Carr for his assistance in difficulties with computer equipment and Derek Heneker and Joe Corvetti for the use of their experimental data for this research.

CHAPTER 1
INTRODUCTION

Australia has long been regarded as an area of low seismicity when compared to the rest of the world. The events of the 1989 Newcastle earthquake and the 1990 Kobe earthquake have shown that even a moderate earthquake can cause devastating destruction to an unprepared city or region. In Australia, following the 1989 Newcastle earthquake, numerous research (discussed in detail in Chapter 2) were initiated all over the country to accelerate the understanding of the behaviour of different types of structures such as masonry, steel frames and reinforced concrete frames under seismic loading. The main objective was to understand how 'typical' Australian designed and detailed structures would react to seismic loading.

A new Australian Standard AS1170.4 [1] - Minimum Design Loads on Structures Part 4 - Earthquake Loads, was introduced in 1993 to bring Australia in line with the latest design philosophy used by other countries in areas with more severe and frequent seismic activities such as Japan, New Zealand and the United States. In areas of low seismic activity, the design of structures is usually governed by gravity and wind loads rather

than earthquake loads. There are many structures in these regions which were only designed for strength and not ductility. These structures would be expected to perform poorly under seismic type loading. There exists a need to investigate how existing Australian designed reinforced concrete frame structures will behave under seismic loading economically and efficiently.

The research presented here examined how reinforced concrete frame structures designed as moment resisting frame structure in accordance with AS3600 - concrete structure code [2] would behave under earthquake loading. Three types of reinforced concrete moment resisting frames are reference to in AS3600: (a) normal moment resisting frames, (b) intermediate moment resisting frames and (c) special moment resisting frames. The normal moment resisting frame was chosen to be investigated because it represented the majority of this type of structures built prior to the increased awareness towards earthquake design in Australia. Furthermore, ordinary moment resisting frames have no special detailing to allow for seismic loading and their designs are usually governed by static or wind load. In this research a computer model was developed using experimental results from the dynamic testing of a 1/5 scale reinforced concrete frame at the University of Adelaide and the quasi-static tests results of 1/2 scale reinforced concrete joints at the University of Melbourne for calibration and incorporating joint stiffness and strength degradation behaviour. This model was then used to predict the ductility, strength and mode of failure of a proposed prototype building.

This work is sectionalised into the following chapters:

- Chapter 2 - consists of a review of research done around the world on seismic behaviour of reinforced concrete beam-column joints and frames both experimentally and theoretically.
- Chapter 3 - describes the development of the computer model, how a hysteresis rule is chosen to model stiffness and strength degradation of the joints and the calibration to the results from experimental testing done at University of Melbourne.
- Chapter 4 - contains the analytical results from using the calibrated computer model to predict the behaviour of the full scale version of the 1/5-scale reinforced concrete

frame tested at the University of Adelaide. These results are then compared to the experimental test data. As an additional comparison, a second computer model was produced using the same hysteresis rule but using the cross sectional properties based directly on design values used to produce the scaled model at Adelaide.

- Chapter 5 - investigates the behaviour of a multi-bay multi-storey prototype building under earthquake loading and the mode of failure will be identified.

In summary, this work aims to give some insight into the suitability of values for the structural response factor (R_f) given in AS1170.4 [1] for ordinary moment resisting frames of reinforced concrete, to comment on whether other design values specified in the code are conservative and to suggest areas which may require further research work.

CHAPTER 2
LITERATURE REVIEW

This chapter consist of two main sections. The first section gives an overview of research associated with reinforced concrete beam-column joint behaviour through experimental studies and the second section reviews the progression of analytical research in reinforced concrete joint hysteresis models under seismic/cyclic loading.

2.1 OVERVIEW ON EXPERIMENTAL RESEARCH

For many years there has been extensive research into the seismic behaviour of structures especially in seismically active areas such as some part of the United States of America, Japan and New Zealand. The use of reinforced concrete frame buildings was found to be a common form of construction and researchers have identified the importance of well designed and detailed frames with respect to their seismic behaviour. Numerous experimental research projects [3-35] into the seismic behaviour of reinforced concrete joints with various joint details and different concrete characteristics have been done all

over the world with pioneer researchers such as Park and Paulay, Popov and Bertero, Hanson and Ehsani and Wight.

In Australia, comparatively little research into the seismic behaviour of Australian designed reinforced concrete structures has been carried out. Most of the low to medium rise reinforced concrete frame buildings designed in Australia were governed by the static load combinations with little allowances for the earthquake loading. Although Australia is considered to be an area of moderate to low seismicity, research into this area has dramatically increased since the 1989 Newcastle earthquake which registered 5.6 on the Richter Scale [36, 37]. More recently, the Hyogo-Ken Nanbu (Kobe) earthquake reinforced the need for research into better seismically behaved structures even in what has been traditionally recognised as an area of low seismic activity. Consequently a series of research into the behaviour of reinforced concrete frame and masonry structures was initiated after the 1989 Newcastle earthquake at the University of Adelaide as well as other universities around Australia.

2.1.1 Beam-Column Joint Behaviour

Most structures are designed to resist seismic loading by being able to behave in a ductile manner and dissipate energy. To achieve this, joints must not fail prematurely. Consequently, much research has concentrated on the behaviour of reinforced concrete beam-column joint regions under seismic/cyclic loading. Alford and Housner [38] used a soon to be demolished 4-story building to study the damping of structures when dynamically loaded. The natural period of the structure was measured as well as the damping. It was concluded that since the resonant amplitude increased less rapidly than the exciting force, damping increased with amplitude. It was also observed that damping did not increase with frequency.

In 1967, Hanson and Connor [22] found that a joint with no hoops needed some joint confinement in order to develop the initial ultimate capacity of the structural members framing into an isolated joint. Megget and Park [17] came to a similar conclusion, that for seismic loading more hoop reinforcement was required. The primary cause of failure

was cracking within the joint region. By adding additional reinforcement it helped confine the concrete in the joint region and prevented the breakdown of anchorage of the longitudinal reinforcement in the joint.

Townsend and Hanson [39] performed a series of experimental tests on beam-column connections. It was found that there are three important parameters describing nonlinear behaviour: (1) column axial load, (2) displacement level and (3) number of cycles of inelastic load. Townsend and Hanson [39] used the results from the experimental tests to derive hysteresis loop equations and presented it as four parabolas (refer to Figure 2.1) where γ is the displacement level and M_y is the computed moment which tensions the top steel to the design yield stress. The steel strains resulting from the effect of column tension tend to open cracks in the connection reducing stiffness and energy absorption capacity of the connection. Lower column axial compression forces were found to produce smaller hysteresis loops for beam hinges near beam-column interface. The experimental results also indicated that increase in the level of yielding causes rapid decrease in the stiffness of the connection of zero displacement.

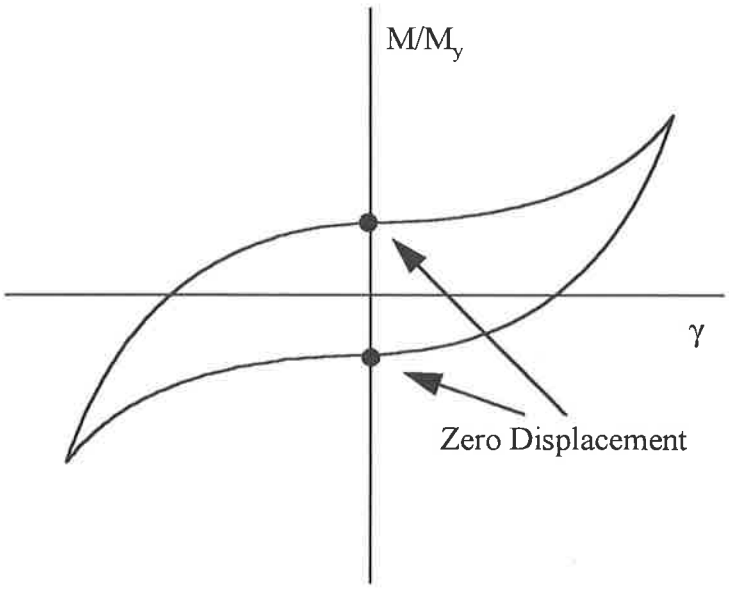

Figure 2.1 - Parabolas in Hysteresis loop
(after Townsend and Hanson, 1973)

Park and Paulay [24] found that most failures of beam-column subassemblages were concentrated at the joint rather than in adjoining members. Improvement of the joint's seismic performance was found by having lateral beams coming into the joint [24, 40] with the possibility of adding beam stubs for exterior joints. Various researchers [3, 11, 18, 20] added to the knowledge of beam-concrete joint behaviour during 1970's. It was found that in a conventional joint, there was insufficient anchorage available for the strut action so excessive stiffness degradation in the joint could occur. This led to new research into different ways of improving the anchorage of longitudinal beam reinforcement. Park, Paulay and Priestley [10] showed that the strength of a joint should not be less than the maximum strength of the weakest members it connects and the maximum capacity of a column should not be weakened by the possibility of strength degradation of the joint.

In 1979, Park and Keong [14] performed a number of tests on beam-column joints with intermediate column bars as vertical shear reinforcement as prescribed in the then new draft SANZ concrete design code. It was found that the strength and stiffness degradation of the joint was worsened by the spalling of the concrete cover at large compressive stresses thereby reducing the section to that within the stirrups. Vertical shear reinforcement was found necessary for truss action and it was needed in the joint core to act with horizontal hoops to form an effective shear resisting mechanism.

When the flexural strength of the beams was reached, the beam-column joint core was bounded by flexural cracks at beam and column faces. The internal beam and column forces caused by flexure and shear acting on the faces of the joint core when the flexural strength of the beams was reached can be calculated accurately. Thus, the horizontal shear forces carried by the joint can be obtained from these forces. As shown in Figure 2.2,

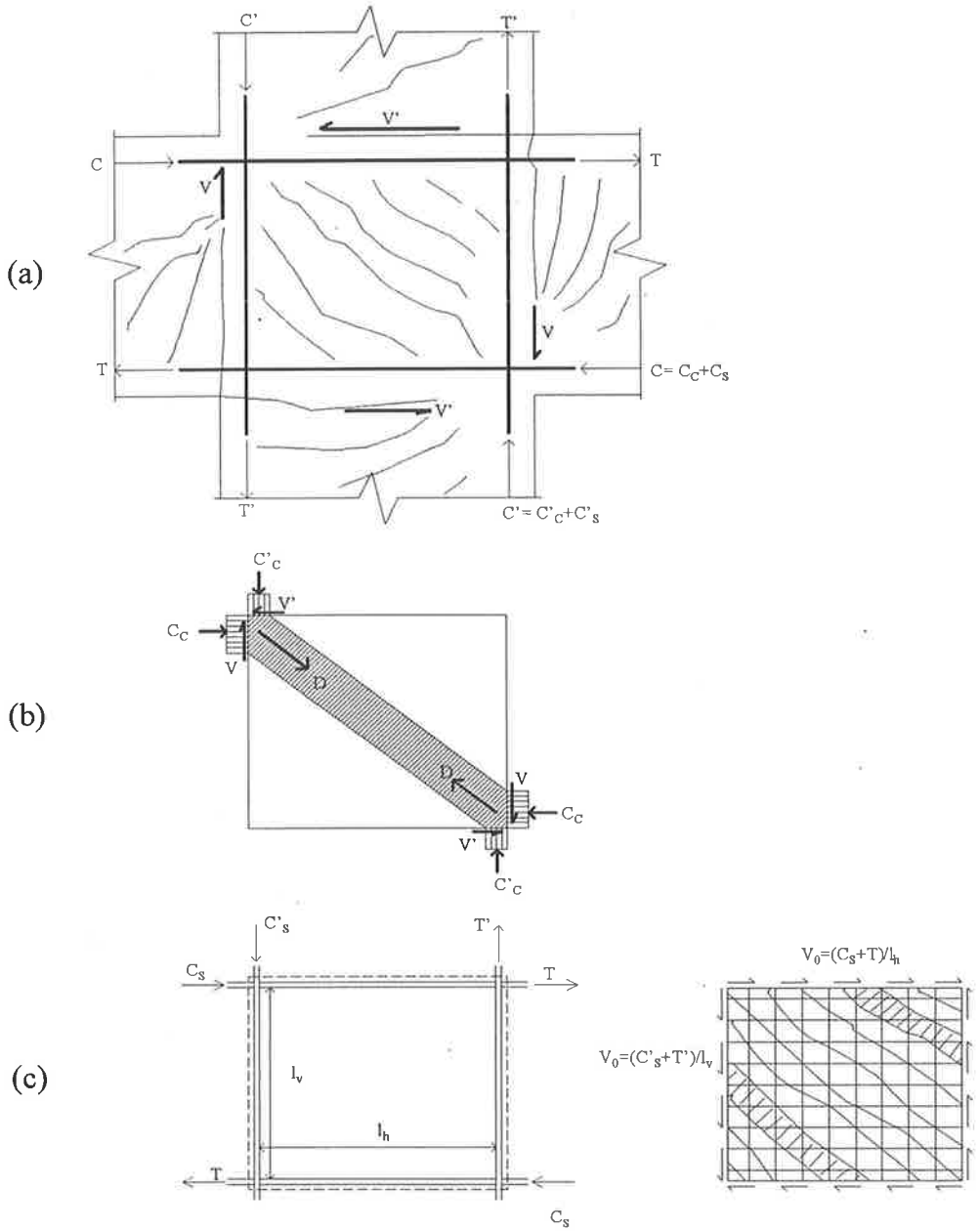

Figure 2.2 - Mechanisms of Shear Transfer of Reinforced Concrete Beam-Column Joint Core: (a) Forces acting on a beam-column joint core; (b) Shear transfer by diagonal compression strut: and (c) Shear transfer by truss action of shear reinforcement (after Park and Keong [14])

the maximum horizontal shear force occurs in the middle region of the beam depth between the neutral axis positions of the beam sections to the left and right of the joint. Similarly, the maximum shear force in the vertical direction can be obtained by

considering the vertical column internal forces and the beam shear acting to one side of a vertical plane in the middle of the joint.

Park et. al [12] tested joints which had intermediate column reinforcement running straight through the joint acting as vertical shear reinforcement but with only 78% of the horizontal shear reinforcement that was required by the same code. This beam-column joint was designed so that the plastic hinges occurred in the beams adjacent to the column faces during seismic loading. It was found that ductile yielding of the plastic hinges in the beams could not dominate the response of the unit because of the stiffness/strength degradation due to the damage concentrated in the joint core.

Paulay and Scarpas [16] found that for an exterior joint, the large flexural cracks previously formed at the column face would not close completely upon load reversal so that a strut force could not be sustained. It was also reported that for an exterior joint, only 50% of the recommended horizontal shear reinforcement was needed for the joint to perform satisfactorily.

A major cause of the loss of stiffness for the beam-column subassemblages was the slippage of the column longitudinal bars and pullout of beam longitudinal reinforcement from the joint [5, 6]. Ehsani & Wight (1984) [5] found that the column bars slipped more than the beam reinforcement bars. Zerbe and Durrani (1988) [7] performed a series of test on multiple reinforced concrete beam-column subassemblages. Strength was not found to be affected by continuity up to a drift level of 1.5%. However, beyond this limit, multiple connection subassemblages were able to resist a higher load partially attributed to an increase in the flexural capacity of the beams due to the presence of axial compressive force. The effects of stiffness degradation were found to be less severe in the multiple connection than in the individual exterior/interior connections. Energy dissipation was not affected by continuity.

The effects of bi-directional loading of reinforced concrete beam-column joints were investigated by Lean and Jirsa [41]. Full-scale versions of a joint assembly were tested. The results showed that the shear stress that can be sustained by an interior joint is very

large and that the effects of biaxial loading and the presence of floor slabs is important in the analysis and design of ductile moment resisting space frames.

In 1990, Pesski et al. [13] tested beam-column joints which were classified to be from lightly-reinforced concrete frames. The type of joint considered had similar detailing to many low to medium rise reinforced concrete frame buildings in Australia (Figure 2.3). It was concluded that the column splices were performed adequately with damage of the column splice concentrated near the beam-column joint. The use of minimum joint reinforcement increased the amount of damage to the column. Bottom beam reinforcement pullout was found to initiate joint failures in joints with non-continuous bottom beam reinforcement.

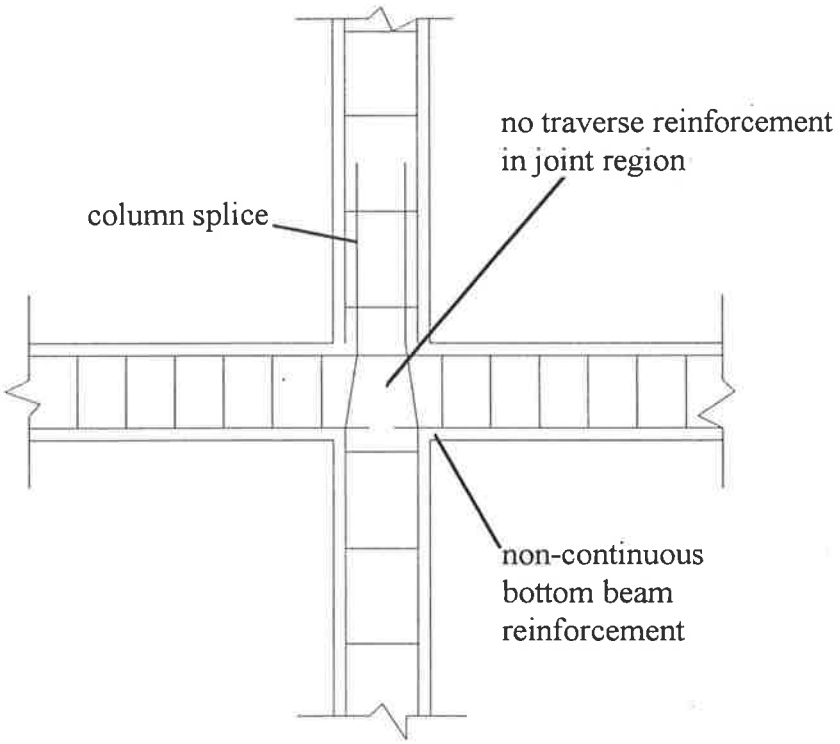

Figure 2.3 - Lightly-Reinforced Beam-Column Connection

Beres et. al [42] tested 34 beam-column connections which were designed for gravity loading only without any special detailing to allow for horizontal loading such as the type of connections being investigated in this research. As expected, there was a rapid strength/stiffness degradation shown by the columns. The interior joint specimens

reached higher total peak column shear strength capacity than the exterior joint specimen. The shear capacity available for the lateral loading of the interior joint was markedly higher than that of exterior connections.

In 1995, Minovwa et. al [43] tested two three story full scale reinforced concrete structures. Two seismic records were used including the 1995 Hyogo-ken Nanbu earthquake. The structures were designed to the strong column-weak beam concept and showed the desired results. The damping was observed to increase with the progress of damage.

Many different research followed on from these [8, 9, 15, 19, 25, 27, 28, 30, 31, 33, 44 - 48] with variations such as light-weight or high strength concrete, multiple connection subassemblages, effects of variations in axial loading, inclined beam bars, prestressed concrete etc.

More recently in Australia, Huang began one of the first beam-column joint testing programs which was followed by Corvetti et al. [23] who tested a series of beam-column reinforced concrete joints designed in accordance with AS3600 (Concrete Structures Code) [2] and AS1170.4 (Earthquake Loading Code) [1]. Joints from three classes of frame were tested (normal, intermediate and special moment resisting frame - AS1170.4 [1]). The normal moment resisting frames had reinforcing details as shown in Figure 2.3 and was designed mainly for strength rather than ductility. Detailing was found to be a key aspect in achieving the required performance for a reinforced concrete beam-column joint. Bottom beam reinforcement that was not cogged up in any way was found to have insufficient bar development length resulting in simple bar pullout without allowing the bars to reach their yielding point. Joints which had better joint confinement (intermediate frames) had improved anchorage allowing the bars to go beyond yield under load reversal.

During the same year, Huang [26] tested Australian designed beam-column joints with extra mechanisms to help improve the beam reinforcement anchorage. The results showed that the majority of damage was confined to the joint region. The bond between

the beam bars and concrete was destroyed due to the crushing of the concrete in the joint region and was found to be a major cause of failure. This slippage of beam bars was also recognised as a major cause of loss of stiffness. Improved joint performance was observed with mechanical anchor plates relative to a normal joint and this highlighted problems with joints designed according to AS3600 [2] in resisting cyclic loading.

2.2 OVERVIEW OF THEORETICAL MODELS

The fact that building structures subjected to strong ground motion will sustain inelastic deformations at certain critical locations is well recognised. The search for an appropriate hysteresis model began with a simple elasto-plastic system and was followed by numerous inelastic analyses of structures where inelastic behaviour was represented by a bilinear hysteresis material relationship. However, many researchers have shown that reinforced concrete members have a more complex post-yield behaviour. Thus to better model the inelastic dynamic response of reinforced concrete structures, it was necessary to use improved models of the hysteresis relations that more closely represented the measured hysteretic behaviour of reinforced concrete members. Consequently more complicated joint hysteresis models have emerged such as the tri-linear model [49] , Takeda model [50] , Q-hyst model [51] and numerous stiffness/strength degradation models.

2.2.1 Stiffness/Strength Degradation and Hysteresis Models

Cyclic tests on small-scale and full-scale reinforced concrete beam-column connections have shown that members loaded beyond their ultimate capacity suffer a deterioration in stiffness and reduction in energy absorption capacity of structural elements at connections. The Portland Cement Association, Chicago, Illinois performed some early tests in 1961 which demonstrated that deterioration in stiffness was particularly true of members subjected to high shear together with bending [52].

In 1966, Clough and Johnston [49] investigated the effect of stiffness degradation on ductility using a single-degree of freedom system (Figure 2.4). A degrading trilinear hysteretic model was developed. It was concluded that degrading stiffness systems have significantly different earthquake response characteristics from ordinary elasto-plastic systems. The dominant effect of the loss of stiffness is an increase in the period of the structure and for long period structures, this tends to eliminate resonance with the earthquake input while for short period structures, the loss of stiffness leads to an increase in amplitude and displacement.

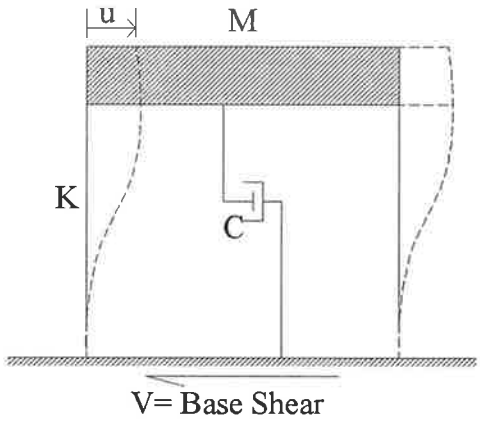

Figure 2.4 - Single Degree of Freedom System

Takeda et al. [50] proposed a hysteresis model and confirmed its applicability by performing dynamic tests on test specimens. The specimens were simple, externally determinate structural units. In the Takeda model, special attention was given to the behaviour of joints during small amplitude deformations. Takeda came up with a series of rules which were used for construction of the load-deflection curve corresponding to load reversals. It was found that a realistic conceptual model for predicting the dynamic response of a reinforced concrete system should be based on a static force-displacement relationship which reflects the changes in stiffness for loading and unloading as a function of the past loading history.

A degrading bilinear system was used by Imbeault and Nielsen [53] and this was compared to a normal bilinear system. The degradation of stiffness only occurred

following inelastic deformations. This model utilised a deteriorating elastic stiffness that represented the average value of unloading and reversed loading stiffness. From beam-column joint experimental results, the load-deflection behaviour of reinforced concrete was found to be characterised by a yield limiting force level and a continually varying stiffness. For a multi-degree of freedom degrading bilinear system subjected to strong long duration earthquakes, a significant increase in the magnitude of ductility requirements was found when compared to that for the bilinear system.

Anderson and Townsend [54] compared different hysteresis models using a 10-storey single bay frame designed in reinforced concrete for loads specified in the Uniform Building Code [55], for a structure located in Seismic Zone 3. It concluded that a degrading trilinear stiffness model was more promising compared to bilinear and degrading bi-linear hysteresis models. The degrading stiffness models resulted in an increase in the relative story to story displacements.

The "Q-hyst" model was developed by Saiidi and Sozen [56] in 1979. A bilinear curve with ascending post-yield branch (Figure 2.5) was used as the primary curve for this model. Stiffness degradation is accounted for at unloading and load reversal. The unloading stiffness at the inelastic segment of the primary curve is defined by K_q in the following equation:

$$K_q = K\left(\frac{D_y}{D}\right)^{0.5} \tag{2.1}$$

in which K is the slope of the elastic portion of the primary curve; D is the absolute value of the maximum deformation experienced; and D_y is the yield deformation.

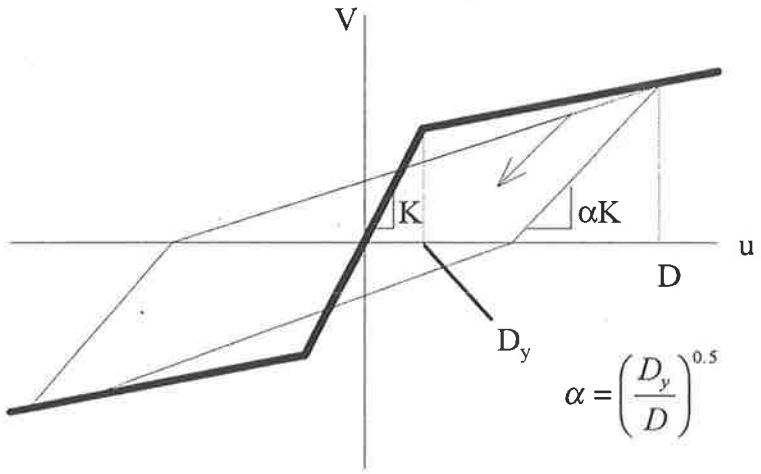

Figure 2.5 - Q-Hyst Hysteresis Model

The Q-Hyst model takes into account hysteretic energy dissipation during low-amplitude deformations if the section has yielded in at least one direction.

Saiidi [51] also compared a number of hysteresis models including the Takeda, Clough and Q-Hysts models as well as the bilinear model to try and find an accurate model. It was found that the elasto-plastic and bilinear models resulted in responses exhibiting poor correlation with the response based on the Takeda model. The Clough degrading model resulted in responses which were closer to that from the Takeda model and the Q-Hyst model showed excellent correlation to the Takeda model.

Shimazu and Hirai [57] from Japan investigated the strength degradation of reinforced concrete columns subjected to cyclic load and found that the strength degradation was greater for anti-symmetrical lateral loading (ie. earthquake loading) than for one central lateral loading with a set magnitude.

Axial force moment interaction was considered by Keshavarzian and Schnobrich [58] in calculating the element stiffness. This two-dimensional line element model was based on a simplified Takeda model and was used for static and dynamic analysis of wall-frame and/or coupled shear wall structures. In this model, the element cord zone (Figure 2.6) comprised of two types of regions, an elastic plus two inelastic zones at each end of the

member with variable length. Inelastic actions were confined to these element ends. The cross sectional stiffness properties of the elastic zone, which were not constant, were calculated based on the change of axial force.

For the inelastic zones, the effective section stiffness properties were obtained from a moment-curvature hysteresis idealisation. For each inelastic zone, the effective stiffness was assumed to be constant throughout the length of that zone with the inelastic length dependant on the loading history and the axial force. While the inelastic zone lengths may be different at the two ends and do not remain constant throughout the response, the inelastic zone changes length only when the end moment is in the strain-hardening phase. Due to the significant contribution to end rotation resulting from bond slippage in the joint, a rotational spring was provided at each member's ends to model the additional flexibility for an element.

It was concluded that this model was very effective in predicting the nonlinear behaviour of reinforced concrete frame members and that is the reason this model will be compared to a few other hysteresis models in the next chapter to find out its performance in modelling Australian designed and detailed reinforced concrete beam-column joints. Analyses which ignored the effect of axial force on flexural strength and stiffness underestimated maximum shear and moment at the base of the shear walls.

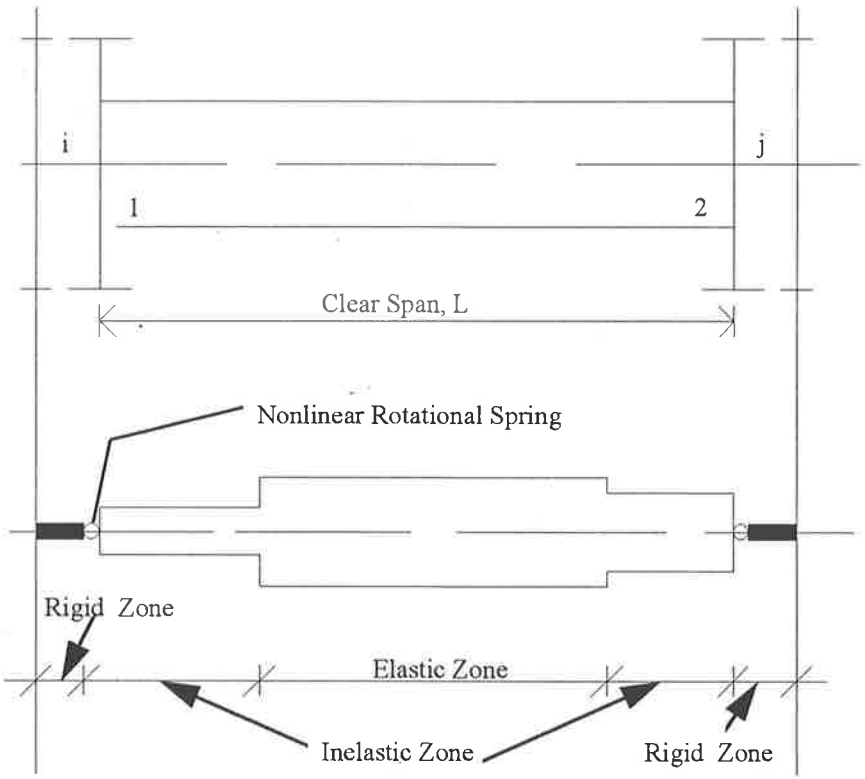

Figure 2.6 - Model Characteristics for Keshavarzian

Sotoudeh and Boissonnade [59] developed a model where stiffness degradation was assumed to be associated with the crack closing phenomenon. The results indicated that the highest level of stiffness degradation in Rayleigh type cases was on average 20% higher than that of the cases with Weibull type inputs [60].

Wang and Subia [61] produced an analytical model based on a damage parameter instead of models by Takeda, Saiidi and Sozen & Nielsen where stiffness degradation was assumed to be a function of the maximum displacement experienced by the structure. Through this research, it was observed that analysis should include a non-linear hysteresis model with stiffness/strength degradation and the effect of stiffness/strength degradation. The Clough and Q-Hyst models were found to perform satisfactorily when damage was not severe.

Sanjayan and Darvall [62] investigated the dynamic response of softening structures. Softening effects were found to be as important as plasticity and hysteresis effects when

computing the full response of concrete frame structures subjected to severe dynamic loads. A method of dynamic analysis which included flexural softening in the analysis of multiple degree-of-freedom unbraced plane frame structures was presented by the same authors [63] in 1987. The element model which then used had finite length hinges which followed a degrading stiffness and softening hysteresis model. A flexural element model of length L was assumed to have discontinuity of hinge lengths at each end as shown in Figure 2.7. The hinges (AB and CD) were the only portions to undergo softening deformations. Points A and D were the only points which could be plastic hinges. The central portion BC had only reversible elastic deformations. In adopting this model, it was assumed that the bending moment maxima occurred at the ends of the elements. The hysteresis model included a modification to account for softening of the model as suggested by Clough. It was concluded that computation of the full response of concrete frame structures to severe dynamic loads requires consideration of softening in addition to plasticity and hysteresis.

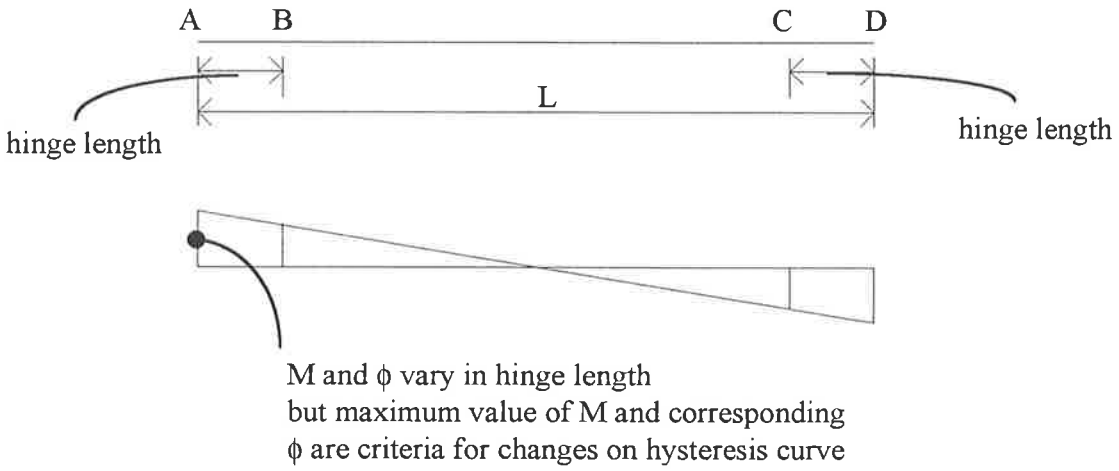

Figure 2.7 - Element Model with plastic-softening hinges

The seismic ductility demands for multistorey rigid frames were studied by Diaz et. al [64] by comparing the response of a seven-story and a fourteen-story building. Two types of models were used, namely a shear-beam model and a rigid frame model. Larger ductility demands were calculated by the shear-beam model from the rigid frame model at the first story. For the upper stories, the case was reversed. P-delta effects provoked

large ductility demands at the first story with the shear-beam model which could lead to collapse due to instability. It was concluded that overstrength for shear at some stories may lead to concentrations of ductility demands at other levels. It seemed to be more pronounced with the shear systems than for rigid frames system.

The effects of the slab on stiffness and strength were studied by Mossalam et. al [65] by creating a three dimensional model of a lightly reinforced concrete joint which was designed mainly for gravity loads. It was found that the presence of the slab reduced the ability of the joint to dissipate energy. In the absence of the slab, the ratio of the energy dissipation through the joint panel shear distortion and the total energy dissipation increased with increased cycling and stabilised at a value of 63%.

In 1995, Priestley [66] proposed a displacement-based seismic assessment method while Park [67] put forward a forced-based procedure. Upon comparison of the two methods over a variety of elastic periods and different inelastic mechanisms, the force-based method was unable to differentiate between the displacement demands for different cases while the displacement method gave a range of required displacements. This will be discussed further in later sections.

Vukazich et. al [68] investigated into using Lanczos vectors in modal analysis. It was found that the proposed Lanczos modal analysis procedure was able to capture the character of the non-linear response but not the full effect of accumulated plastic strain. The advantage of this method was the reduction in time to approximately one quarter to one sixth of that required normally and could be used as a preliminary design tool for finding undesirable mechanisms such as column yielding and excessive interstorey drift. The new method compared favourably to full nonlinear dynamic finite element analyses but more investigation work must be done before this technique will provide usefulness to the structural designer.

Spacone et. al [69, 70] developed a reliable and computational efficient beam-column finite element model for the analysis of reinforced concrete members under cyclic loading. The non-linear behaviour of the element is monitored at several control sections

that are discretized into longitudinal steel and concrete fibres. It was concluded that there were several advantages with the proposed model over the traditional stiffness based beam-column based elements: (1) it required fewer elements for the representation of the non-linear behaviour of a structure, (2) no numerical difficulties arise in connection with the possible strength loss and softening of individual sections, (3) the element could readily incorporate distributed element load. The proposed non-linear solution strategy also presented a significant in computational time saving.

2.3 CONCLUSION

There has been much research in the field of earthquake behaviour of reinforced concrete structures. Some experimental work has been done here in Australia in addition to the extensive amount done abroad especially in the United States and New Zealand with seismic behaviour of beam-column joint and how to increase the performance of these joints. These experimental results have provided information and data for the development of theoretical models. Researchers such as Takeda, Sozen and Nielsen; Park and Paulay, just to name a few have developed joint hysteresis models which mathematically describe the behaviour of reinforced concrete joints during an earthquake.

Research here in Australia has been accelerated after the 1989 Newcastle earthquake and to a lesser extent the 1995 Hyogo-Ken Nambu earthquake in Japan. These two earthquakes showed the need for research in regions considered to be of low to medium seismicity such as Australia. The majority of reinforced concrete frame buildings in Australia are governed by strength and have no allowances for ductility required to withstand earthquake type forces.

In this thesis, a computer model is produced, calibrated against both large scale reinforced concrete joint tests performed at the University of Melbourne by Corvetti [71] and small scale frame modelling at the University of Adelaide by Heneker [72] to try and predict the behaviour of reinforced concrete frame buildings which have no particular special detailing to account for seismic loading. The importance of stiffness and strength

degradation (softening of the joint) has been highlighted by many researchers such as Mendis [73] 1986 and has been taken into account here in this computer model. The results from this research will give design engineers some insight into the behaviour of reinforced concrete frame buildings under seismic loading and highlight weak areas of structures.

CHAPTER 3
COMPUTER MODELLING OF BEAM-COLUMN JOINTS

3.1 INTRODUCTION

The formulation of a non-linear computer model of a reinforced concrete beam-column joint will be discussed in this chapter. The type of reinforced concrete beam-column joint modelled was representative of a joint from an ordinary moment resisting frame as specified in the Appendix B of AS1170.4 [1], the Minimum Design Loads on Structures, Part 4: Earthquake Loads. This type of frame was detailed in accordance with AS3600 [2], excluding the provisions provided in the Appendix A of that same standard.

Various hysteretic models were examined. The model was required to be able to represent inelastic beam behaviour together with stiffness/strength degradation characteristics. The computer joint model was calibrated to the results obtained from quasi-static tests performed at the University of Melbourne on a 1/2 scale reinforced concrete beam-column joint designed as part of an ordinary moment resisting frame.

3.2 RUAUMOKO

The computer program Ruaumoko [74] used to carry out the analysis was designed to produce a step-by-step time history analysis of non-linear general two dimensional framed structures subject to ground acceleration or time varying force excitation. The program was developed by Dr. Athol Carr of the Department of Civil Engineering, University of Canterbury, New Zealand.

Within Ruaumoko, several options were available for the modelling of the mass, damping and stiffness matrices. This was discussed in the following sections.

3.2.1 Mass Matrix

The mass of the structure can be input in the form of weights and from this the program converts them into mass units. There are two ways to specify the mass of the structure: (1) nodal weights or (2) member weight per unit length.

For this research, all the weights for both the columns and beams were entered into the computer model as member weight per unit length. The mass of the slab were taken into account but distributing the slab load on to the beam as additional uniformly distributed load.

3.2.2 Damping Matrix

Ruaumoko has a variety of options for defining the damping matrix [74]. The damping model used for this research was the linear variation of damping with elastic natural frequencies to ensure that higher modes were not overdamped (Figure 3.1).

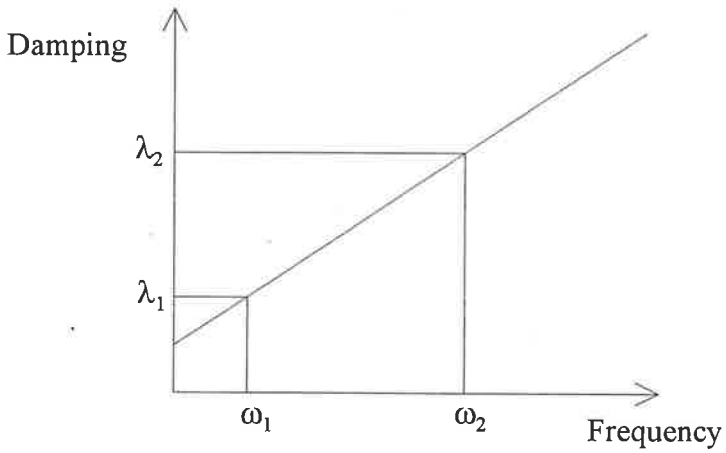

Figure 3.1 - Linear Damping

3.2.3 Stiffness Matrix

There are a number of member models that can be used to represent the stiffness of the structure in Ruaumoko. They are categorised into six types: Frame members, Spring members, Structural-Wall members, Dashpot members, Tendon members and Contact members. Frame members were used in this research as this type of member covered both beam and beam-column members.

3.2.4 Hysteresis Rules for Stiffness Degradation

Ruaumoko has many different hysteresis rules available. The most suitable models for this research were (discussed in Section 2.2 of the literature review) the Q-Hyst degrading stiffness hysteresis model, the Muto degrading tri-linear hysteresis model and the Mehran Keshavarzian degrading and pinching hysteresis model. In this research, all the hysteresis rules mentioned above were used in the model to see which rule can best simulate results obtained from experimental testing at the University of Melbourne by Corvetti [71].

Most of the degrading rules were developed to represent the behaviour of reinforced concrete members. To cater for strength degradation, the yield levels in the interaction diagrams were reduced as a function of the ductility (used in the frame modelling) or of the number of load reversals (used in the joint modelling).

3.2.5 Loading

Ruaumoko allows for both static and dynamic loading. For the joint modelling, a sinusoidal time varying force excitation was used to simulate the quasi-static cyclic loading used in the experiment at the University of Melbourne [71]. The sine wave was defined by 100 points (Figure 3.2) with a frequency of 0.1Hz.

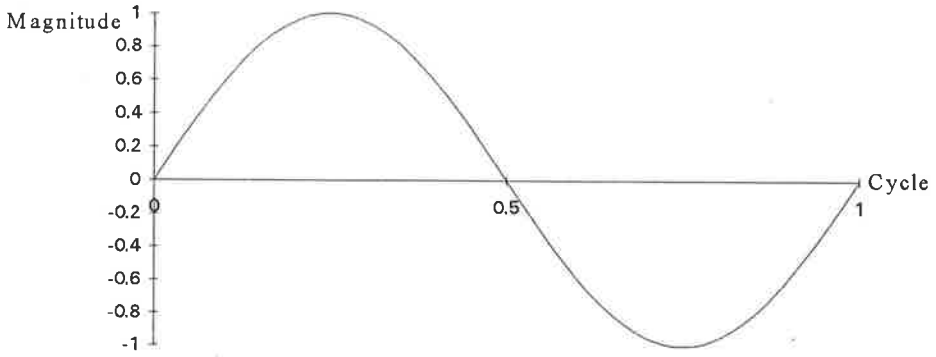

Figure 3.2 - Sinusoidal Loading

3.2.6 Time-History Integration

The unconditionally stable Newmark Constant Average Acceleration (Newmark β=0.25) method was used to integrate the dynamic equations of equilibrium. The time step of the analysis should be less than 0.5 to 0.1 of the period of the highest mode of free vibration that contributes significantly to the response of the structure and in this research, the second mode was considered to be the highest mode which influenced the response of the structure. The period of the second mode was 0.03 second and the analytical time step used was 0.01 second.

3.3 MELBOURNE UNIVERSITY 1/2 SCALE JOINT MODEL CALIBRATION

The first part of the modelling involved calibrating the computer model to the test results for the 1/2-scale reinforced concrete joint which was tested at the University of Melbourne by Corvetti [71]. The joint was tested in a quasi-static manner, using a cyclic loading function which was displacement controlled. The frequency of the cycles was set at 0.1Hz. This type of joint is typically designed for strength rather than ductility. Figure

3.3 and Figure 3.4 show the testing setup and reinforcement details used in the Melbourne research.

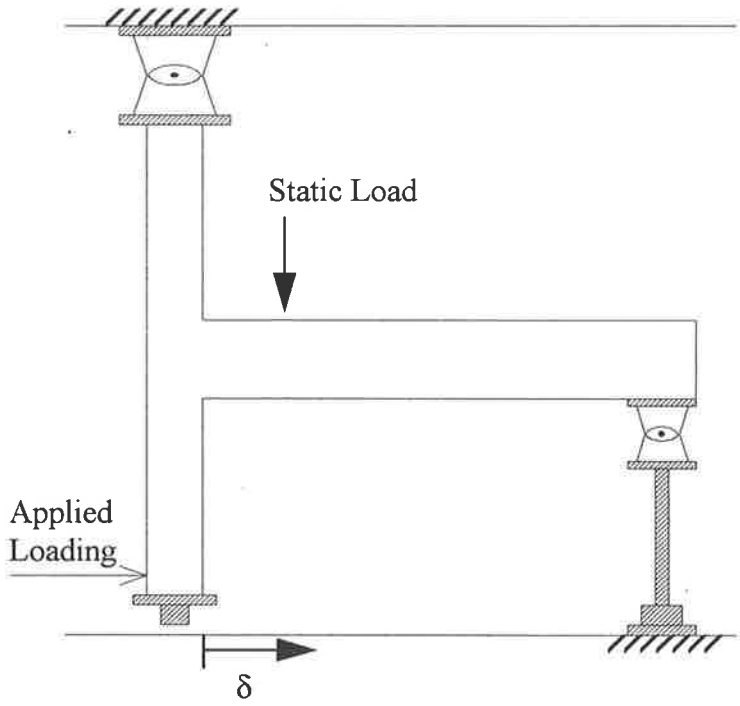

Figure 3.3 - Testing Setup at the University of Melbourne

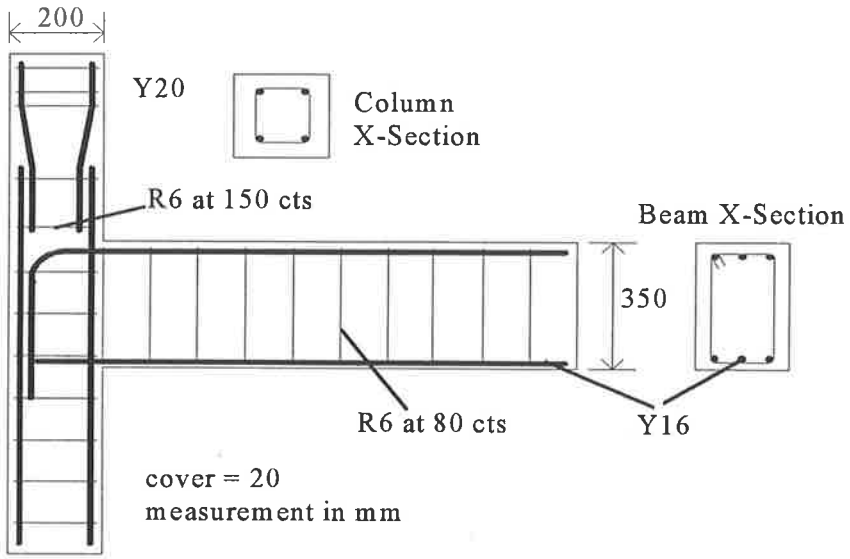

Figure 3.4 - Reinforcement Details for 1/2 Scale Joint Tested at Melbourne University

Figure 3.5 shows the load-displacement plot for the specimen detailed in accordance with the AS3600 [2] specifications for a reinforced concrete moment frame of the "ordinary" classification as per the Australian earthquake loading code AS1170.4 [1].

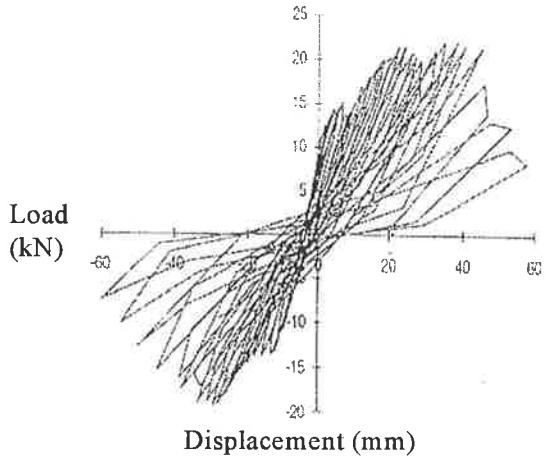

Figure 3.5 - Load-Displacement Plot for Ordinary Moment Frame Specimen (after Corvetti et.al, 1993)

3.3.1 Hysteresis Model

This part of the research involved the identification of the most appropriate hysteresis model for the ordinary moment resisting frame joint. For this research, three hysteresis models were identified out of the available 23 as being the most suitable for the simulation of the behaviour of reinforced concrete members under seismic loading. They were the Q-Hyst degrading stiffness hysteresis, the Muto degrading tri-linear hysteresis and the Mehran Keshavarzian degrading and pinching hysteresis. The decision as to which of the hysteresis models was preferred was based on the result (shape and numerical) of the storey hysteresis obtained from the experimental testing of the 1/2 scale reinforced concrete beam- column joints at the University of Melbourne [71].

3.3.1.1 Q-HYST Degrading Stiffness Hysteresis Model

The Q-Hyst degrading stiffness (Figure 3.6) was developed by Saiidi [56] in 1979 and this rule is the same as the Modified Takeda rule with the parameter BETA set to 0.0

[50]. This hysteresis rule requires only one additional input parameter ALFA (α) which gives the unloading stiffness and is within the range of 0.0 to 0.5 inclusive.

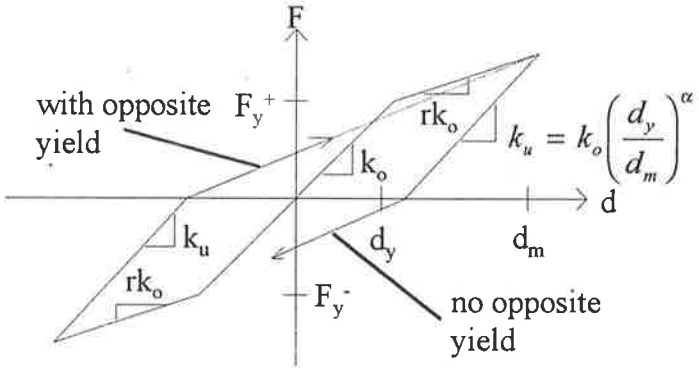

Figure 3.6 - Q-Hyst Degrading Stiffness Hysteresis Model

3.3.1.2 MUTO Degrading Tri-linear Hysteresis

This hysteresis model is based on a tri-linear rule (Figure 3.7) which was developed by Muto [75] in 1973. After cracking, the model is an origin-centred rule. After yield level is reached, the model becomes a bi-linear hysteresis with equivalent elastic stiffness equal to the secant stiffness to the yield point. For concrete beam-column sections, symmetry in moments is required.

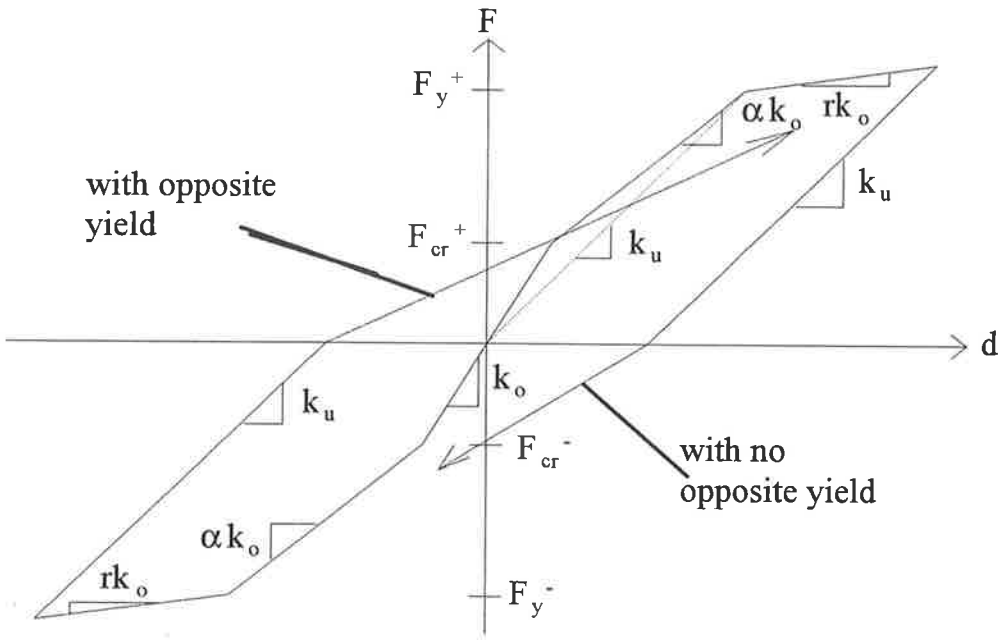

Figure 3.7 - MUTO Degrading Tri-linear Hysteresis

The Muto degrading model requires five additional input parameters which are summarised in Table 3.1.

Table 3.1 - Input Parameters for Muto Hysteresis Model

ALFA	Bi-linear factor (cracking to yield)
FCR1+	Cracking moment or force at A (>0.0)
FCR1-	Cracking moment or force at A (<0.0)
FCR2+	Cracking moment or force at B (>0.0)
FCR2-	Cracking moment or force at B (<0.0)

3.3.1.3 MEHRAN KESHAVARZIAN Degrading and Pinching Hysteresis Model

The Mehran model (Figure 3.8) was developed in 1984 by Keshavarzian [58] based on research done on reinforced concrete wall-frame and coupled shear wall structures. After comparison between experimental results and analytical results by the Mehran model, the conclusion was drawn that this model was very effective in predicting the non-linear behaviour of reinforced concrete column frame members.

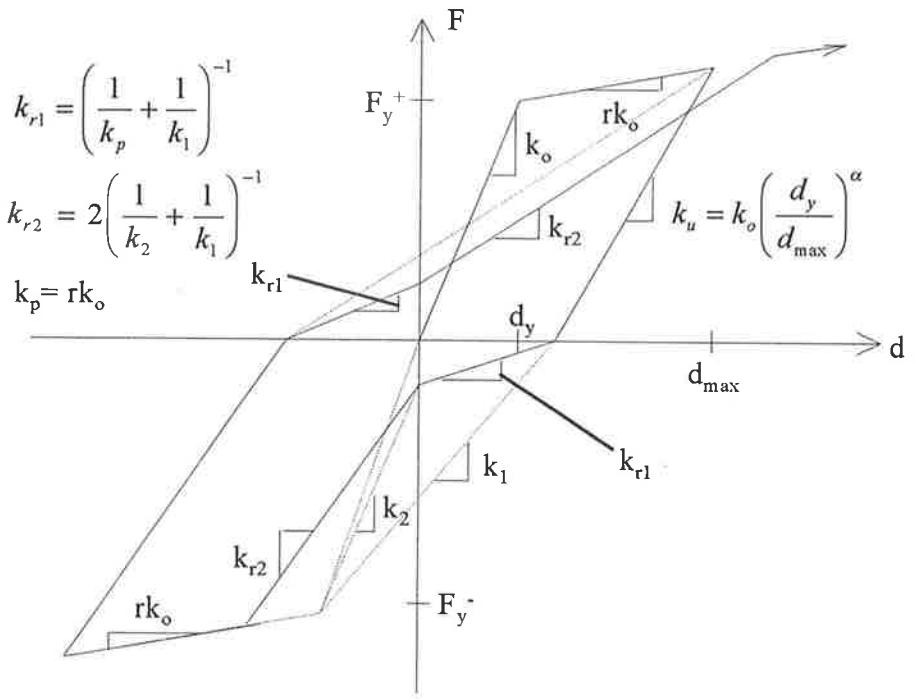

Figure 3.8 - Mehran Keshavarzian Degrading and Pinching Hysteresis Model

Only one additional input parameter is required for the Mehran model ALFA (α) which governs the unloading stiffness and is between 0.0 and 0.5 inclusive.

In all three hysteresis models, the strength degradation option was used to better model the behaviour of the joint

3.3.2 Pilot Computer Joint Model

A pilot computer joint model was setup using each of the three hysteresis rules with degrading stiffness/strength relative to the number of cycles. No calibration was done at this stage to the sections properties (I, A and P-M interaction curve for each member). To match the testing setup of the Melbourne results, displacement and not force time history was required for loading. Unfortunately, Ruaumoko does not have the option of displacement controlled loading. Hence the following model was used to achieve what was needed.

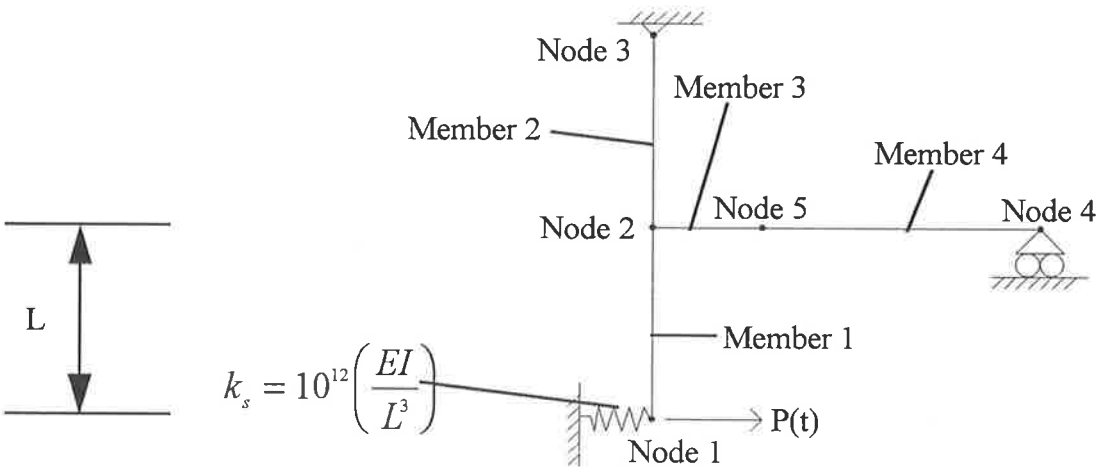

Figure 3.9 - Schematic of Computer Joint Model

By putting a very stiff spring (relative to the stiffness of the frame members) at the point where the cyclic load was to be applied, enforced displacements were simulated. The equation of the cyclic force pattern is as shown in equation 3.1

$$P(t) = A\mathrm{Sin}\omega t \qquad (3.1)$$

Also, for the spring

$$F = \delta k_s \qquad (3.2)$$

thus, equation 3.2 becomes

$$\delta = \frac{F}{k_s} \tag{3.3}$$

Equating the two forces F and P(t) gives

$$A = k_s \delta_{max} \tag{3.4}$$

with "A" being the scale factor required for the cyclic loading pattern, k_s is the stiffness of the spring which was calculated from the E (modulus of elasticity), I (moment of inertia) and L (length refer to Figure 3.9) of the structure and δ_{max} is the desired maximum displacement applied to the structure. By adjusting the scale factor "A", the level of enforced displacement could be altered.

The cyclic loading on the joint was governed by a sine wave pattern which was defined by one hundred points per cycle (refer to Figure 3.2). This record was input as a text file in the Caltech format, as defined in the Ruaumoko user's manual [74].

The storey hysteresis diagram for each of the hysteresis models from the pilot joint study are shown in Figures 3.10 to 3.12 and for the input files for each hysteresis models, refer to Appendix A.

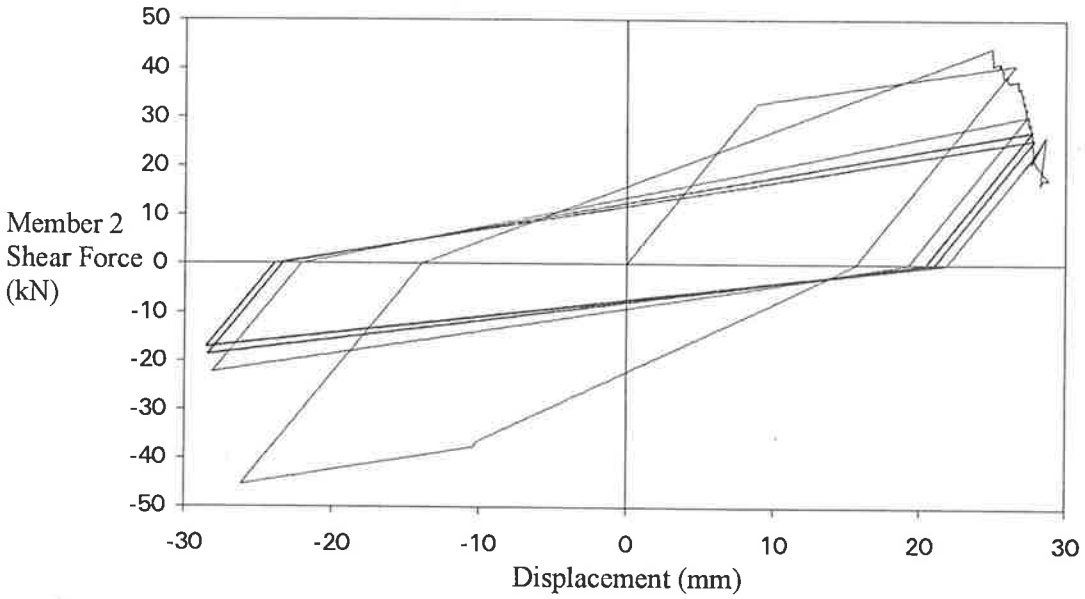

Figure 3.10 - Storey Hysteresis for Pilot Computer Joint Model Using Q-Hyst Degrading Stiffness Model

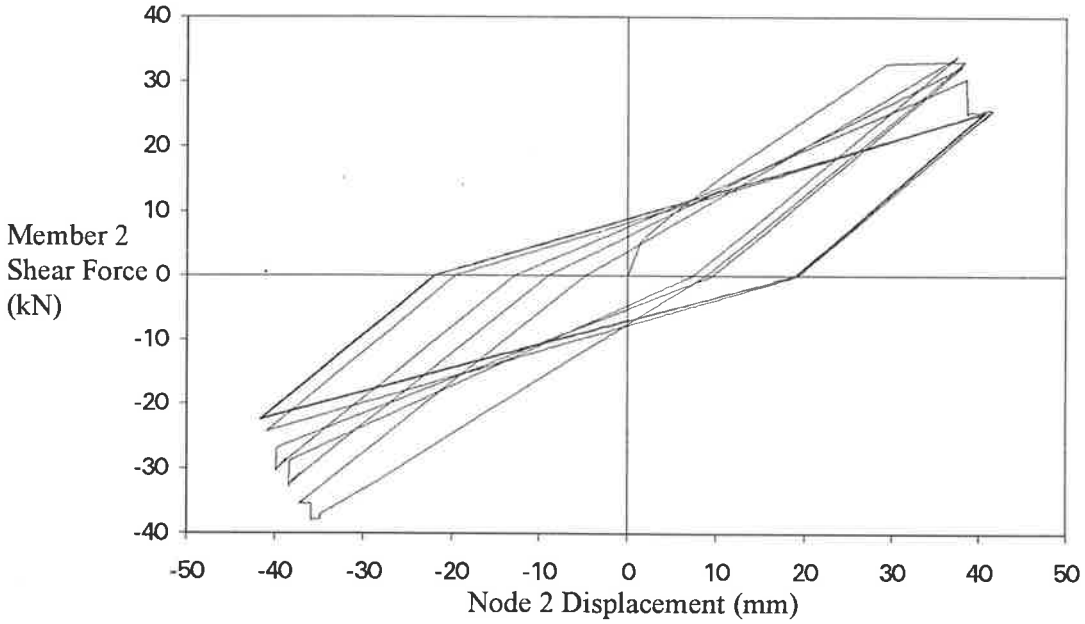

Figure 3.11 - Storey Hysteresis for Pilot Computer Joint Model Using Muto Degrading Tri-linear Hysteresis Model

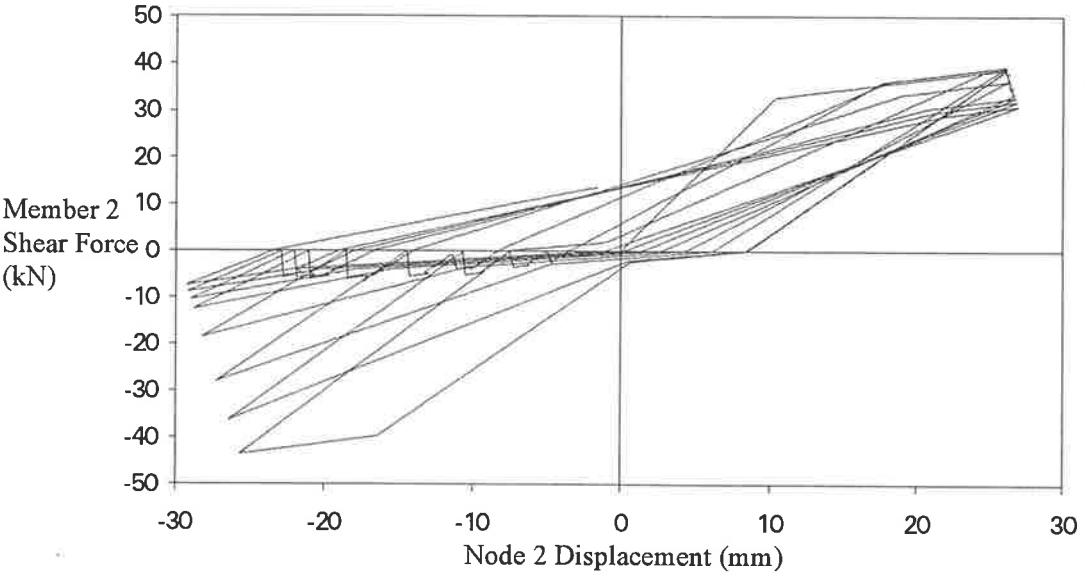

Figure 3.12 - Storey Hysteresis for Pilot Computer Joint Model Using the Mehran Keshavarzian Degrading and Pinching Hysteresis Model

After comparison of the results for each of the three pilot joint models to the Melbourne test results, it could be seen that all three performed relatively well. However, the Q-Hyst degrading stiffness model and the Muto degrading tri-linear model had loops which were

too large or "fat", indicating that these models overestimated the energy dissipation of the reinforced concrete joint specimen. Experimental results from Melbourne (Corvetti [71]) showed that the loops were quite narrow for the same joint (Figure 3.5). Judging from the shape of the hysteresis the Mehran Keshavarzian degrading and pinching model was felt to best represent the experimental results. The hysteresis obtained from this simple analysis showed that the Mehran model could best match the experimental results with respect to the shape, narrowness and was also able to model the characteristic pinching seen in the experimental hysteresis loops. It was observed that there existed a small numerical instability for all three models as the joints reached failure.

3.3.3 Computer Joint Model Calibration

The joint model was defined as shown in Figure 3.11 using the Mehran hysteresis model with the analysis options chosen listed in Table 3.2. The actual input file for this analysis is given in Appendix A.

Table 3.2 - Joint Model Analysis Options

Member Type	Frame/Reinforced Concrete BC Member
Joint Type	Members Built-In to Joint
Time History Integration	Newmark Constant Average Acceleration
Mass Matrix	Diagonal Mass Matrix
Damping Model	Linear Variation of Damping with Elastic Natural Frequencies
Small /Large Displacements	Small Displacement Assumed

The analytical time step was set at 0.01 second. This satisfied the requirement of being less then 0.1 of the period of the highest mode (2nd mode in this case) of free vibration that contributed significantly to the response of the structure. The joint was loaded with a sinusoidal force pattern at Node 1 (Figure 3.9) with a period of 10 seconds (the cycle frequency of the loading at the University of Melbourne was 0.1Hz). The loading pattern was increased after every cycle by 2mm starting from 2mm and ending with 40mm of enforced displacement. The hysteresis diagram of Node 2 displacement versus Member 2 shear is shown in Figure 3.13.

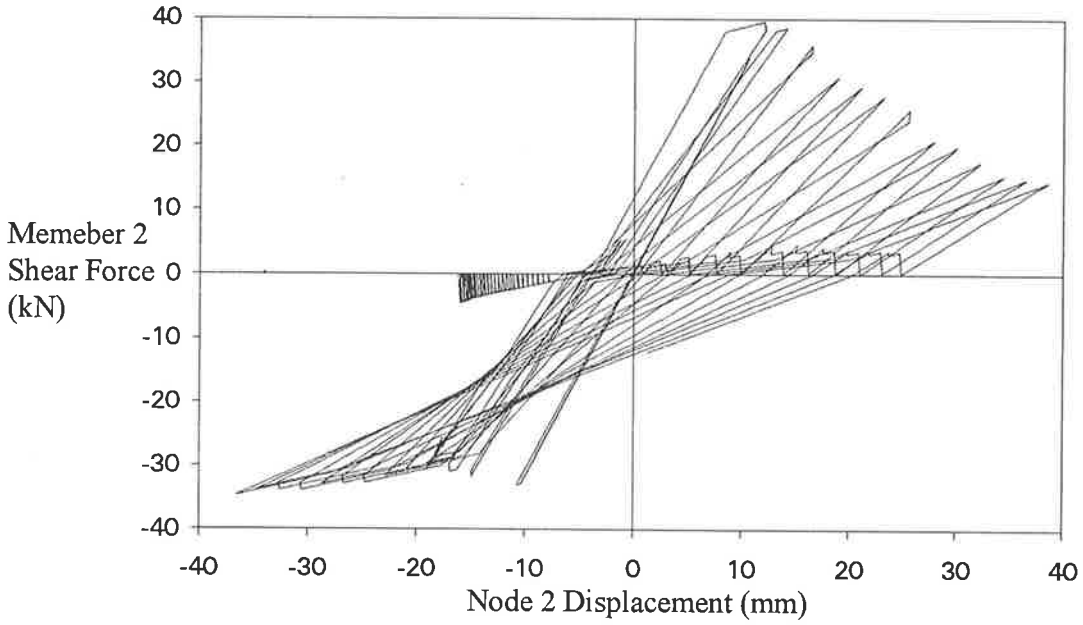

Figure 3.13 - Storey Hysteresis for Mehran Model Loaded with an Increasing Cyclic Load Pattern

From the hysteresis diagram of this pilot model (Figure 3.13), the initial stiffness was estimated to be 3.19kN/mm and the yield force was 37.8kN. The initial stiffness from the experimental test was 1.72kN/mm and the yield force was approximately 20kN (Corvetti [71]) (refer to Figure 3.5).

A quick comparison of the results showed that the computer joint model was both stiffer and stronger than the results from the experimental tests in Melbourne.

Calibration of the computer model was then undertaken by adjusting a few parameters so that the analytical results matched the initial stiffness and yield levels observed in the experimental tests. The parameters adjusted were I (moment of inertia), E (Young's modulus) and yield strengths (in tension, compression and bending) of the members. After calibration, it was found that the moment of inertia was reduced to 30% of I_g and yield values were reduced to 64% of original. Figure 3.14 shows the force-Δ hysteresis of the calibrated model. Note the yield force for the computer model was about 20kN and the initial stiffness of the joint was about 1.8kN/mm.

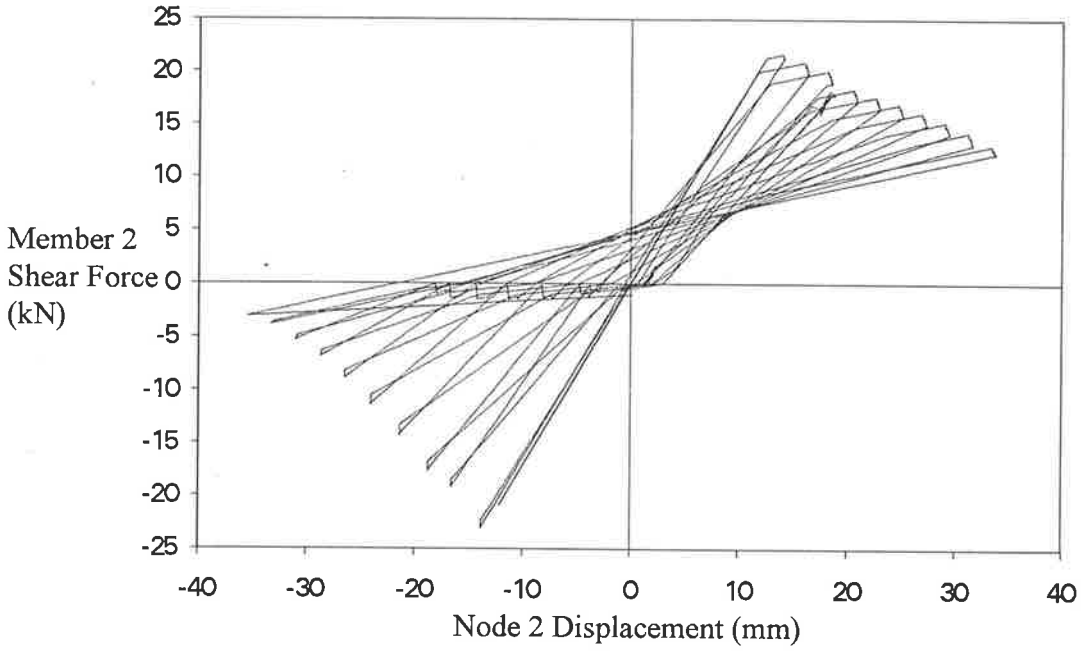

Figure 3.14 - Storey Hysteresis for Calibrated Computer Joint Model

Due to limitations of the program, stiffness/strength degradation could not be modelled in the linear elastic range. A qualitative comparison was made and the hysteresis loops from the computer model appeared to have similar areas to those observed during experimental testing.

3.4 CONCLUSION

A computer joint model of a beam-column joint from an ordinary moment resisting frame was produced and calibrated to the experimental results obtained from 1/2 scale quasi-static joint tests performed at the University of Melbourne.

Three hysteresis rules for stiffness degradation, namely the Q-Hyst Degrading Stiffness Hysteresis Rule, the Muto Degrading Tri-linear Hysteresis Rule and the Mehran Keshavarzian Degrading and Pinching Hysteresis Rule, were examined. By comparing the hysteresis obtained from the computer model using each hysteresis rule (Figures 3.10 to 3.12) , it was concluded that when compared to the experimental results, both the Q-Hyst Rule and the Muto Rule gave hysteresis loops which over-estimated the energy dissipation seen in the Melbourne experiments. The Mehran model was chosen to be the most suitable as it gave the thinnest hysteresis loops while allowing the pinching effect of the loops to be modelled as well.

Using the Mehran hysteresis rule, a computer joint model was produced and calibrated to the experimental results from the University of Melbourne in terms of initial stiffness and the yield levels. The storey hysteresis from this model (Figure 3.14) gave a satisfactory simulation of what was seen at the 1/2 scale test in Melbourne in terms of initial stiffness, yielding behaviour and stiffness/strength degradation of the joint system.

CHAPTER 4
COMPUTER MODELLING
FRAME MODELLING

4.1 INTRODUCTION

A computer model of the full scale version of the three-storey reinforced concrete frame dynamically tested by Heneker [72] in 1993 at the University of Adelaide was produced using the beam-column joint model calibrated (Chapter 3) to the Melbourne 1/2-scale joint test results [71] which is based on the Mehran-Keshavarzian degrading and pinching hysteresis model. The structure was dynamically loaded with three acceleration records recorded during three different magnitude shake table tests in Adelaide corresponding to effective peak accelerations (EPA) of 0.047g, 0.078g and 0.105g designated to be EQ05, EQ08 and EQ11 where the numbers represented the effective peak accelerations of the earthquakes.

A second computer model was produced by calibrating the properties directly to the full-scale equivalent of the University of Adelaide 1/5-scale model test results. The

"Adelaide" calibrated model was then loaded with the same three earthquakes which were used with the "Melbourne" calibrated model. The analytical results for both computer models were compared with the full-scale equivalent of the experimental results from the Adelaide tests.

4.2 UNIVERSITY OF ADELAIDE 1/5-SCALE FRAME TEST COMPARISON

The 1/5-scale reinforced concrete frame structure tested at the University of Adelaide was a single bay portal frame (Figure 4.1). The member and joint reinforcing details were the same as those used on the 1/2-scale joint tested at the University of Melbourne: namely, only nominal shear reinforcement, bottom beam bars terminating half way into column and column splices located just above the top of each floor slab (Figure 4.2-4.3). The concrete strength (f'c) of the micro concrete was 64MPa and the yield strength (f_{sy}) of the steel was 450MPa.

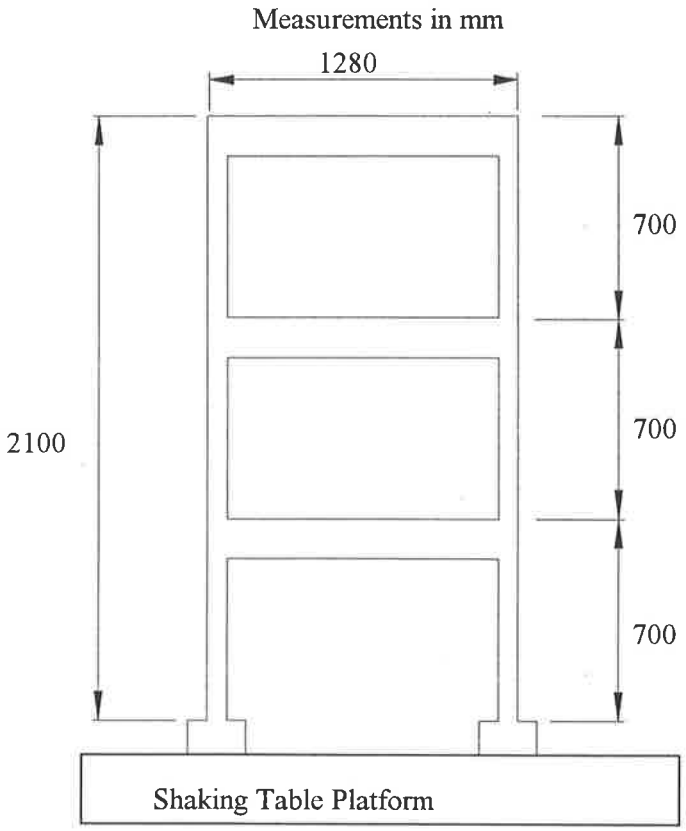

Figure 4.1 - 1/5-Scale Reinforced Concrete Frame Tested at The University of Adelaide

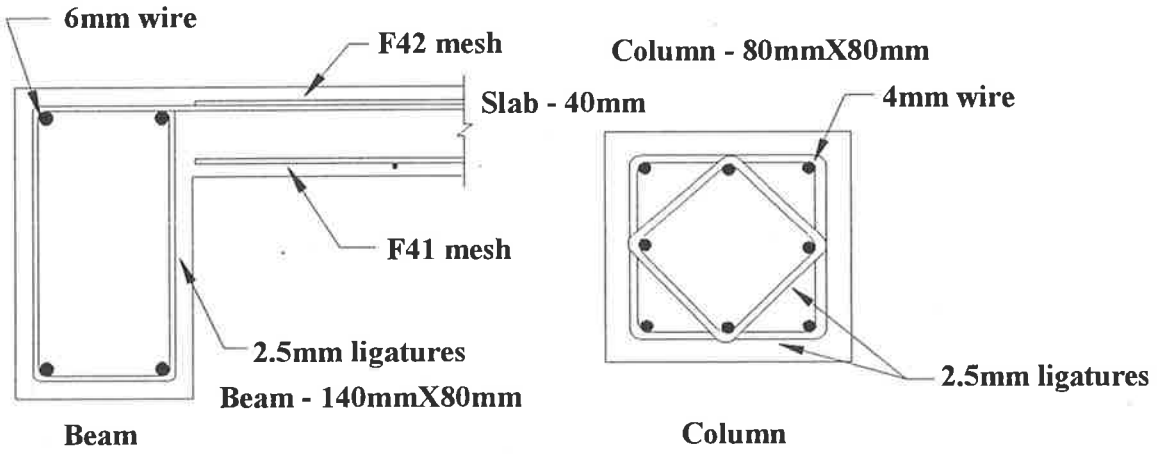

Figure 4.2 - Reinforcing Details of Beams and Columns

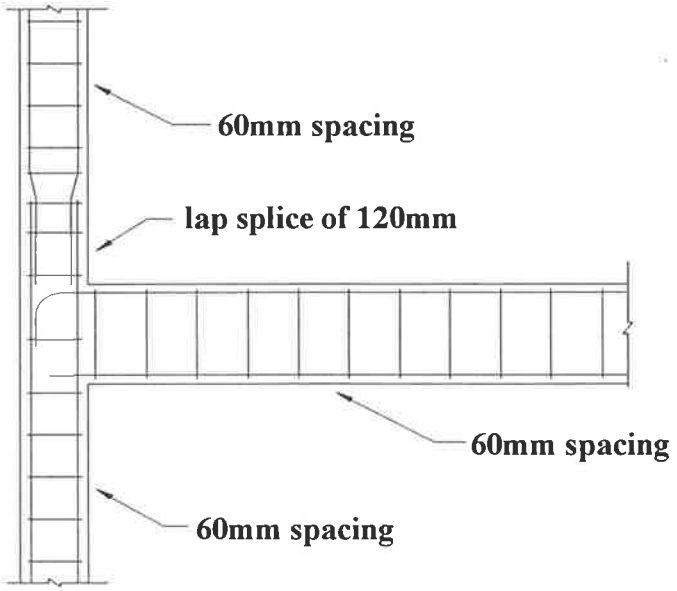

Figure 4.3 - Joint Reinforcing Details

The 1/5-scale frame was loaded dynamically with the time-scaled North-South component of the 1940 El-Centro earthquake acceleration record [77] (Figure 4.4) using the Department of Civil and Environmental Engineering earthquake simulator. A free vibration test was carried out prior to testing to calculate the period of the structure and it was found to be 0.31 second. The damping of the structure was also measured and was found to be 3% of critical.

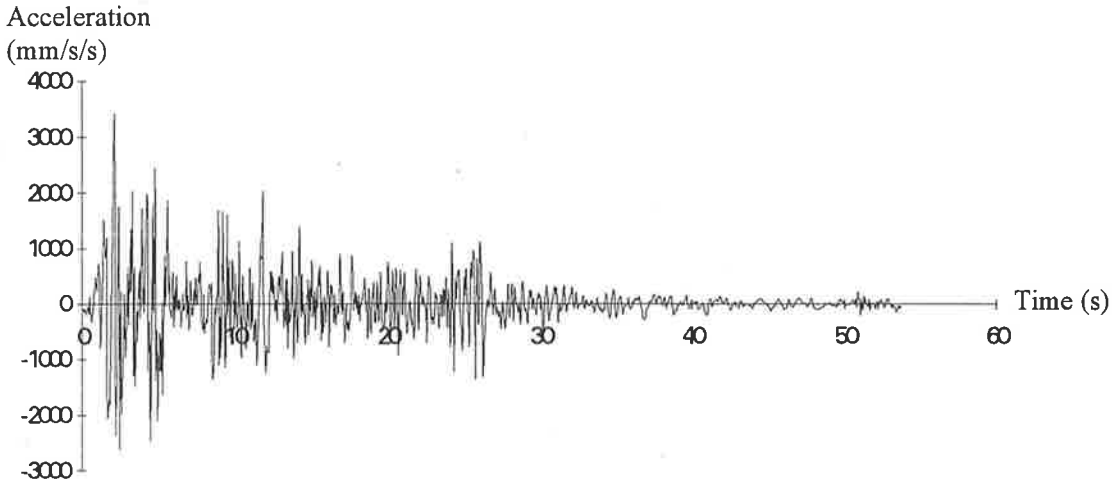

Figure 4.4 - Acceleration Record of the 1940 El-Centro Earthquake

A set of three different magnitude earthquake tests from the Adelaide shake table test series were chosen for use as a comparison with the analytical models. These tests had shake-table accelerations which corresponded to the El-Centro earthquake with maximum effective peak accelerations (EPA) of 0.047g, 0.078g and 0.105g, respectively. Effective peak acceleration corresponds to the design acceleration coefficient " a " in the earthquake loading code AS1170.4 [1]. Thus, this range of magnitude of earthquakes covers the range of design values for all major Australian capital cities, from Adelaide (0.1), Melbourne and Sydney (0.08) down to Hobart (0.05).

The measured shake-table acceleration records were used as the loading input for all subsequent analyses. This enabled direct comparison of analytical results to be made with the experimental results.

4.2.1 Calibrated Model - Melbourne Joint Model

A computer model of the full-scale equivalent of the 1/5-scale reinforced concrete frame structure tested at the University of Adelaide was produced using the full-scale equivalents of the properties and characteristics of the computer joint model developed

for the beam-column joint tested at Melbourne University (refer to Chapter 3). A two-dimensional computer model consisting of 8 nodes and 9 members (Figure 4.5) was produced. The computer program *Ruaumoko* [74] was used for this analysis. Hence only half the mass of the slab and the orthogonal beams were lumped at the nodes (2,3,4,6,7 and 8). By modelling in two dimensions, the torsional effects were not included. However, torsion was not expected to be significant since the structure was designed to be symmetrical with respect to mass and stiffness. The properties of the members such as Young's modulus, moment of inertia and yield strengths (both for beams and columns) were taken from the calibrated joint model discussed in Chapter 3 but were scaled up to the full scale equivalent values. The conversion factors from 1/2-scale properties to full-scale properties are given in Table 4.1. The effect of the slab was included by adding the effective width of the slab (in accordance with AS3600 [2]) to the beam and calculating the moment of inertia of this modified section.

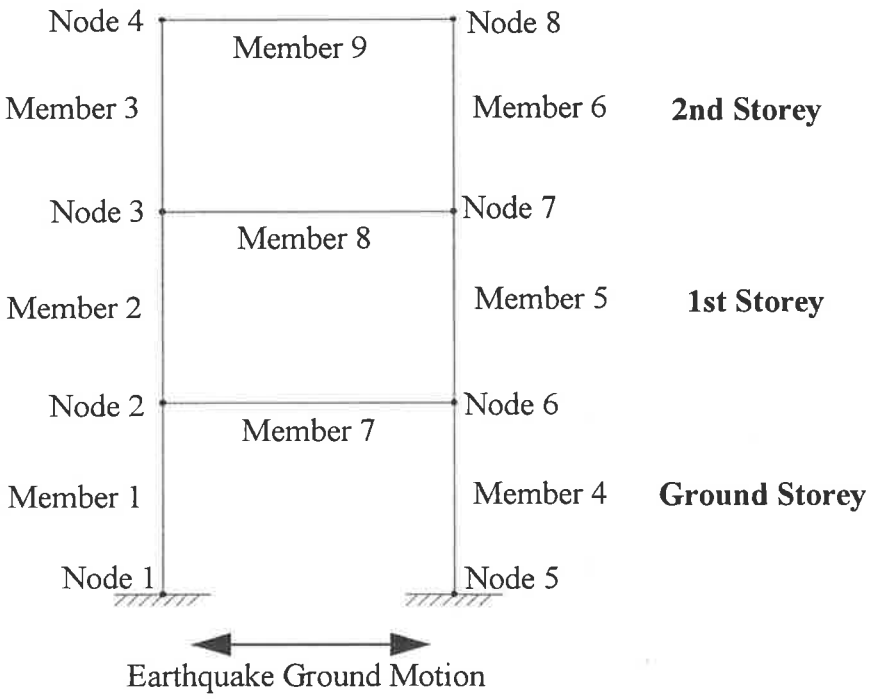

Figure 4.5 - Schematic Diagram of Computer Model

Table 4.1 - Conversion from Scaled Model to Full Scale Equivalent

1/5 Scale Model (S=5)	1/2 Scale Model (S=2)	Full Scale Equivalent
Length	Length	S*Length
Area	Area	S^2*Area
Force	Force	S^2*Force
Moment	Moment	S^3*Moment
Moment of Inertia (I)	Moment of Inertia (I)	S^4*Moment of Inertia

4.2.1.1 EQ05 (EPA=0.047g)

The full-scale computer model of the 3-storey reinforced concrete frame was loaded dynamically with a 0.047 EPA El-Centro earthquake. A modal analysis determined the period of the structure to be 0.62 second whereas the experimentally determined value was 0.6932 second (full-scale equivalent). The moment of inertia of the columns and beams were subsequently reduced to produce a slightly less stiff structure in order to match the period of the real structure. Thus, the moment of inertia of the beams and columns were reduced to 60% of the original values. Table 4.2 and Figure 4.6 show the cross sectional inputs and the yield interaction surface for the beam and column members used and in Appendix B, a copy of the input file used in Ruaumoko for the frame analysis is provided.

Table 4.2 - Cross Sectional and Yield Interaction Surface Properties

	Beam	Column
Cross sectional area, **A**	36.4×10^{-2} m^2	16×10^{-2} m^2
Moment of inertia, $\mathbf{I_{cr}}$	15.39×10^{-3} m^4	392.54×10^{-6} m^4
Axial compression yield force, **PYC**	-7.44×10^{6} N	-4.85×10^{6} N
Axial compression force at balance point, **PB**	-2.57×10^{6} N	-1.33×10^{6} N
Yield moment at balanced point, **MB**	862.4×10^{3} Nm	333.6×10^{3} Nm
Yield moment at P = (2/3)*PB, **M1B**	758.72×10^{3} Nm	307.2×10^{3} Nm
Yield moment at P = (1/3)*PB, **M2B**	586.1×10^{3} Nm	257.6×10^{3} Nm
Yield moment at P = 0.0, **MO**	372.0×10^{3} Nm	190.4×10^{3} Nm
Axial tension yield force, **PYT**	624×10^{3} N	326.8×10^{3} N

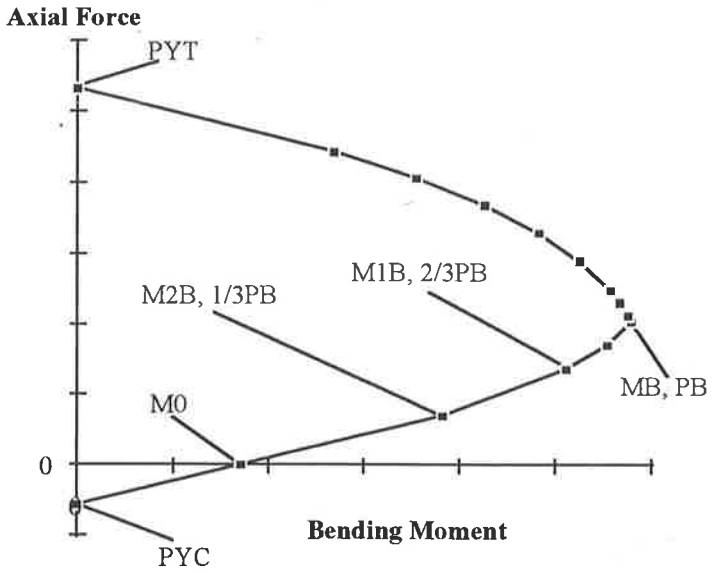

Figure 4.6 - Beam-Column Yield Interaction Surface

Figure 4.7 shows the time history storey displacement relative to the ground (Node 2, 3 and 4 were ground, first and second storey respectively). The maximum roof displacement was found to be 22mm and 17mm in either direction. For comparison, all the theoretical storey shear and storey hysteresis were converted to the equivalent values of four columns by doubling the shear values obtained from the two-dimensional model. In this way, a direct comparison with the experimental results was made possible.

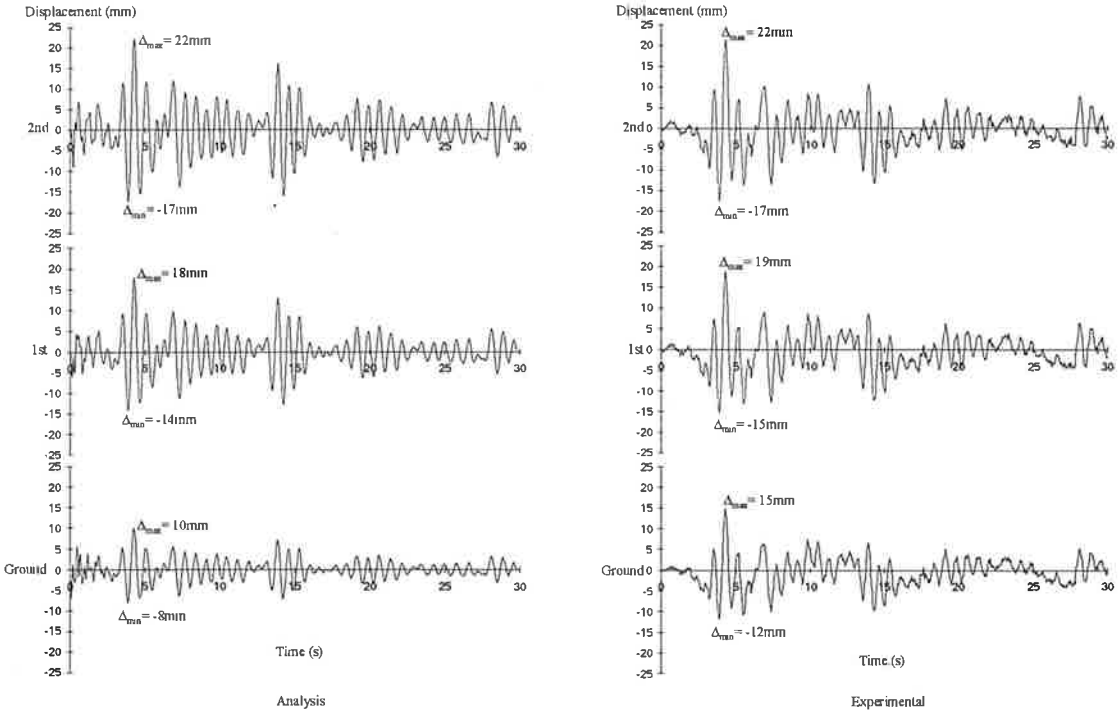

Figure 4.7 - Storey Displacement for EQ05

By comparing the displacements relative to the ground (Figure 4.8), it was noticed that the computer model predicted the maximum displacement at roof level very well when compared to experimental results but under-estimated displacements at the lower two levels. The calculated deformations were more linearly distributed between the lower two levels in the computer model whereas in the experiment, most deformation occurred in the first level. Thus, this implied that for this level of earthquake, the computer model over-estimated the stiffness of the lower levels of the frame or under-estimated the non-linear behaviour of the frame.

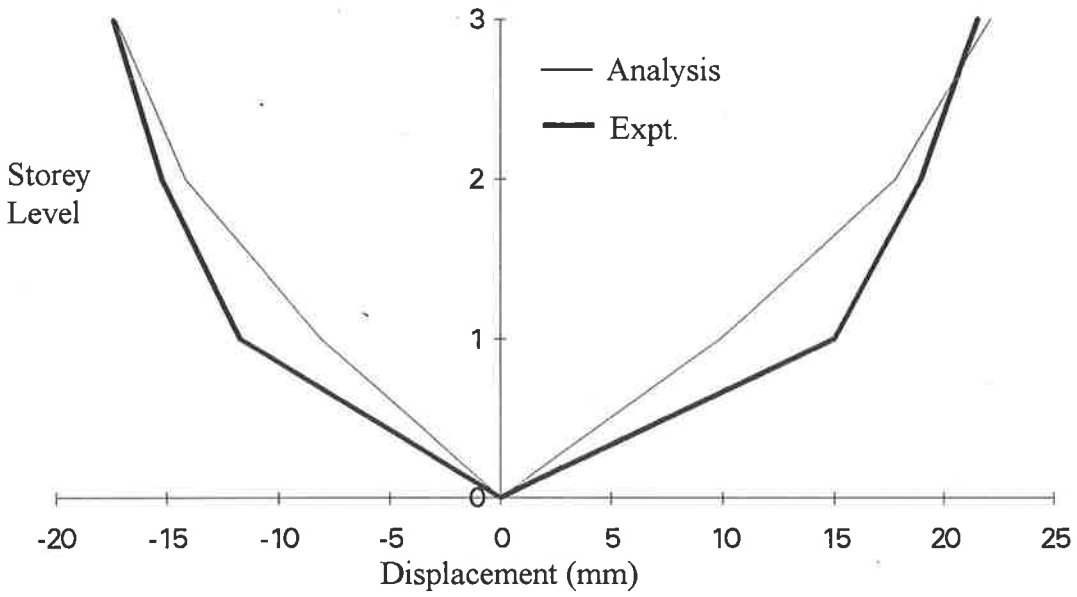

Figure 4.8 - Maximum Displacement Profile for EQ05

Figure 4.9 shows the shear forces experienced by the columns at each level of the structure. The sum of the column base shear forces from the computer model was 145kN and 119kN respectively in both directions. The experimentally observed sum of the column base shear forces was 137kN and 87kN correspondingly. The computer model predicted higher level of shear forces experienced by the columns than was recorded from the experimental test results.

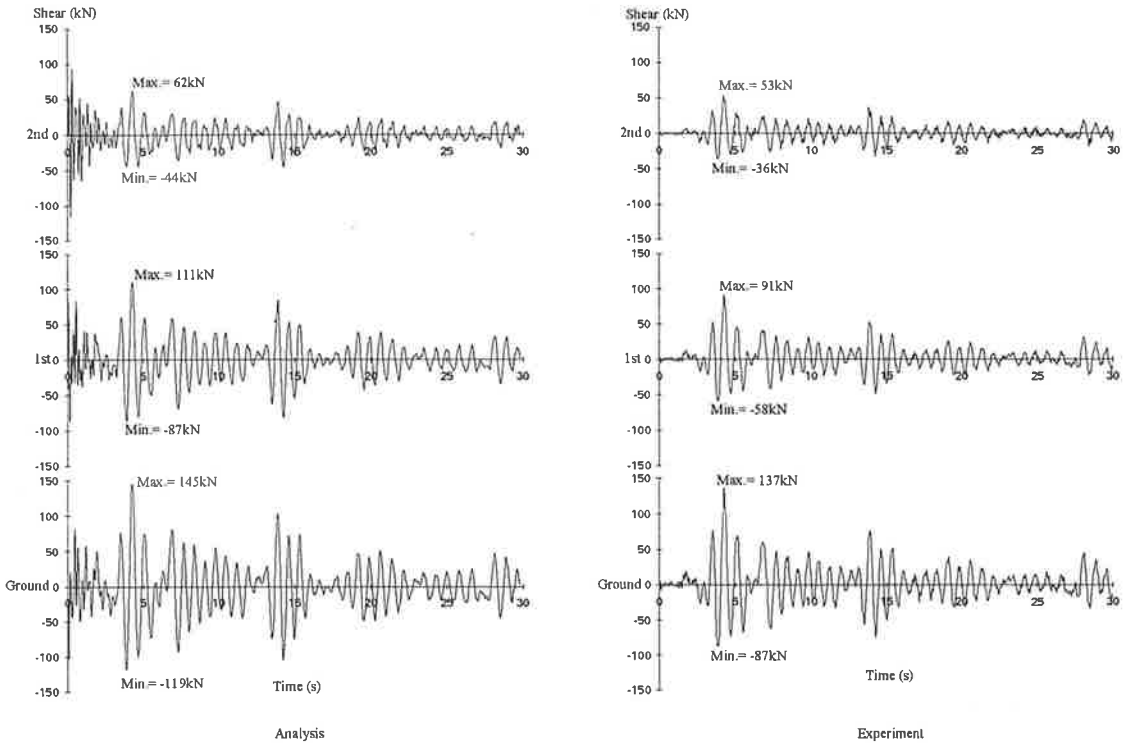

Figure 4.9 - Storey Shear Forces for EQ05

Figure 4.10 shows the normalised storey shear profile of the structure. The plot shows that the inertia forces were uniformly distributed in the frame as shown by the relatively even increments in both the experimental and analytical results.

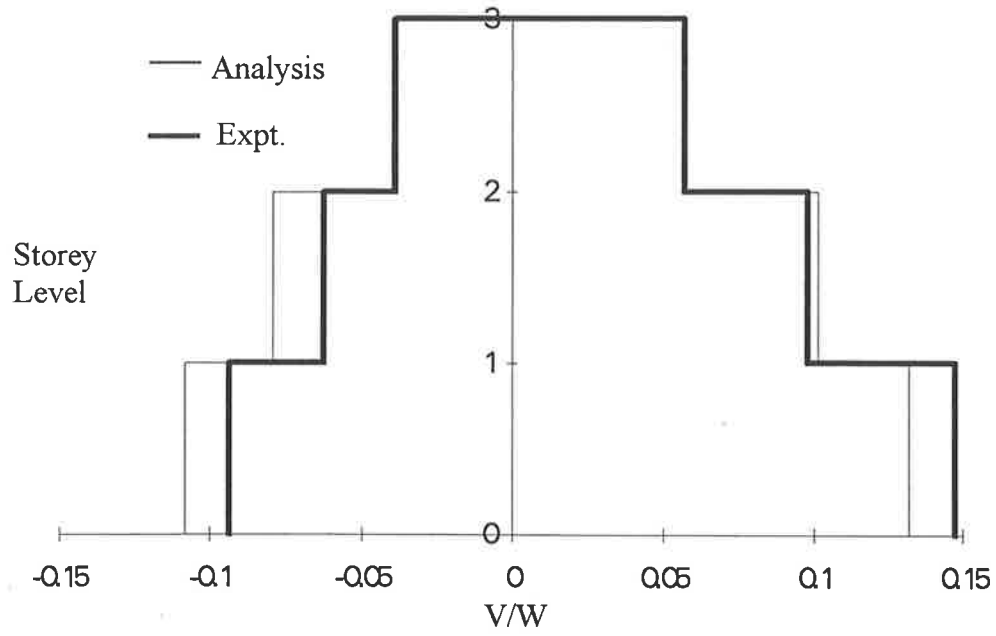

Figure 4.10 - Normalised Storey Shear Profile for EQ05

Figure 4.11 shows the storey hysteresis for the three levels. It can be seen that all three hysteresis loops are very narrow indicating that very little energy was dissipated by the structure and that the structure was behaving essentially in a linear elastic manner. The storey stiffness estimated from the storey hysteresis for each level gave a fairly uniform stiffness throughout the three levels. They were 15.7kN/mm, 14.0kN/mm and 14.5kN/mm from bottom to top level. However, the experimental results were 9.0kN/mm, 17.5kN/mm and 16.7kN/mm (equivalent full scale values) from bottom level to the top. This implies that the computer model was not "yielding" where as the experimental structure did.

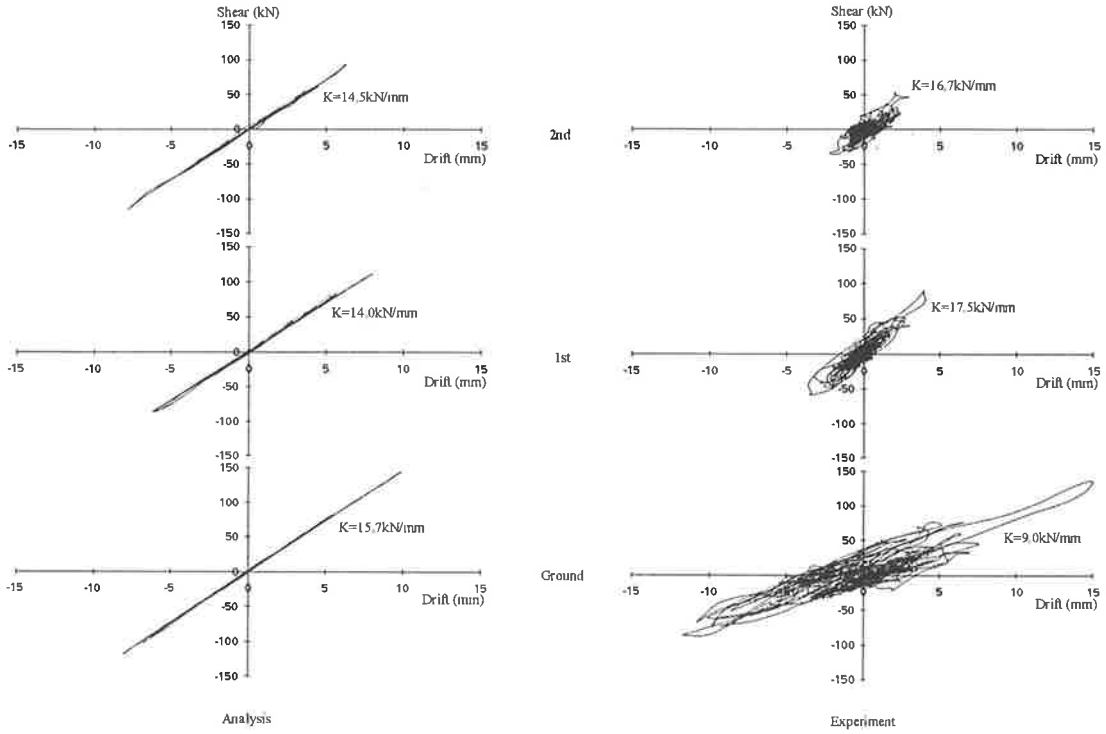

Figure 4.11 - Storey Hysteresis for EQ05

4.2.1.2 EQ08 (EPA=0.078g)

The computer model was used to simulate the behaviour of the three-storey structure during an earthquake with an effective peak acceleration of 0.078g corresponding closely to the earthquake loading code (AS1170.4 [1]) acceleration coefficient of 0.08 for cities such as Melbourne and Sydney.

Figure 4.12 shows the displacement time history of each of the three floors.

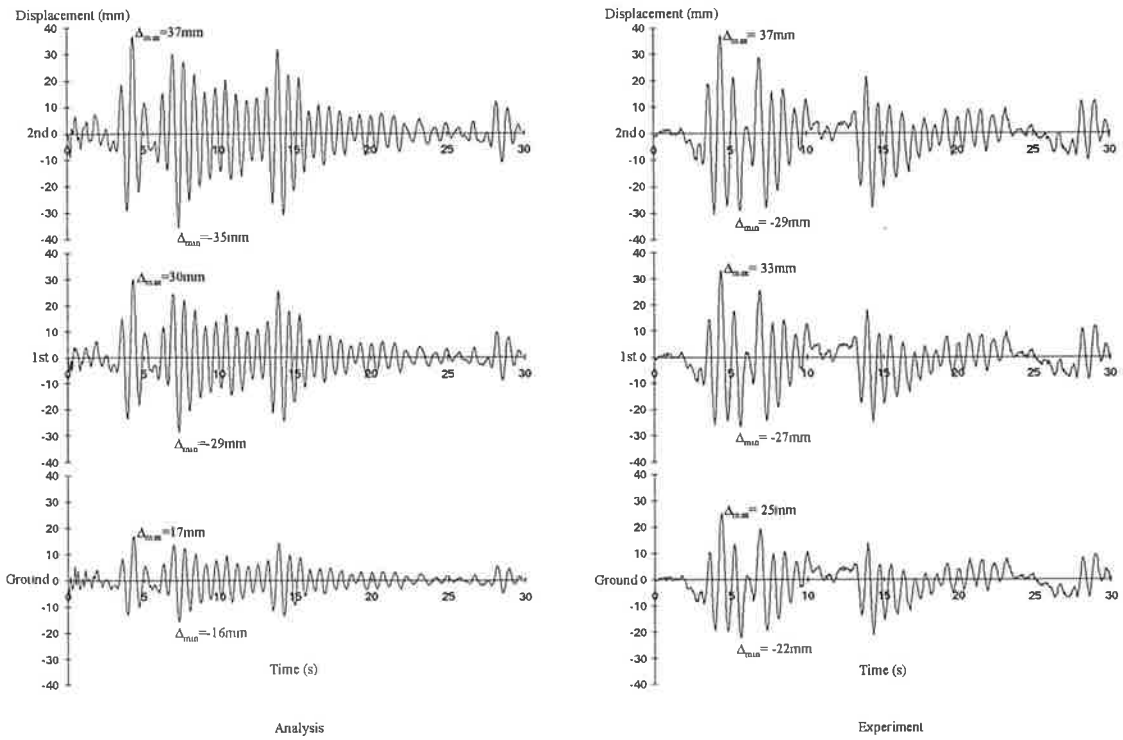

Figure 4.12 - Storey Displacement for EQ08

Comparison of the maximum displacement profile for both the computer model and the experimental results for the same structure are given in Figure 4.13. In one direction, the maximum displacements were accurately predicted by the model for the top floor but the displacements of the lower floors were under-estimated. In the other direction, the maximum top floor displacement indicated by the model was more than observed during

testing (35.4mm compared to 30.6mm). However, the first floor displacement was still under-estimated by the computer model.

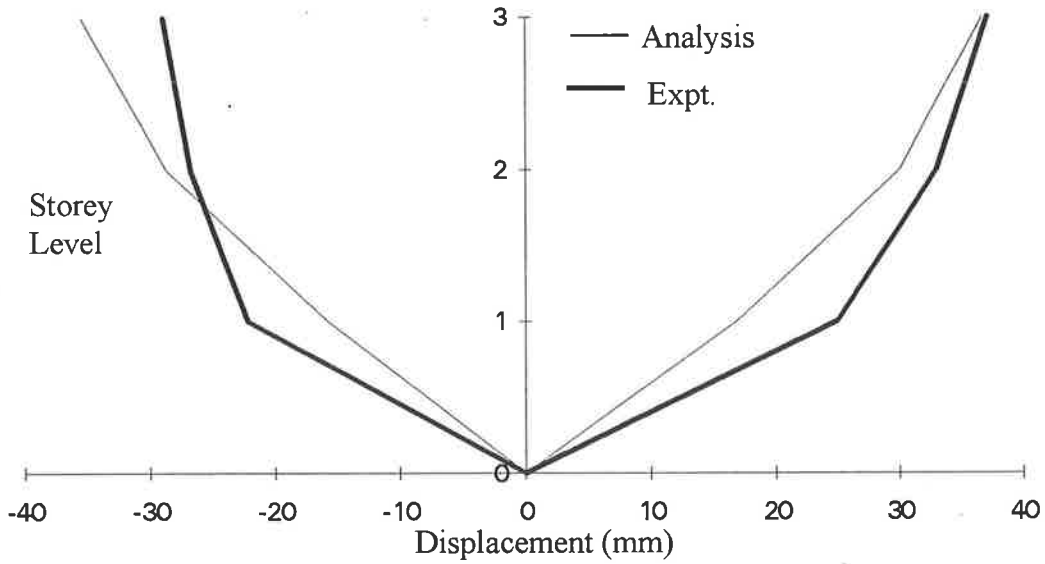

Figure 4.13 - Maximum Displacement Profile for EQ08

Storey shear forces in the three levels are shown in Figure 4.14. The sum of column base shear forces measured from the experiment was 205kN and 148kN respectively in both directions. Correspondingly, the computer model predicted 247kN and 231kN. As with EQ05, the computer model had over-estimated the base shear forces experienced by the structure. The reason for this are as follows.

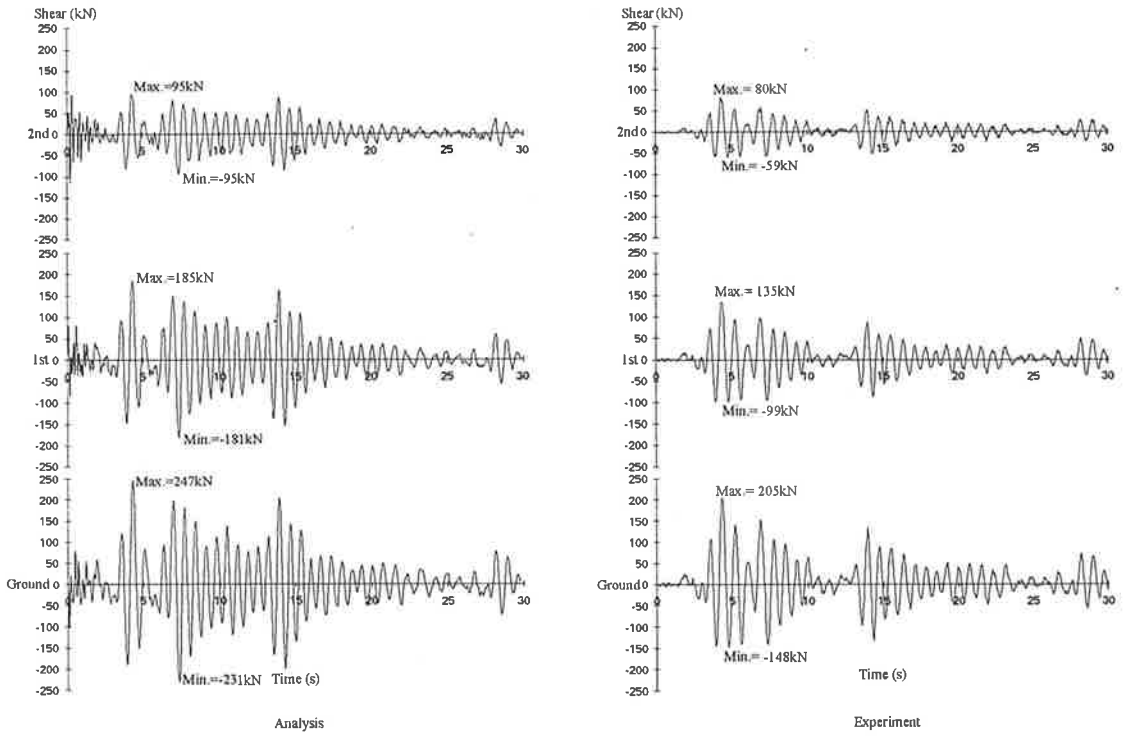

Figure 4.14- Storey Shear Forces for EQ08

Shear forces can be thought of as a product of stiffness and displacement, i.e.

$$V = k \cdot \delta \tag{4.1}$$

As the base shear forces were overestimated and the displacement at ground level was also lower than that observed from experimental testing (Figure 4.12), this indicating that the stiffness of the joint was overestimated. The natural period of this structure (refer to page 21) is greater than that corresponding to the peak elastic spectral response T_m for the 1940 El-Centro earthquake [77]. (Refer to Figure 4.15).

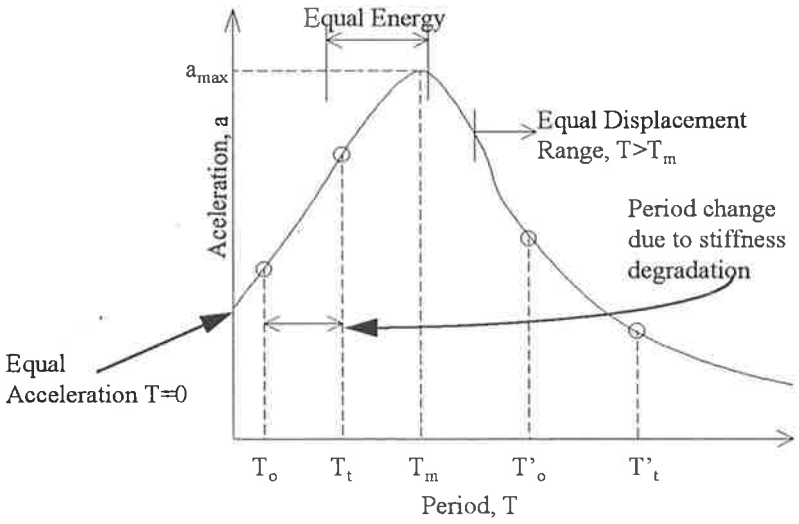

Figure 4.15 - Influence of Period on Ductile Force Reduction

The ductility achieved by the inelastic system of such a structure is approximately equal to the force reduction factor for the equal-displacement region of the spectrum as given by Priestley and Paulay [76], i.e.

$$\mu = R \tag{4.2}$$

The shear profile of the structure expressed as a fraction of the self weight of the structure is shown in Figure 4.16. The distinctive step profile was again observed and the computer model results gave closer correlation to the experimental results than it did for EQ05.

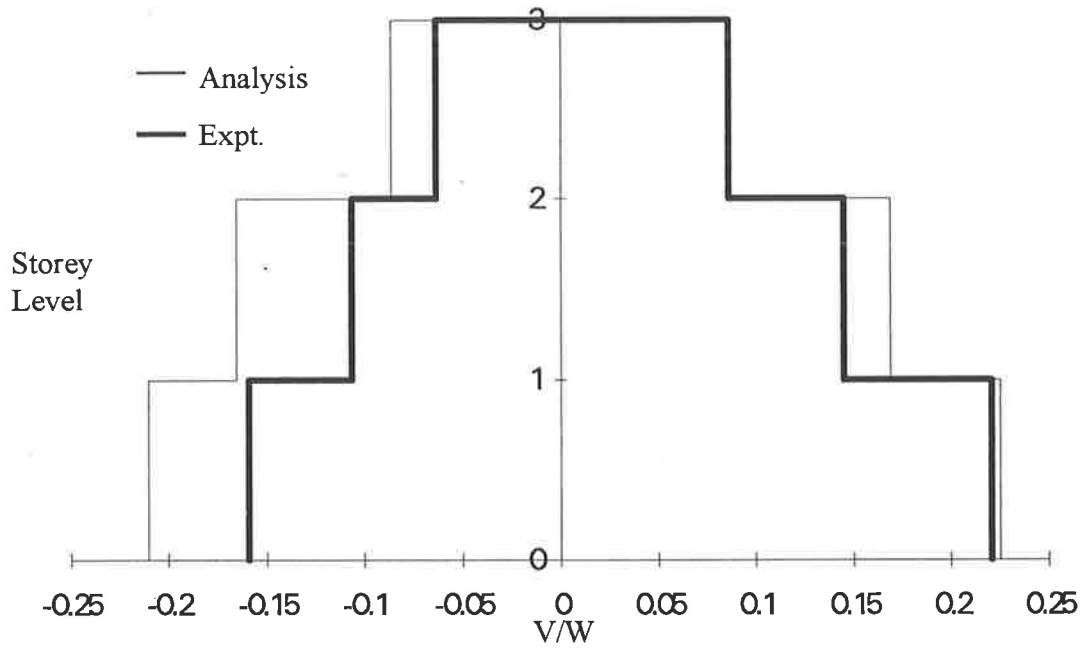

Figure 4.16 - Normalised Storey Shear Profile for EQ08

The storey hysteresis diagrams (Figure 4.17) indicated that the structure was still behaving in an elastic manner with very little stiffness and strength degradation. The tightness of the loops, for the computer model especially, again implied that little energy dissipation occurred. The storey stiffness measured from the scale model testing was 8.3kN/mm, 16.7kN/mm and 17.2kN/mm for ground to second level. The corresponding values from the computer model were 14.6kN/mm, 15.0kN/mm and 14.6kN/mm. The computer model gave a fairly uniform storey stiffness for all three levels whereas the experimental testing showed that the storey stiffness of the ground level was lower than the higher two levels. As shown by the underestimations of displacement and shear, stiffness was overestimated at ground level.

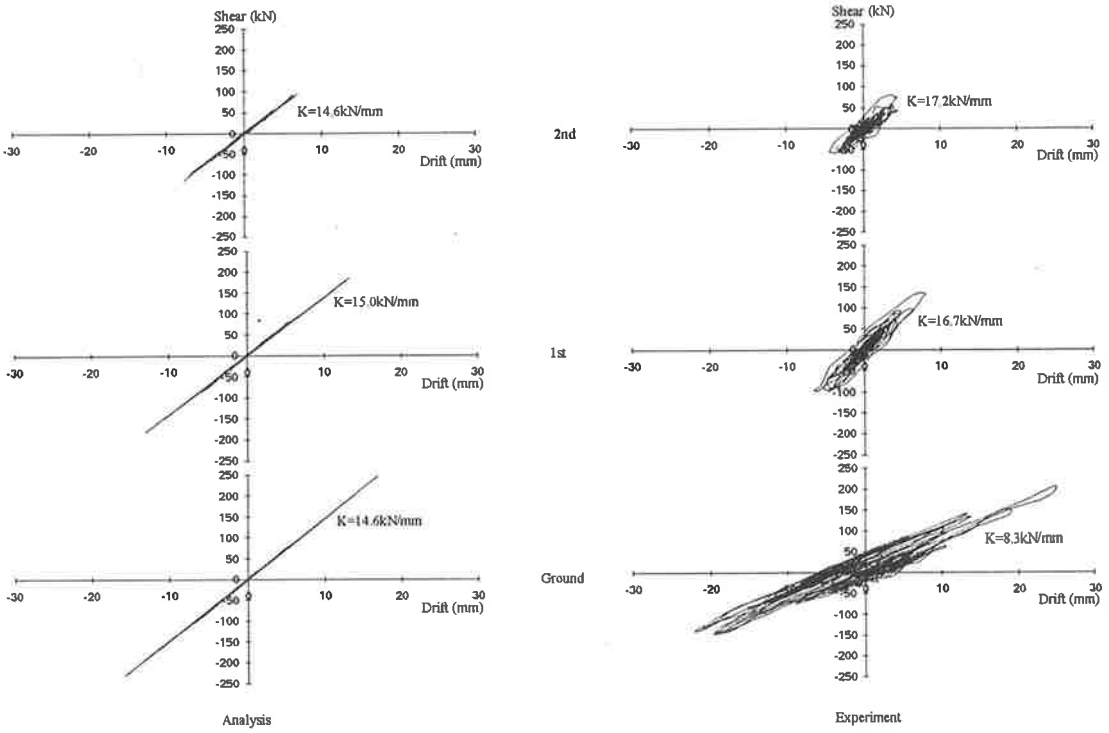

Figure 4.17- Storey Hysteresis for EQ08

4.2.1.3 EQ11 (EPA=0.105g)

The third analysis used an EPA=0.105g earthquake. This was the largest earthquake, in terms of magnitude, used for this comparison and was comparable in magnitude to the design coefficient (AS1170.4 [1]) from Adelaide (a=0.10) and Newcastle (a=0.11).

The displacement time histories during EQ11 (EPA=0.105g) of each floor are given in Figure 4.18.

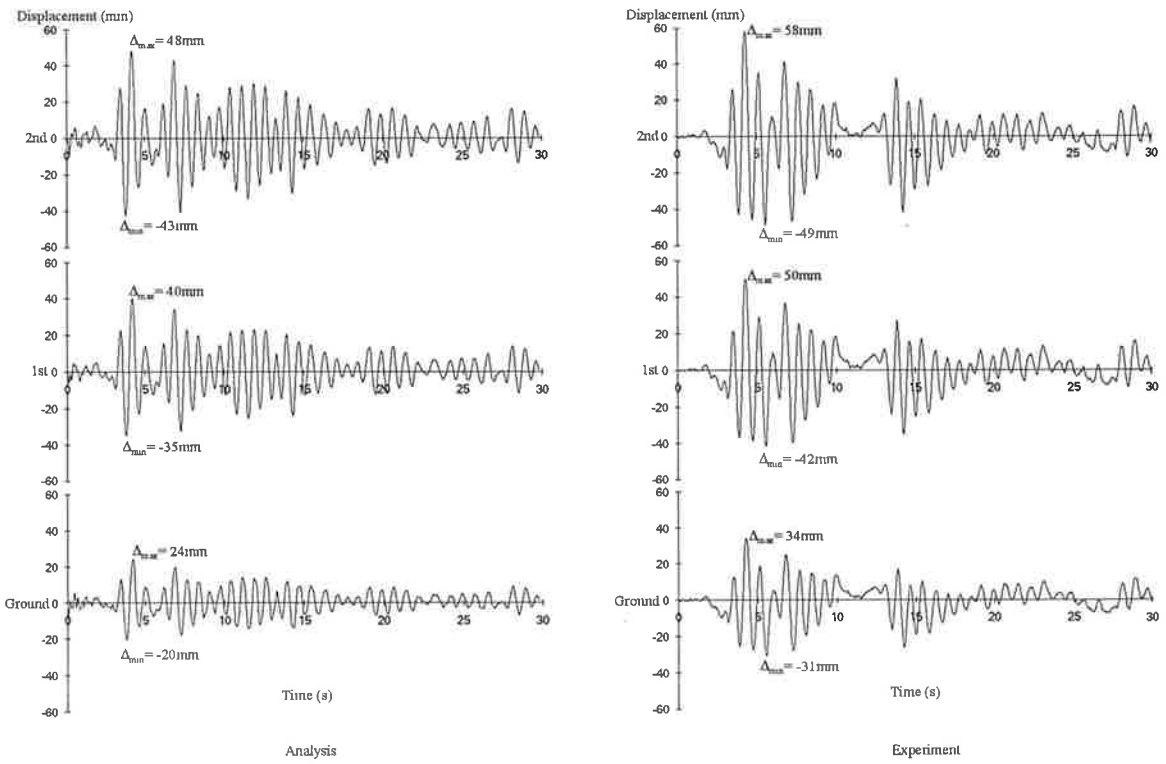

Figure 4.18 - Storey Displacement for EQ11

The maximum displacement profile (Figure 4.19) once again showed that the computer model under-estimated the displacement at all three levels during EQ11. The maximum roof displacement predicted by the model was 48mm and 43mm in either direction while the scale

model experiment gave 56mm and 61mm of displacement. This represented approximately 15% and 30% below experimental results respectively. However, the shape of the calculated profile matched quite well with that obtained from the shake table test. This seem to indicate that the amplitude of shaking has been reached so that the computer model could begin to yield.

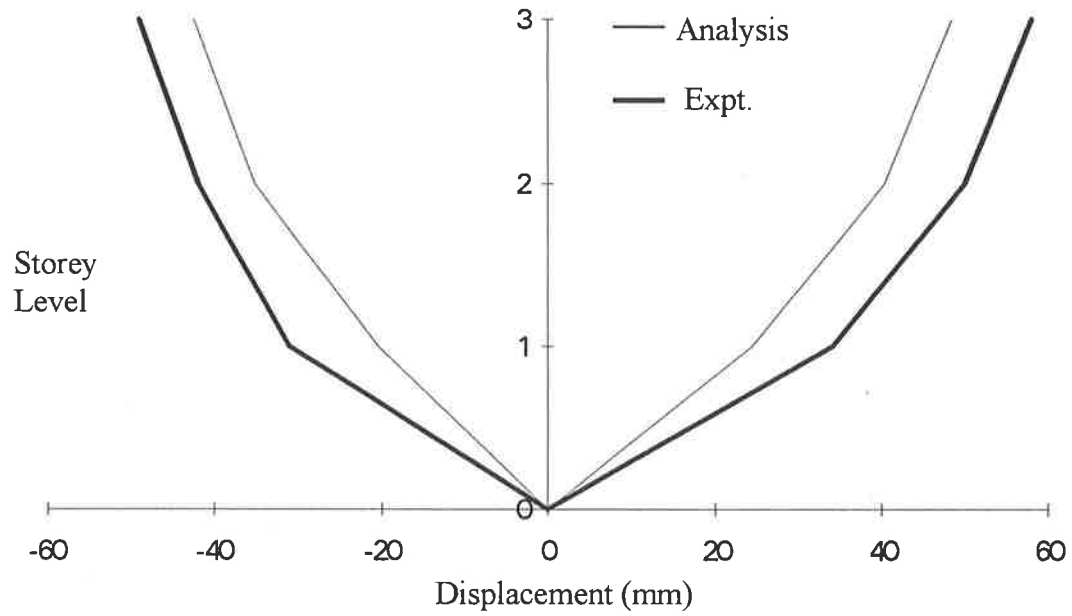

Figure 4.19 - Maximum Displacement Profile for EQ11

Figure 4.20 shows the storey shear forces at each level of the structure during EQ11. The maximum base shear forces experienced from the computer model were 304kN and 283kN in either direction respectively. The experimentally observed values were 255kN and 218kN respectively. As was seen with the comparison of EQ05 and EQ08, the computer model consistently over-estimated the total base shear forces.

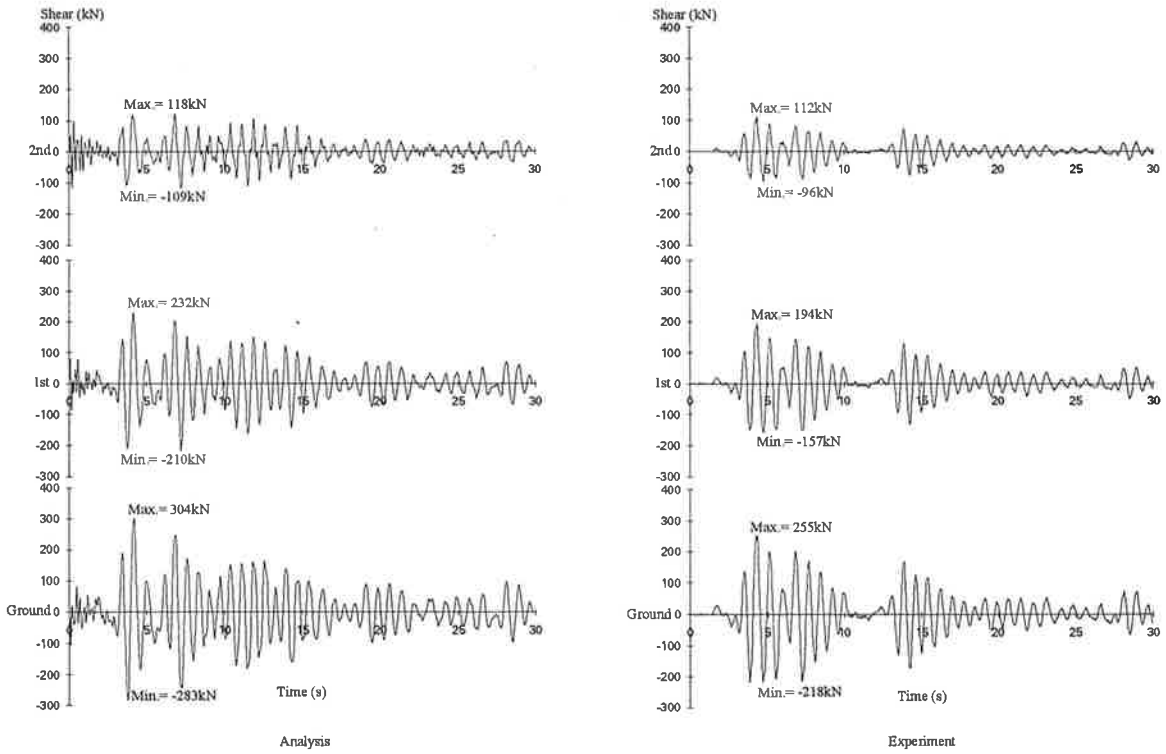

Figure 4.20 - Storey Shear Forces for EQ11

Figure 4.21 shows the normalised shear profile for the structure during EQ11. The experimental results and the analytical results for the upper two storeys were quite close while for the base shear, the analytical model over-estimated the shear forces.

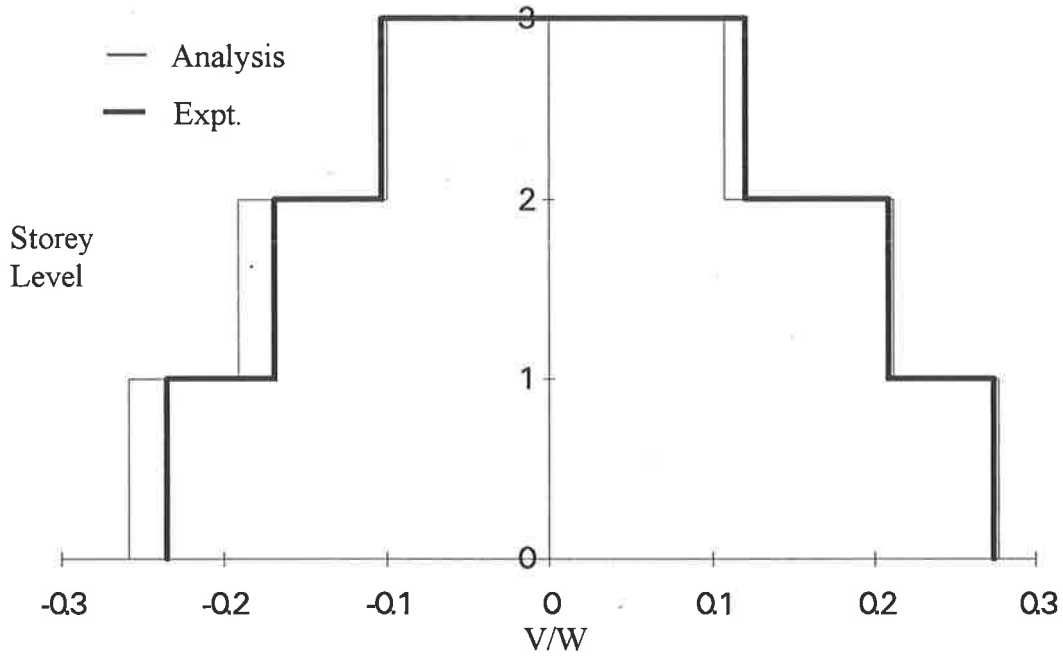

Figure 4.21 - Storey Shear Profile for EQ11

For EQ11, the storey hysteresis diagrams (Figure 4.22) show significant yielding behaviour. They indicated that there was significant yielding in the ground storey corresponding to a shear force of 273kN and a displacement of 18mm. The storey hysteresis for the second and third levels showed considerably less damage to the columns. From the hysteresis diagrams (Figure 4.22), slight stiffness degradation could be detected for the upper two levels, otherwise, the members were still behaving, in most part, mainly elastically. The initial storey stiffness were 15.1kN/mm, 13.8kN/mm and 13.8kN/mm from bottom to top level. The storey stiffness recorded during the experimental test were 10kN/mm, 13.3kN/mm and 13.4kN/mm.

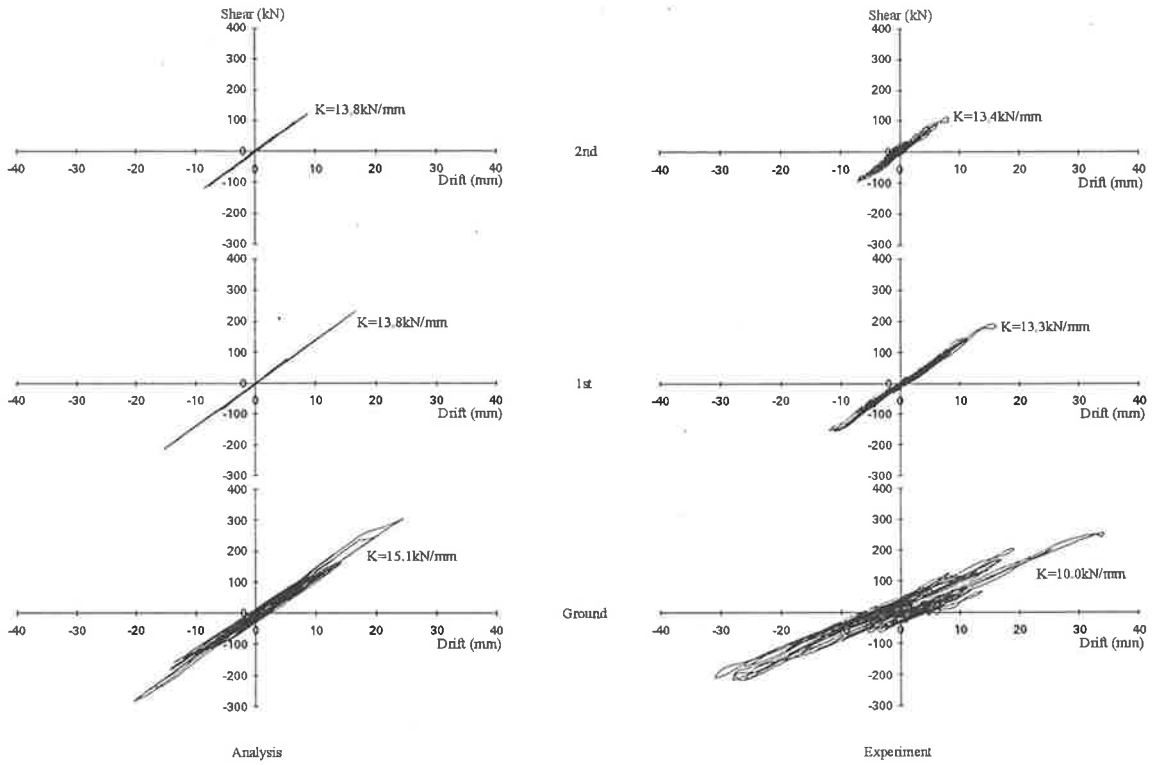

Figure 4.22 - Storey Hysteresis for EQ11

By comparing the displacements and shear values from both experimental testing and computer analysis, there again exists a slight difference which can be traced back to the overestimation of the stiffness at ground level as previously observed at lower magnitude earthquakes.

4.2.2 Adelaide Calibrated Model

A second full scale computer model of the three storey frame was developed using the properties (moment o inertia (I), cross-sectional area (A) and strength interaction characteristic of the member (N/M interaction values)) from the design values of the 1/5-scale structure tested at the University of Adelaide. Similar to the previous computer model, the structure was modelled in two dimensions only so that just half the mass of the slab and the orthogonal beams was lumped at the nodes. The Young's Modulus value was the only parameter to be adjusted so that the analytical period of the structure matched the experimentally obtained value. The computer model again consisted of 8 nodes and 9 members (refer to Figure 4.5). The contribution of the slab was taken into account in the calculation of the moment of inertia of the section. The model was loaded with the same three acceleration records used with the Melbourne calibrated model, namely, EQ05, EQ08 and EQ11 from the Adelaide shake table test series. The only difference in the two computer models - the "Adelaide" calibrated model and the "Melbourne" calibrated model, was that the "Adelaide" calibrated model was tuned to the Adelaide measured period (from experiment) using the Young's Modulus instead of the moment of inertia.

4.2.2.1 EQ05 (EPA=0.047g)

The "Adelaide" calibrated model was loaded with the acceleration record recorded during test EQ5 at Adelaide University. Figure 4.23 shows the time history storey displacement relative to the ground during the EQ05.

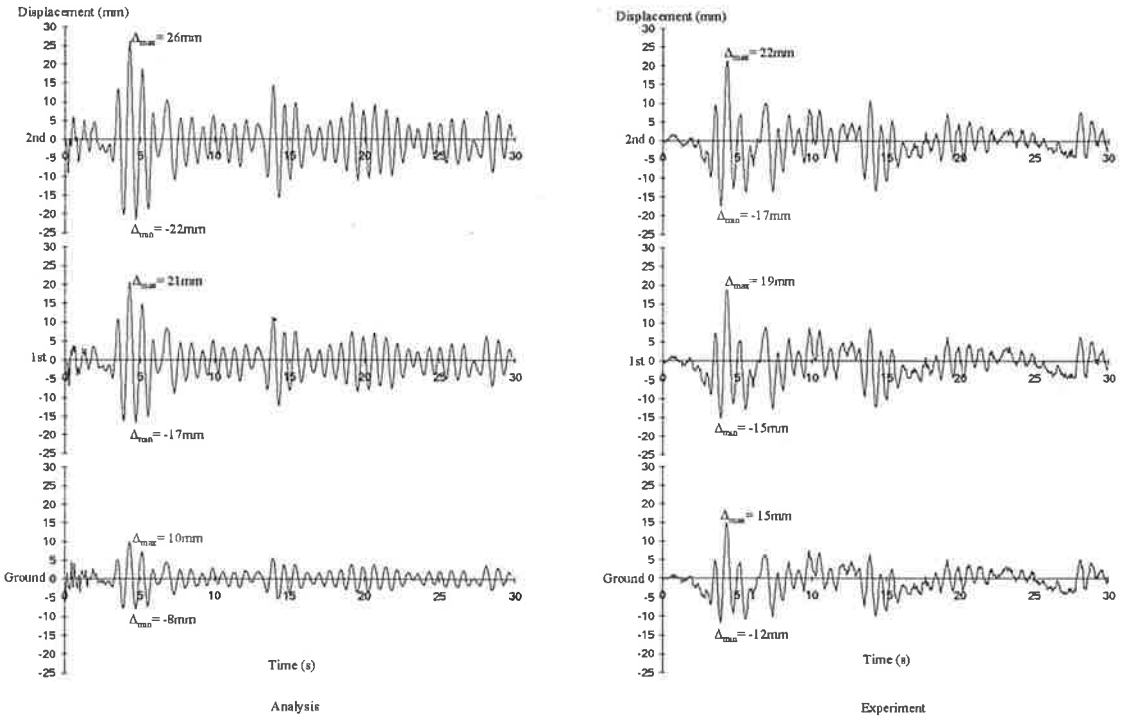

Figure 4.23 - Storey Displacement for EQ05

After comparing the maximum displacement profile of the computer model and the experimental results (Figure 4.24) it was found that the first storey displacement was under-estimated by the analysis as was the case for the Melbourne calibrated model. For the computer model, deformations were uniform for the ground and first storeys whereas the experimental results showed the majority of the deformation occurred at the first storey. The calculated maximum displacement at the top of the structure was greater than that observed in the experimental test. The most noticeable difference was that the computer model under-estimated the first storey drift when compared to the experimental results.

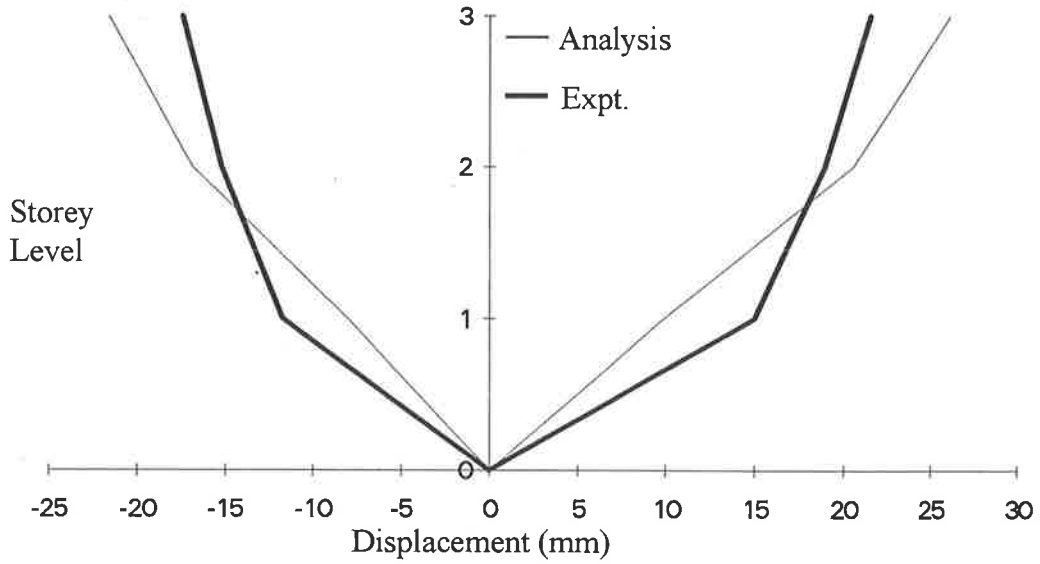

Figure 4.24 - Maximum Displacement Profile for EQ05

The storey shear forces are shown in Figure 4.25. The total base shear was 149kN and 126kN respectively in either direction compared to the experimental values of 137kN and 87kN which are 8% and 44% higher than the experimental results indicated. The analytical values were similar in magnitude to those from the analysis using the Melbourne calibrated model indicating that both computer models were over-estimating the shear experienced by the structure for this magnitude earthquake.

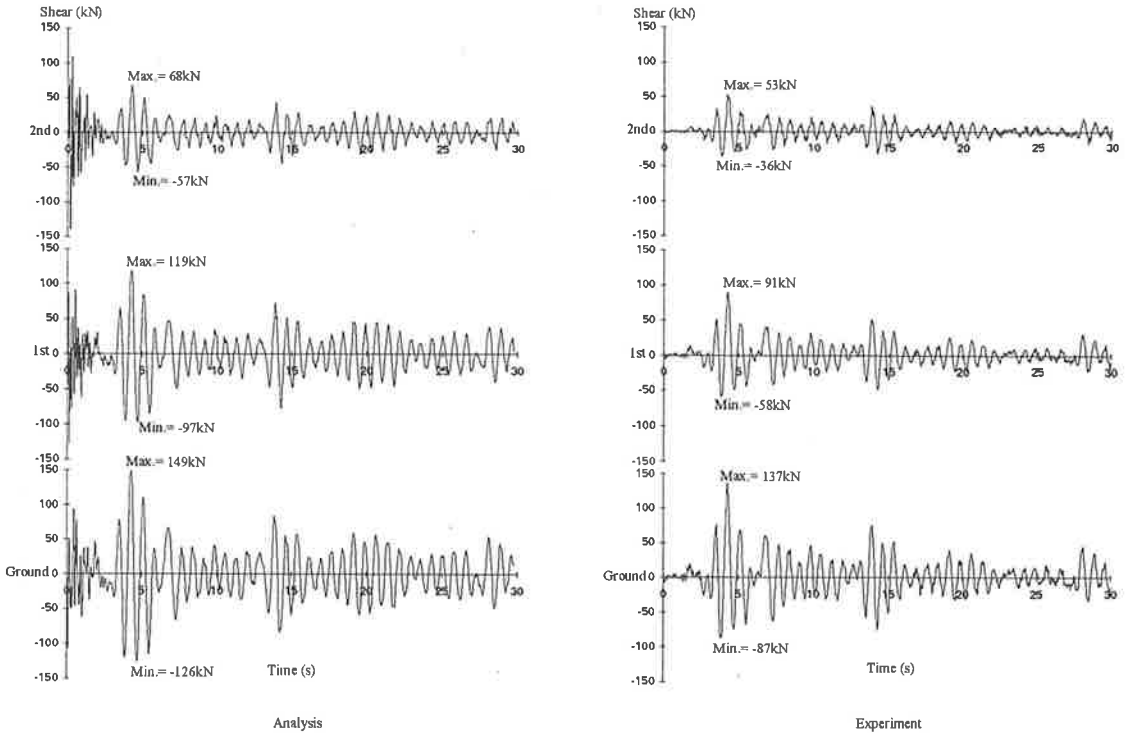

Figure 4.25 - Storey Shear Forces for EQ05

Figure 4.26 shows the normalised shear profile of the structure. The results from the analytical model indicated that both the computer models (Melbourne based and Adelaide based) gave very similar results.

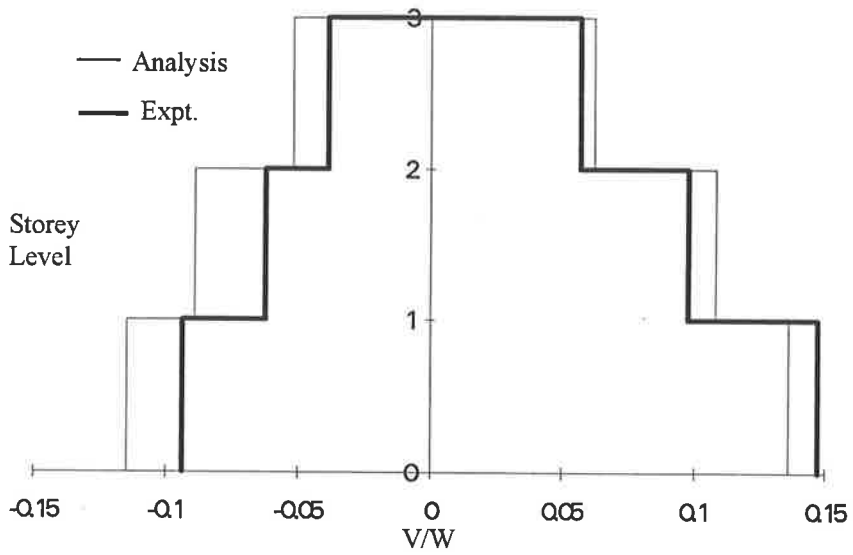

Figure 4.26 - Normalised Storey Shear Profile for EQ05

Figure 4.27 presents the storey hysteresis plots for the structure based on the Adelaide calibrated model analysis. The ground storey showed some indications of stiffness degradation (Figure 4.27). The second level also showed signs of degrading stiffness but the top storey was still behaving, for the most part, elastically. Noticeably more yielding was observed with this model than was noticed for the Melbourne calibrated model for the same magnitude earthquake. The storey stiffness from the shake table test were 9.0kN/mm, 17.5kN/mm and 16.7kN/mm from the ground storey to the second storey. The corresponding analytical values from the computer model were 15.2kN/mm, 11.2kN/mm and 15.0kN/mm.

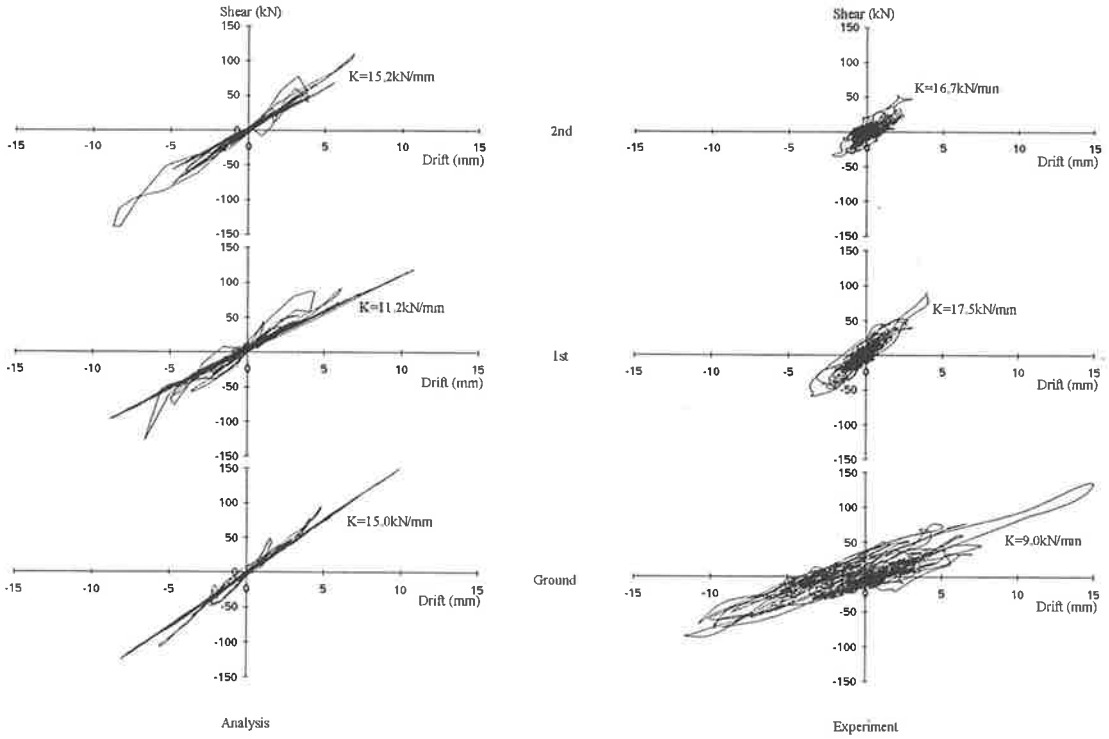

Figure 4.27 - Storey Hysteresis for EQ05

4.2.2.2 EQ08 (EPA=0.078g)

The second analysis with the Adelaide calibrated model was loaded with accelerations recorded during test EQ08. The effective peak acceleration of this earthquake was 0.078g.

Figure 4.28 shows the storey displacement time histories of the three levels.

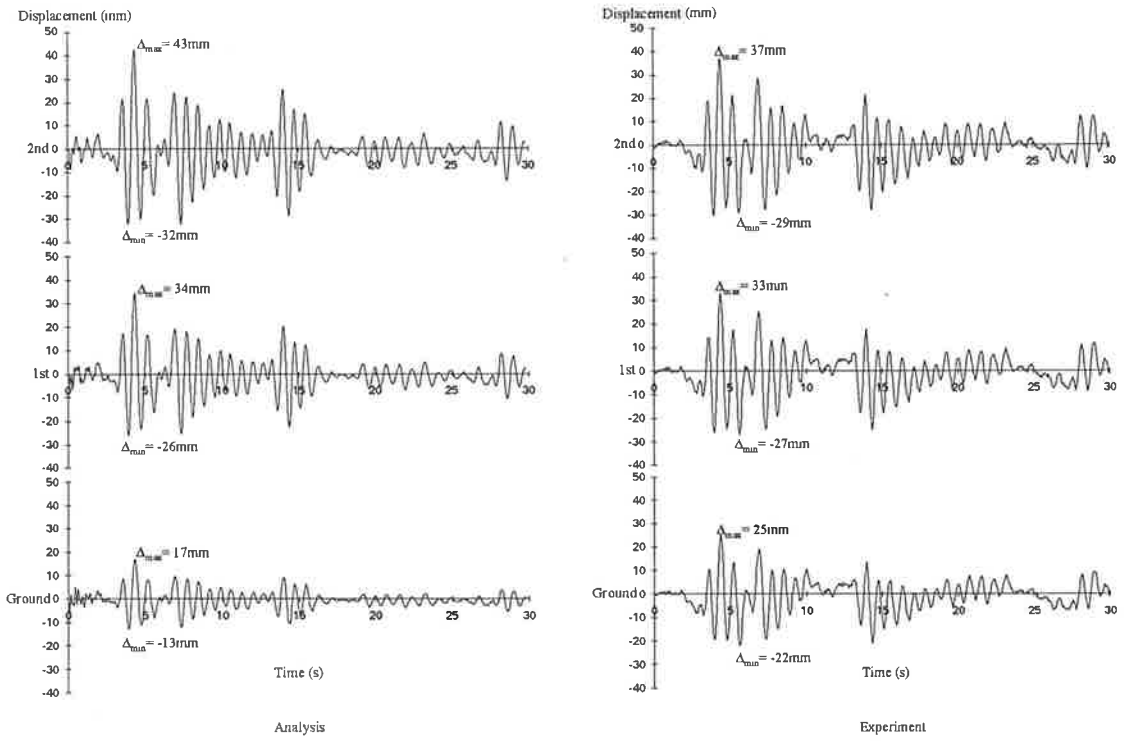

Figure 4.28 - Storey Displacement for EQ08

Figure 4.29 shows the maximum displacement profile of the structure. The computer model predicted that most of the deformation occurred in the ground and first storeys (similar to the Melbourne calibrated model) whereas the experimental results showed it occurred predominantly in the first level. The shape of the profile was similar to the one for EQ05. The first storey interstorey drift was under-estimated as was observed in EQ05. There existed an offset in the displacement time history plot which indicated non-linear inelastic response which lead to a permanent offset displacement.

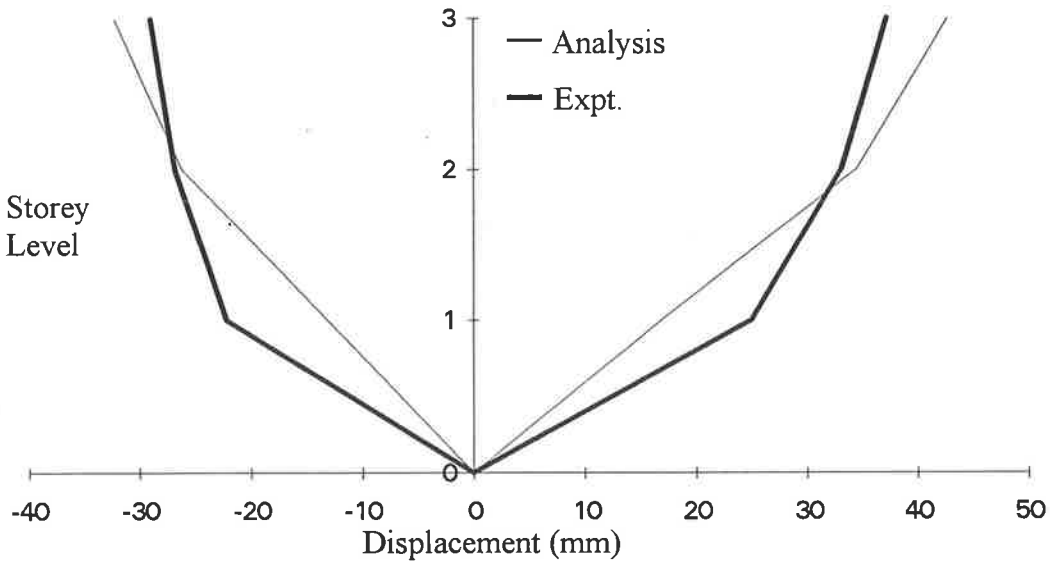

Figure 4.29 - Maximum Displacement Profile for EQ08

The storey shear forces are shown in Figure 4.30. The maximum base shear force recorded for this magnitude earthquake during the shake table test was 205kN and 148kN in each direction. For the same magnitude earthquake, the computer model predicted results of 243kN and 203kN. Both computer models (Melbourne calibrated and Adelaide calibrated) were found to over-estimate the total base shear forces with the Adelaide based model results lower than the Melbourne calibrated model results.

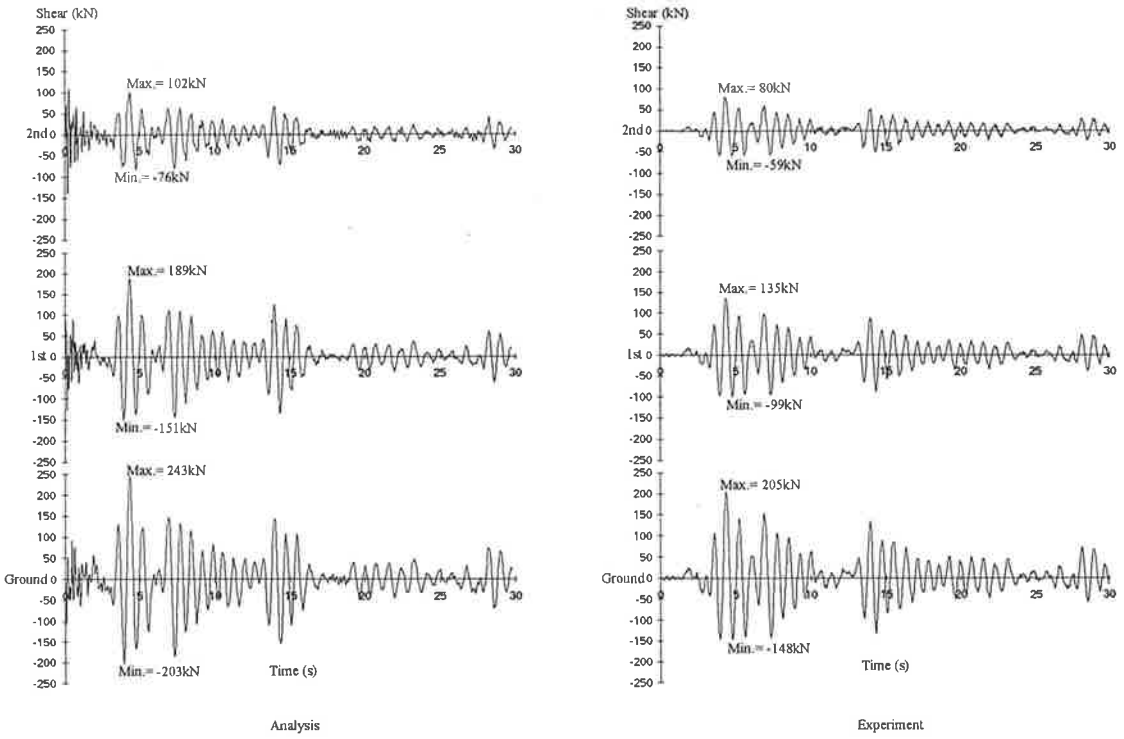

Figure 4.30 - Storey Shear Forces for EQ08

Figure 4.31 shows the comparison of the experimental and the analytical normalised storey shear profile of the structure. The computer model again had a distinct "uniform step" profile which was quite similar to the results obtained from the experimental shake table test.

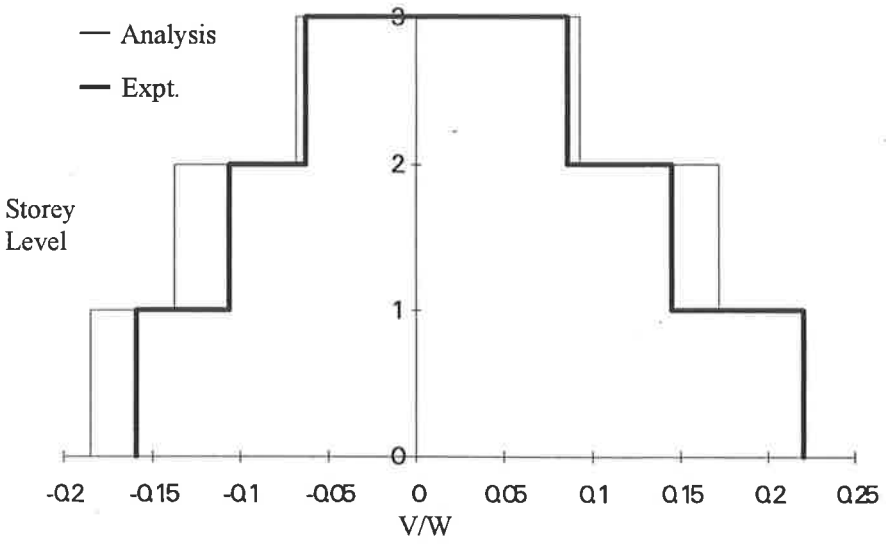

Figure 4.31 - Normalised Storey Shear Profile for EQ08

The storey hysteresis loops are shown in Figure 4.32. For the ground storey, more significant yielding occurred than observed in EQ05 for the same computer model. When compared to the Melbourne calibrated model (for the same magnitude earthquake), it was found that the Adelaide based model showed more non-linear/inelastic response than was observed with the Melbourne calibrated model which was still behaving essentially in an elastic manner for EQ08. The initial storey stiffness were 15.6kN/mm, 10.9kN/mm and 15.6kN/mm from level one to level three. The corresponding experimental results were 8.3kN/mm, 16.7kN/mm and 17.2kN/mm.

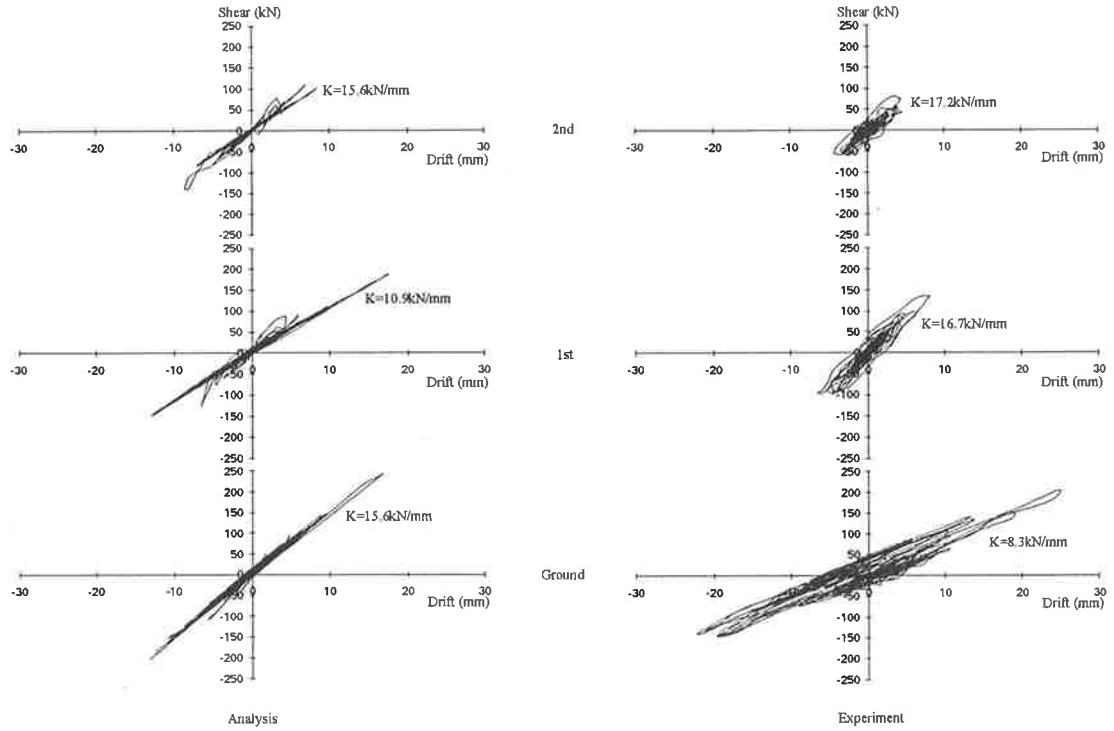

Figure 4.32 - Storey Hysteresis for EQ08

4.2.2.3 EQ11 (EPA=0.105g)

The final analysis of the Adelaide based model was loaded with accelerations recorded during the earthquake test series. This magnitude earthquake had an EPA of 0.105g which is approximately equal to the design magnitude earthquake for Adelaide and Newcastle.

The storey displacement time histories of each level are given in Figure 4.33.

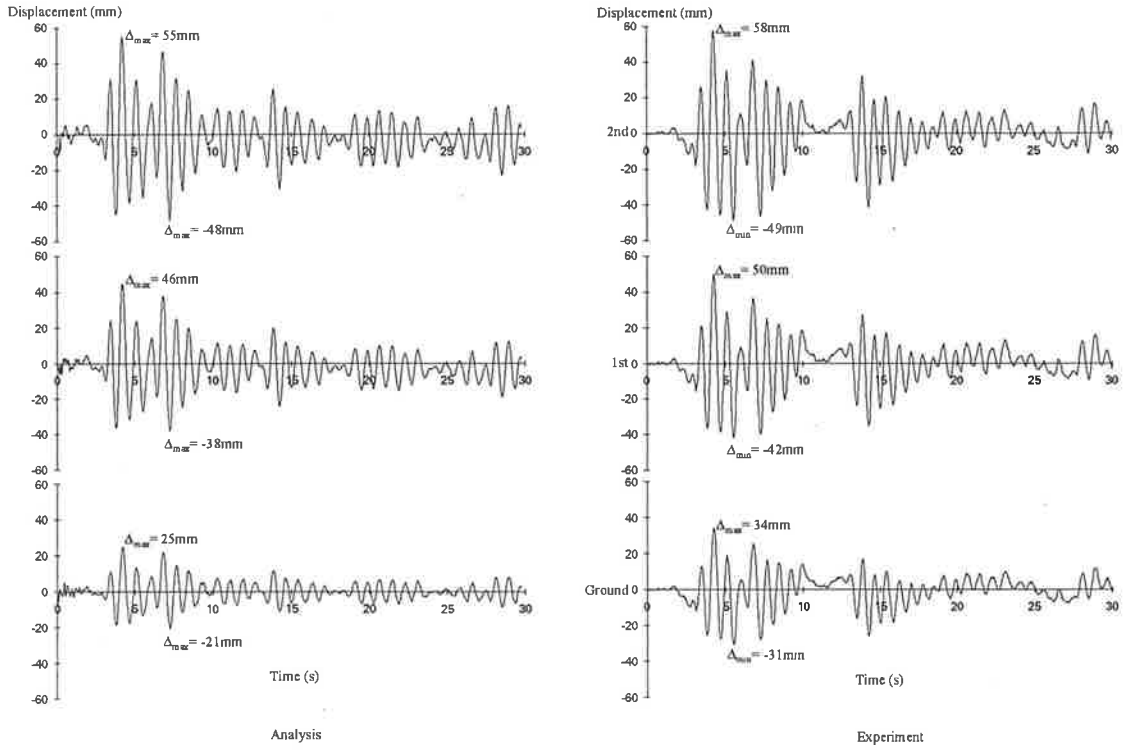

Figure 4.33 - Storey Displacement for EQ11

From the maximum displacement profile, it was found that the computer model under-estimated the displacements at each level when compared to experimental results. In one direction, the calculated maximum roof displacement was quite close to the observed value in the shake table test while in the opposite direction, there was a significant difference (Figure 4.34). As before, the first storey drift was under-estimated. Therefore

it showed that this characteristic of the model was independent of the earthquake magnitude.

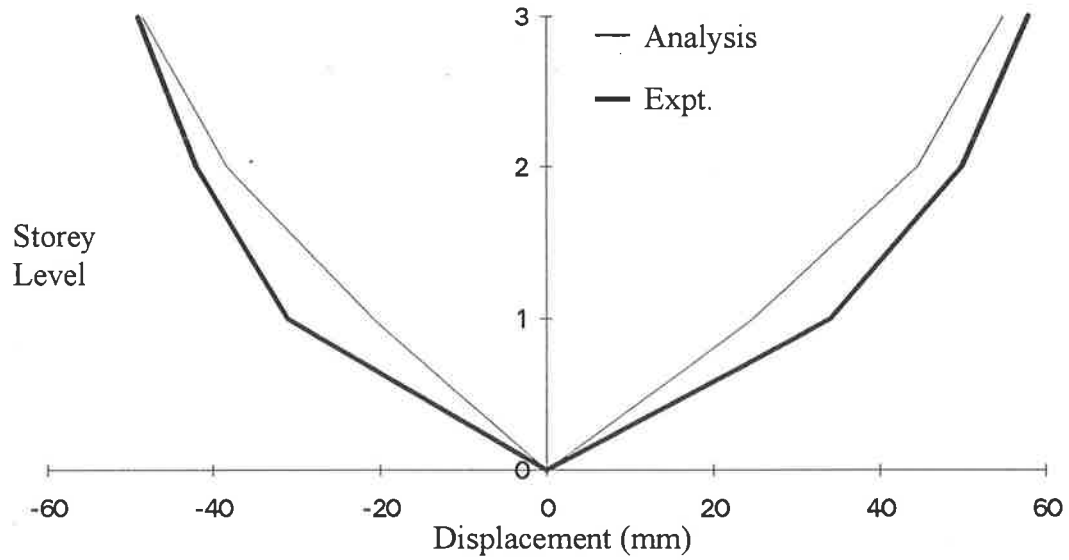

Figure 4.34 - Maximum Displacement Profile for EQ11

The maximum total base shear forces for the structure during EQ11 were 293kN and 265kN (Figure 4.35) in each direction according to the computer model. The measured base shear force during the shake table test was 255kN and 218kN respectively. Once again the computer model had over-estimated the maximum base shear forces when compared to experimental results. It was also noticed that the Adelaide based model was consistently less accurate (irrespective of the magnitude of the earthquake) in predicting the shear forces than the Melbourne calibrated model.

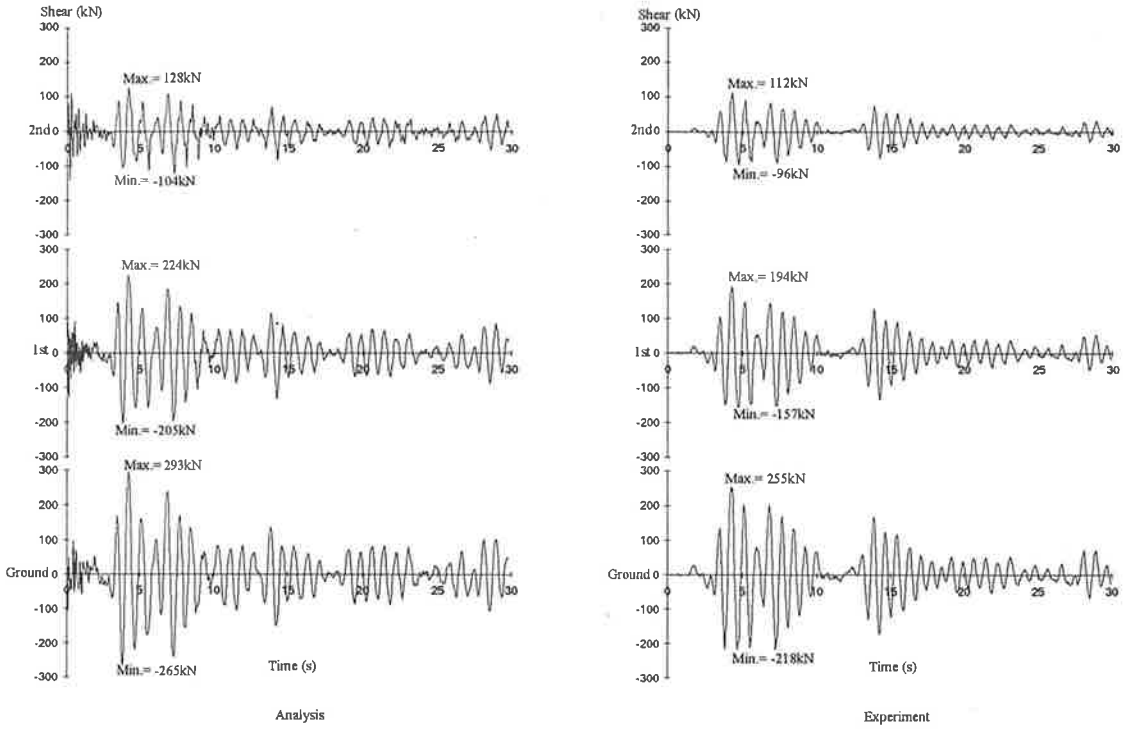

Figure 4.35 - Storey Shear Forces for EQ11

From the normalised shear profile of the structure, Figure 4.36, it can be seen that the shear profile from the computer model closely matched the experimental results unlike the results seen in the smaller magnitude earthquakes EQ05 or EQ08.

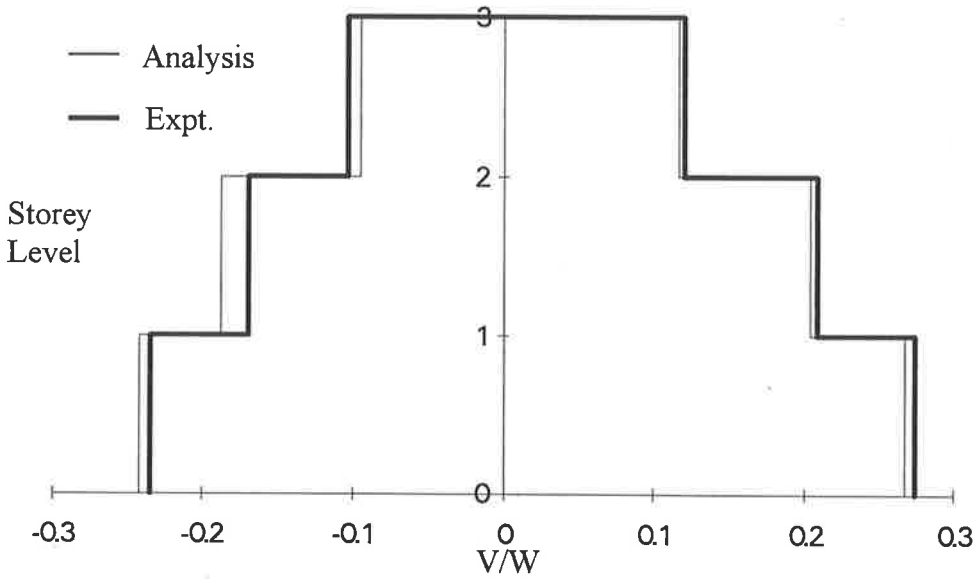

Figure 4.36 - Normalised Shear Profile for EQ11

As expected the storey hysteresis diagrams (Figure 4.37) showed that more yielding occurred at the first level than with the smaller magnitude earthquakes. The hysteresis loops for the upper two levels were much bigger than those seen in EQ05 and EQ08, indicating larger amounts of energy was being dissipated by the structure. The initial stiffness of each storey was as follows from bottom to top: 14.0kN/mm, 15.0kN/mm and 13.8kN/mm. This compared to the experimental results of 10.0kN/mm, 13.3kN/mm and 13.4kN/mm correspondingly.

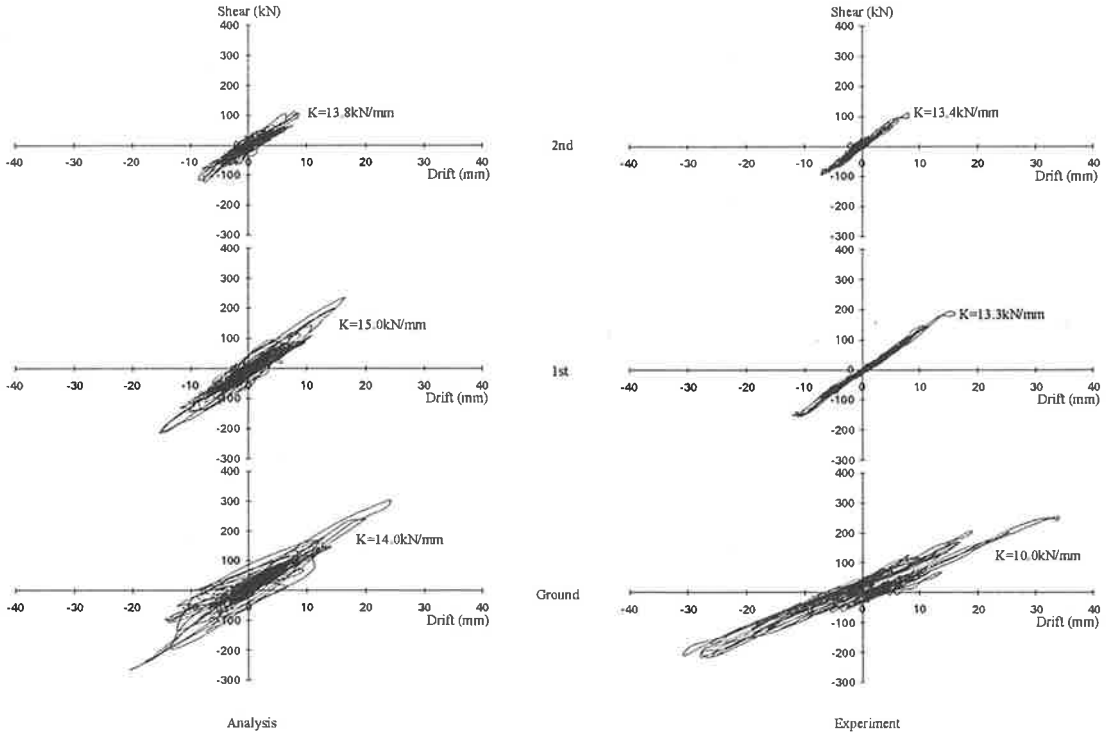

Figure 4.37 - Storey Hysteresis for EQ11

4.3 SUMMARY AND CONCLUSION

A series of dynamic analyses of a full scale three-storey reinforced concrete frame were performed using two different computer models. The first model was developed using a reinforced beam-column joint model calibrated against Melbourne University quasi-static joint test results. The second model was developed using full-scale equivalent properties of a 1/5-scale frame tested dynamically at the University of Adelaide. The analytical

results for both models were then compared to the experimental results from the 1/5-scale frame shake table tests.

Comparison of results showed that the Melbourne calibrated model gave good predictions of storey displacement (especially roof displacement) but the maximum displacement profile indicated that the model predicted uniform distribution of deformations over the ground and 1st storey with less at the 2nd storey while experimental results showed most deformations were concentrated in the ground storey. As the magnitude of earthquake loading was increased, the predicted storey displacements became less accurate when compared to the experiment results. However, the shape of the maximum displacement profile showed improvement when compared to the experimental results (especially EQ11 - Figure 4.19). Shear forces were consistently over-estimated irrespective of earthquake magnitude. Initial storey stiffnesses, obtained from the analytical storey hysteresis plots, were found to be fairly constant for all three storeys while results from the shake table tests showed that the bottom level was less stiff than the top two levels. No significant yielding of the structure was indicated by the analytical model until EQ11 (EPA=0.105g).

Results from the Adelaide calibrated model showed that the model over-estimated roof displacement for EQ05 and EQ08. When loaded with EQ11, the displacements were under-estimated (very similar to the Melbourne calibrated model). The maximum displacement profile (Figure 4.24, 4.29 and 4.34) showed that deformations were again uniformly distributed through the bottom two storeys (for all three magnitude earthquakes) while the experiments showed that the majority of deformations occurred in the ground storey. Shear forces were again over-estimated when compared to experimental results and it was more significant than for the Melbourne calibrated model. The initial storey stiffness was fairly constant for all three storeys whereas experimental results showed a much less stiff ground storey. Yielding was first noticed during EQ08 which was sooner than occurred with the Melbourne calibrated model.

It is observed that the experimental results showed a soft ground storey while both the computer models were not able to predict this analytically. This clearly identified a short

coming of the computer model. The computer model is trying to model non-linear behaviour of the concrete with a simple bi-linear arrangement. Therefore until yielding has occur, the stiffness calculated by the computer model is higher than that of the real non-linear behaviour. The calibration process in Chapter 3 concentrated on the initial stiffness and the level at which yielding occur and not on storey drift. Hence, the ground storey drift predicted by the computer model was less than that observed during the experimental testing. Using a storey stiffness versus storey drift relationship such as shown in Figure 4.38, it can be seen why the stiffness predicted by the computer model was higher than that of the actual behaviour. It can be concluded that there is a limitation to the computer model using section yield interaction curves and a hysteresis model to reflect non-linear behaviour of concrete section at levels of stress less than yield stress.

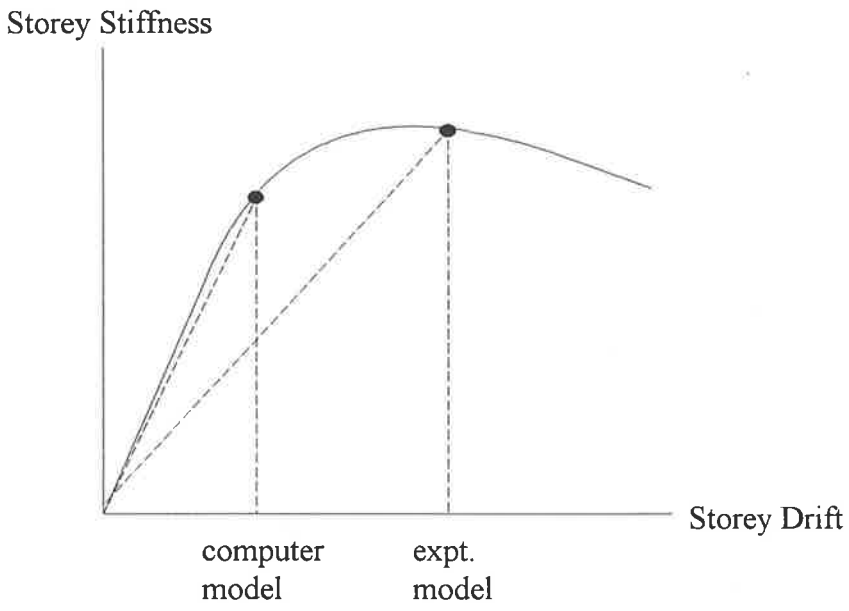

Figure 4.38 - Storey Drift versus Storey Stiffness for Reinforced Concrete Members

After reviewing both sets of analytical results and comparing them with the corresponding experimental observations, it appeared that the stiffness (especially at ground storey) was overestimated by the computer model and conclusion was made that the overall performance of the Melbourne calibrated model gave closer correlation of results to what was observed in experimental tests. Therefore it was this computer model

(Melbourne calibrated) which was used to simulate the behaviour of a prototype building in the next chapter.

CHAPTER 5
PROTOTYPE BUILDING

5.1 INTRODUCTION

In this chapter, the calibrated computer joint model from Chapter 3 (using the Melbourne University 1/2-scale joint testing data) was used to simulate the behaviour of a more realistic prototype building during an earthquake. This model was chosen because it proved to be more accurate when compared to experimental results (refer to Chapter 4) and to avoid any scaling effects of small scale modelling. A multiple bay multi-storey prototype building was chosen to examine the behaviour of the beam and columns at both exterior and interior joints of the external and internal frames of the structure. Due to the limitations of two-dimensional analysis, a computer model was set up to represent an internal frame of the prototype building.

The internal frame of the prototype building was analysed with three different magnitude earthquakes which had effective peak accelerations corresponding to 0.047g, 0.078g and

0.105g. Finally, the frame was loaded with scaled up versions of the 0.105g earthquake until failure was imminent. The results from the analysis are discussed in the following sections where critical members are identified to study the behaviour of the structure under collapse load conditions.

5.2 PROTOTYPE BUILDING

A multi-bay multi-storey reinforced concrete frame structure was used as the prototype building for the computer analysis. By using a multi-bay multi-storey building, the effects of adjacent bays were examined to quantify the effects of redundancy on the structural system during earthquake loading.

Figure 5.1 shows the configuration and geometry of the prototype building. It had three storeys and four bays in the direction of the loading and three bays in the orthogonal direction to loading.

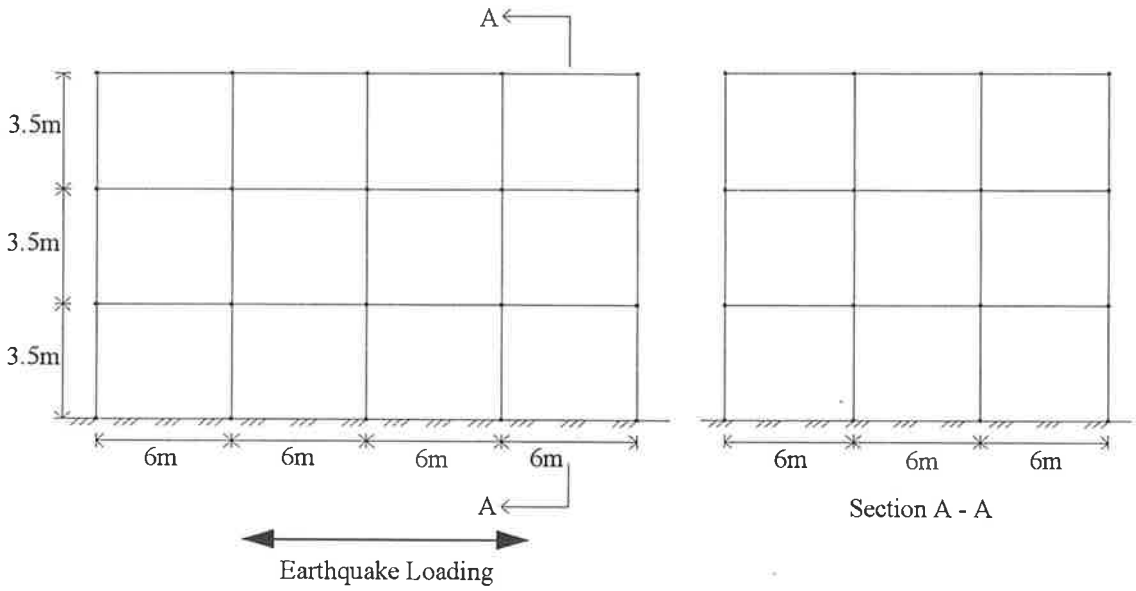

Figure 5.1 - Elevations of Prototype Building

The member sizes and cross sectional properties were the same as the full scale members for the single bay portal frame used in Chapter 4. As the computer analysis was restricted

to two dimensions, two types of frame existed. Figure 5.2 shows the plan view of the building and the two frame types that were present. They were an internal frame and an external frame. The two frames had different column loads due to the different contributing areas from the floor slab. Only the internal frame was investigated. Torsional effects on the frame were ignored since the analyses were conducted in two dimensions. Contributions of the floor slab towards the beam stiffness was accounted for by adding the effective width (in accordance with AS3600 [2]) from the slab on to the cross section of the beams.

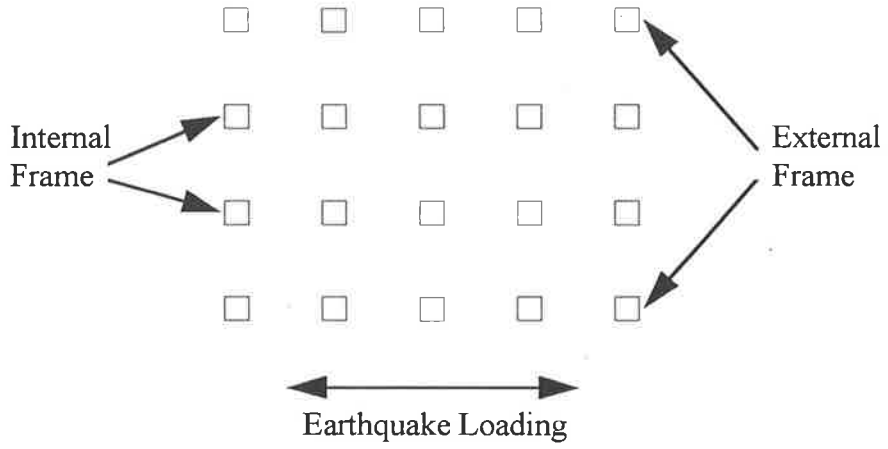

Figure 5.2 - Plan View of the Columns Layout of the Building

The computer model of the internal frame was defined using the properties from the Melbourne calibrated model. The model configurations are shown in Figure 5.3. It contained 20 nodes and 27 members. There were three different member properties: one for columns, one for the beams in external bays and one for the beams in internal bays.

The 1940 El-Centro earthquake acceleration record [77] was used to dynamically load the building frame for a set of three analyses having effective peak ground accelerations of 0.047g, 0.078g and 0.105g.

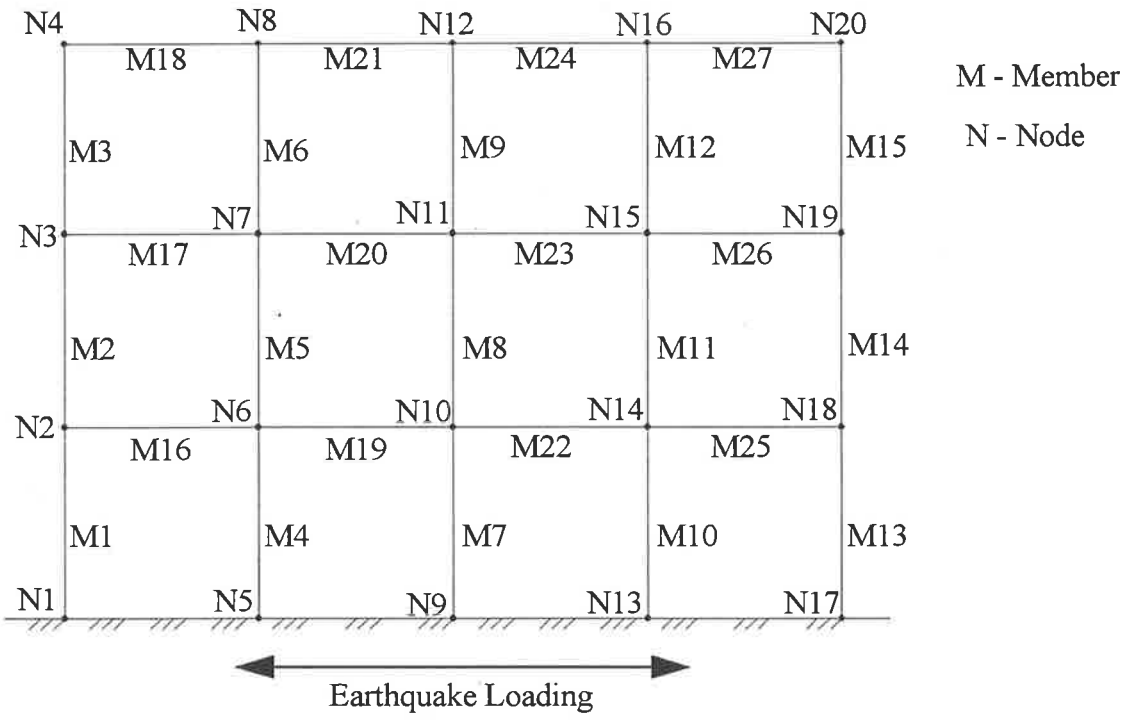

Figure 5.3 - Schematic Diagram of Computer Model of Prototype Building

5.3 INTERNAL FRAME

The internal frame (Figure 5.2) of the prototype building was subjected to three earthquake loadings with increasing magnitudes. The dead loads carried by the internal frame were larger than those of the external frame due to the presence of a floor slab on both sides of the frame. The load from the floor slabs was distributed back to the beam members. The period of the internal frame was 1.042 seconds. The stiffness of the internal frame beam was also different from that of the external frame because of the slab contribution on both sides. Two regions of the frames were examined in detail: the exterior columns with members M1 to M3 and the interior columns with members M7 to M9 (refer to Figure 5.3).

5.3.1 Earthquake Test 5 (EPA=0.047g)

The internal frame was firstly loaded with the earthquake signal recorded during the shake table test 5 (EQ5) at The University of Adelaide which had an effective peak acceleration of 0.047g. Figure 5.4 shows the displacement of each level of the internal frame during EQ5. The maximum displacements reached were 42mm and 48mm (2nd floor, Figure 5.4).

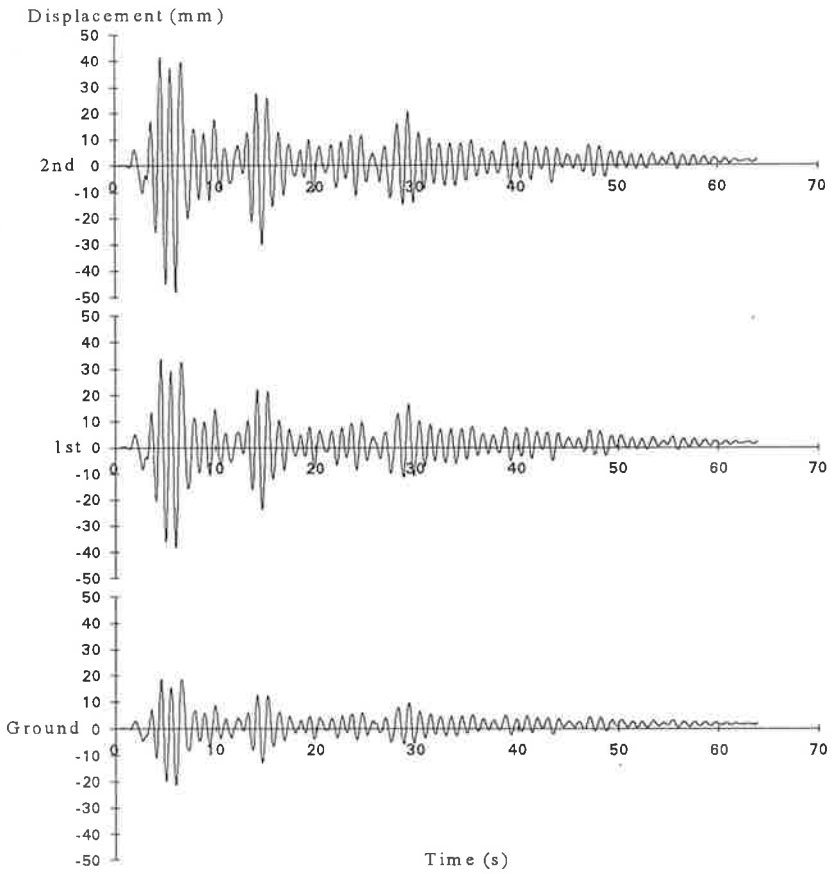

Figure 5.4 - Storey Displacement for EQ5

The maximum displacement profile for the frame is shown in Figure 5.5. The deformations were distributed evenly through the ground and 1st storey giving a linear profile for the two storeys. This suggests that the structure exhibited an essentially elastic response.

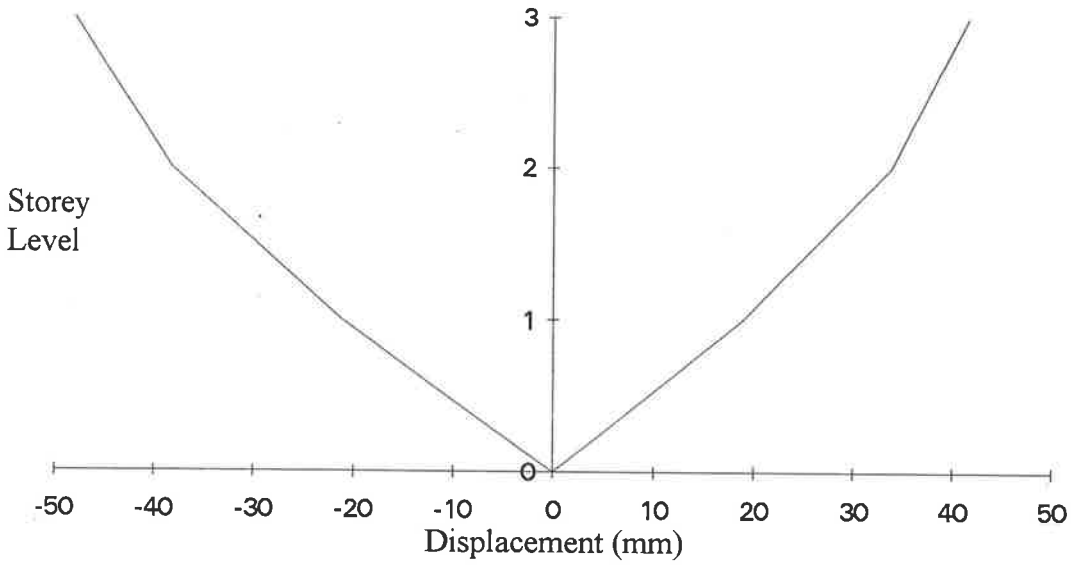

Figure 5.5 - Maximum Displacement Profile for EQ5

Exterior Columns: Figure 5.6 shows the shear forces experienced by the exterior columns (members M1 to M3) at each level with the maximum base shear forces equal to 70kN and 79kN respectively in each direction.

Figure 5.7 shows the maximum shear profile of the exterior columns (members M1 to M3). The profile was symmetrical with uniform increments indicating that the inertia forces were evenly distributed throughout the levels.

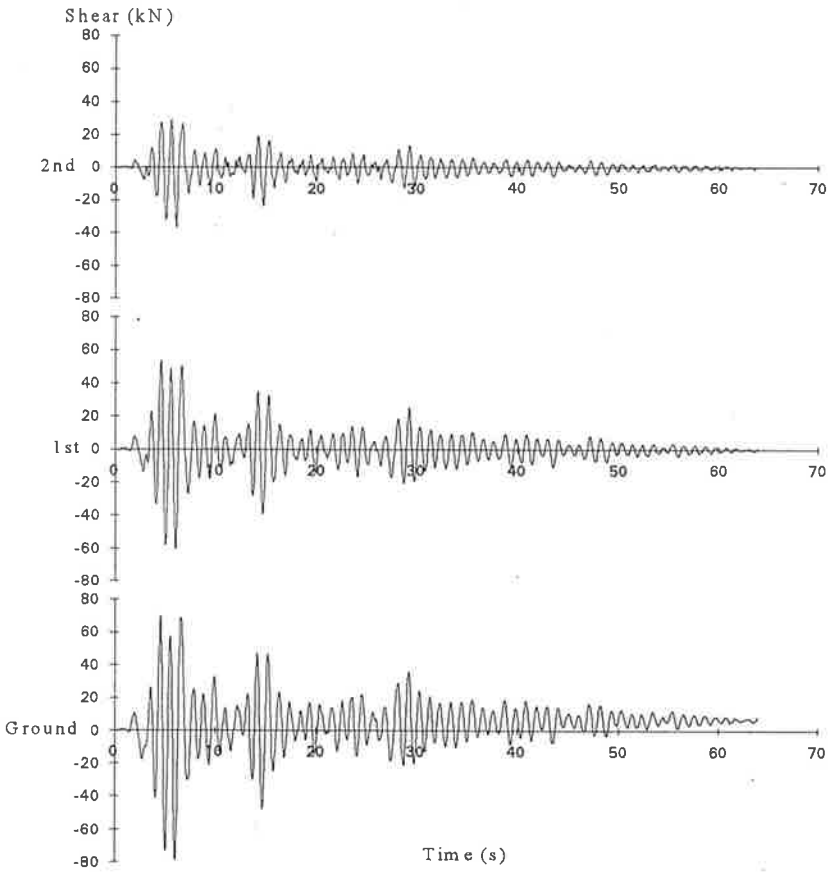

Figure 5.6 - Storey Shear Forces for Exterior Columns for EQ5

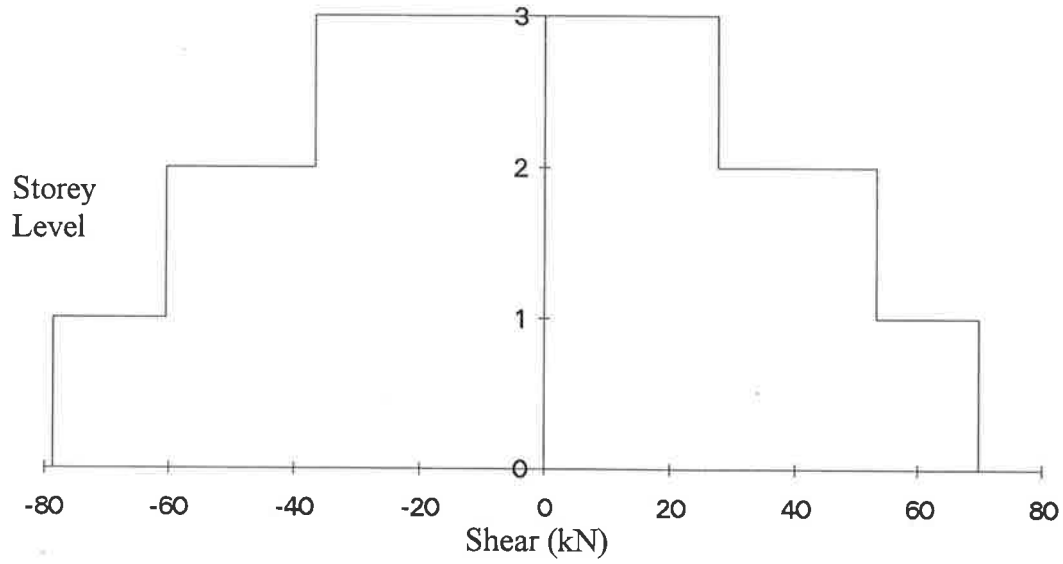

Figure 5.7 - Maximum Shear Profile of Exterior Columns for EQ5

The hysteretic behaviour of the exterior columns (Figure 5.8) showed no indication of yielding. Instead, it showed that the columns at each exterior joint at each level behaved in an elastic manner.

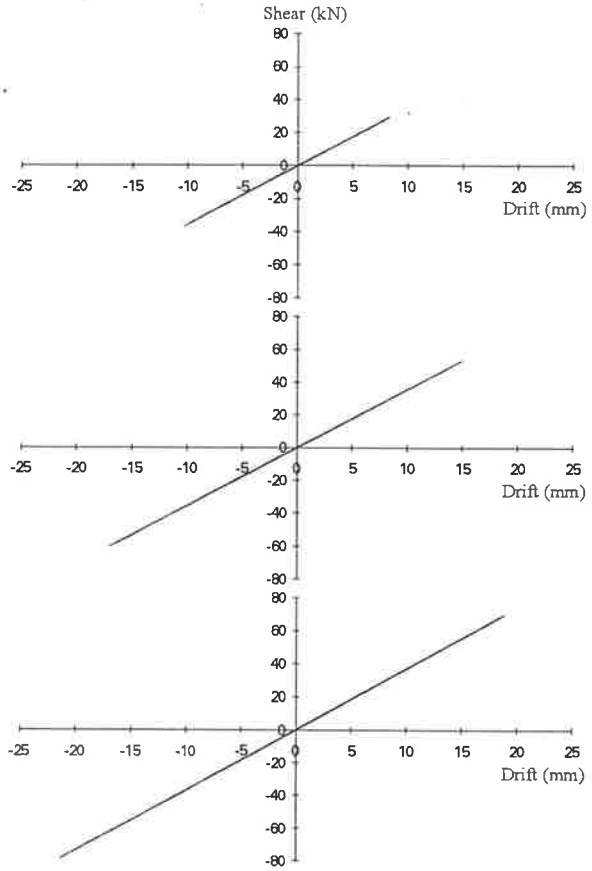

Figure 5.8 - Shear Force Hysteresis for Exterior Columns for EQ5

Interior Columns: As can be seen in Figure 5.9 the maximum base shear forces for the interior column (member M7) were 71kN and 80kN. These were a little higher than the maximum base shear forces for the exterior column (member M1). For the interior columns the maximum shear profile (Figure 5.10) was similar to the one for the exterior columns: symmetrical shape and uniform "step" size in both directions.

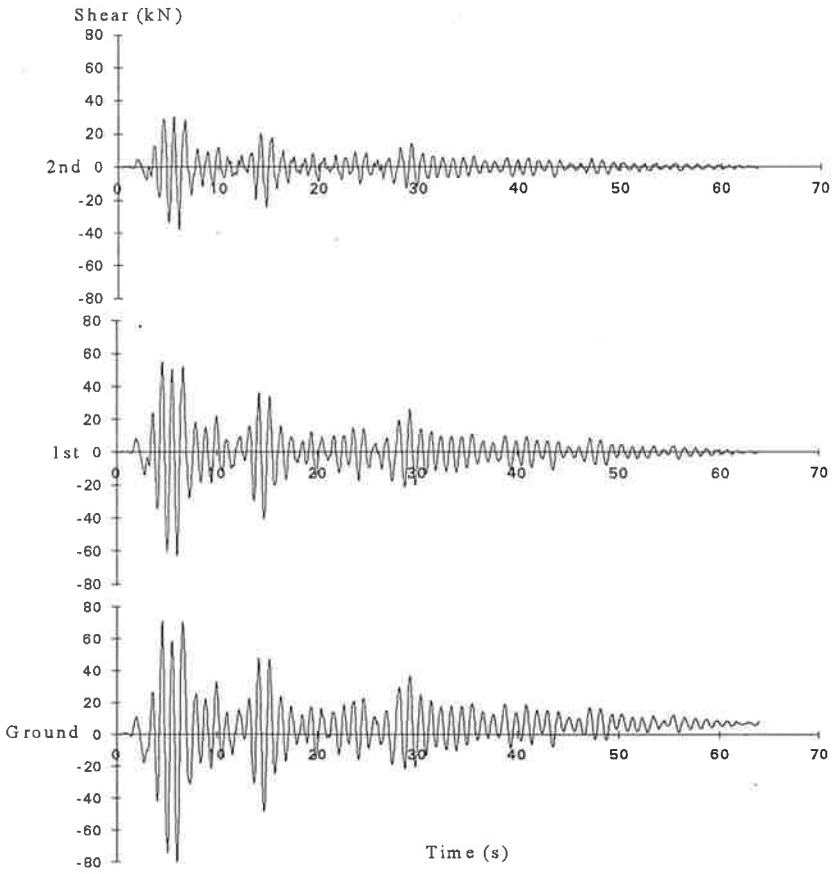

Figure 5.9 - Storey Shear Forces for Interior Columns for EQ5

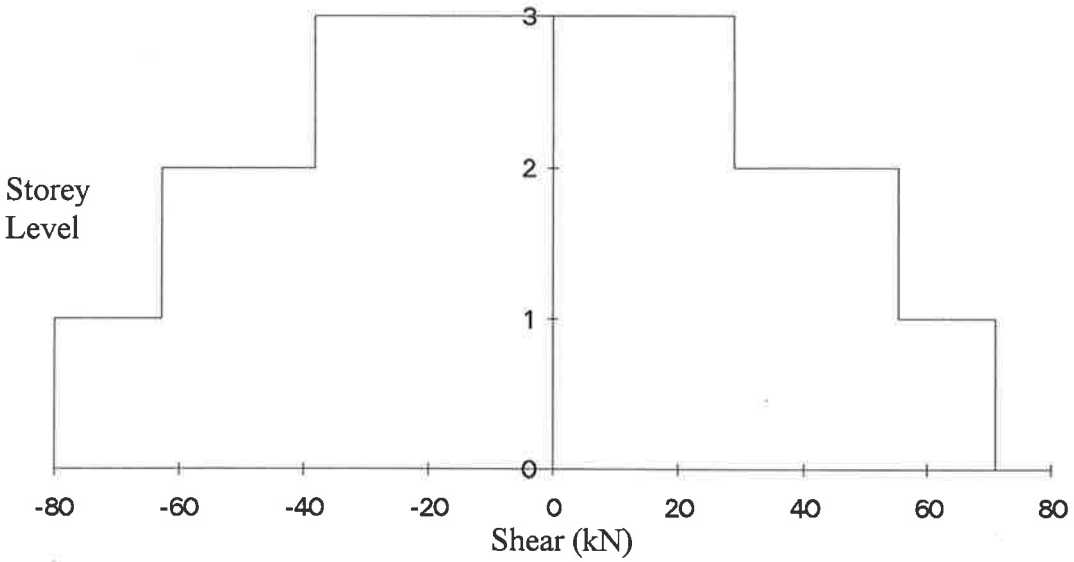

Figure 5.10 - Maximum Shear Profile of Interior Columns for EQ5

Similarly, no yielding or stiffness degradation of the interior columns was observed after being loaded with EQ5 (Figure 5.11). The columns were still within the elastic range of behaviour for this level of loading.

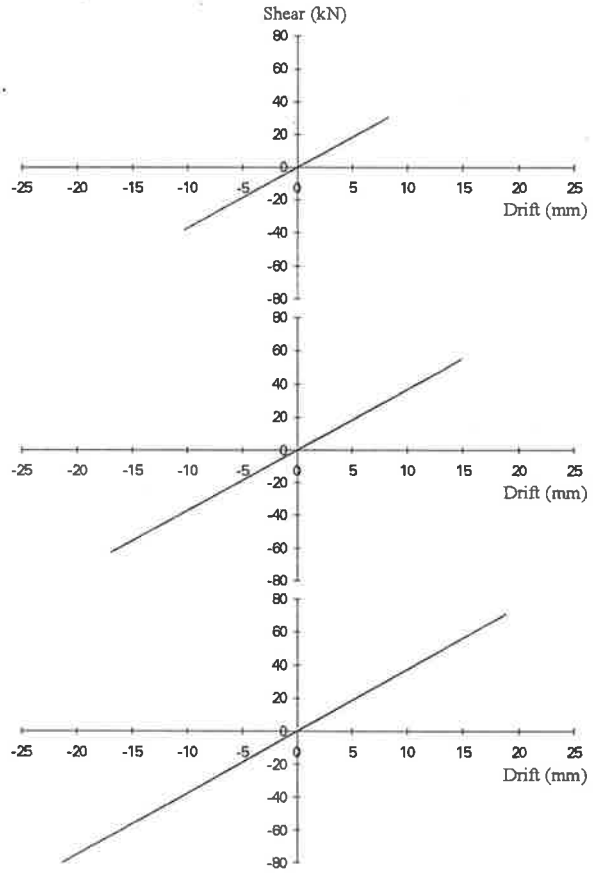

Figure 5.11 - Shear Force Hysteresis for Interior Columns for EQ5

5.3.2 Earthquake Test 8 (EPA=0.078g)

The second analysis involved loading the internal frame of the prototype building with the acceleration time history recorded during earthquake test 8 described in Chapter 4. It had an effective peak acceleration of 0.078g.

Figure 5.12 shows the storey displacements for the internal frame during EQ8. The maximum roof displacements were 70mm and 61mm.

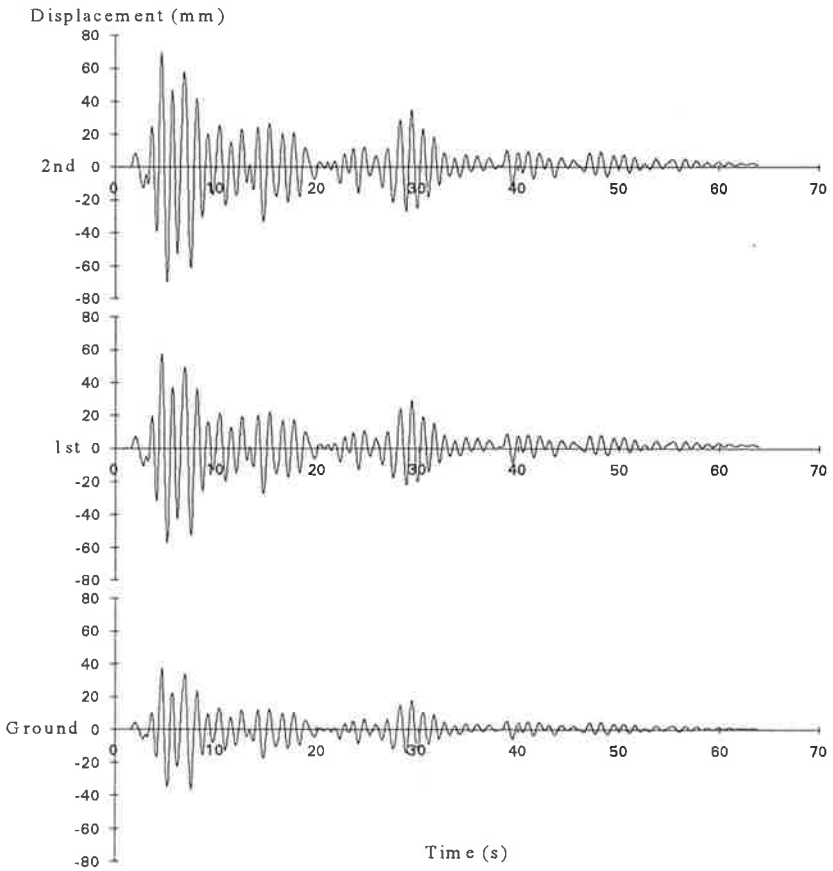

Figure 5.12 - Storey Displacement for EQ8

Upon examining the maximum displacement profile (Figure 5.13), a larger displacement for the ground storey gave a more non-linear profile than was seen in the one loaded with EQ5 (Figure 5.5).

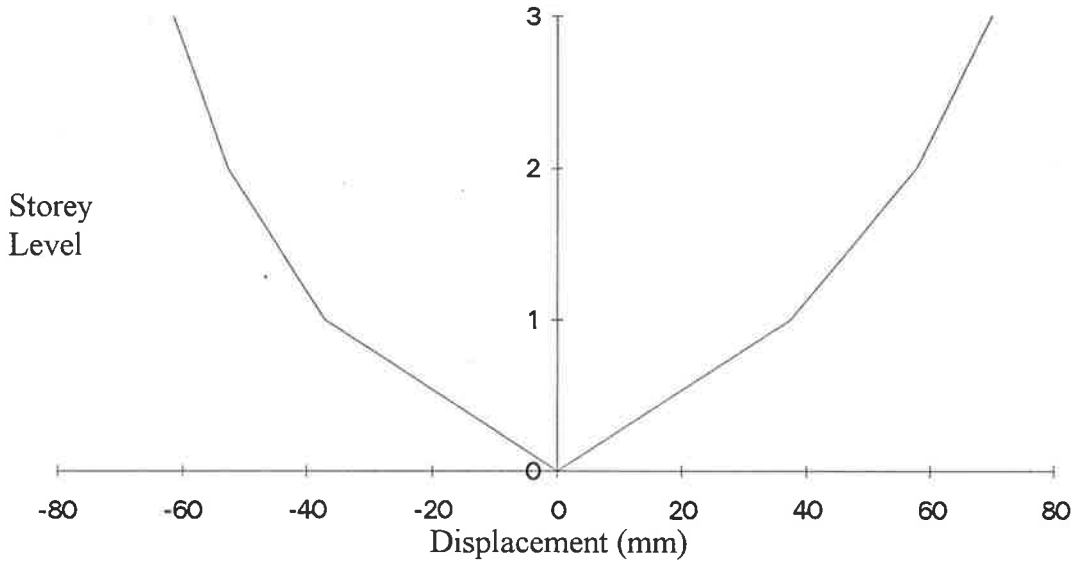

Figure 5.13 - Maximum Displacement Profile for EQ8

Exterior Columns: The maximum base shear forces calculated for the exterior columns were 79kN and 102kN (Figure 5.14). A residual shear force in the columns at ground storey existed after the earthquake loading had ended. This was probably due to the fact that it was an exterior joint with only one beam member. This situation indicated that shear was greater in one direction than in the other. This was caused by opening and closing of the cracks along the face of the joint which had no beam member adjoined to it to help confinement of the concrete (see ref. [23, 40]). A check for static equilibrium of the structure at the end of the earthquake loading was later performed. This proved that the existence of a residual shear force in a single member did not violate the principal of static equilibrium for the structure (i.e. the residual shear forces in the interior columns balanced that in the exterior columns). As a result of this inelastic behaviour the maximum shear profile for the exterior columns (Figure 5.15) was found to be unsymmetrical.

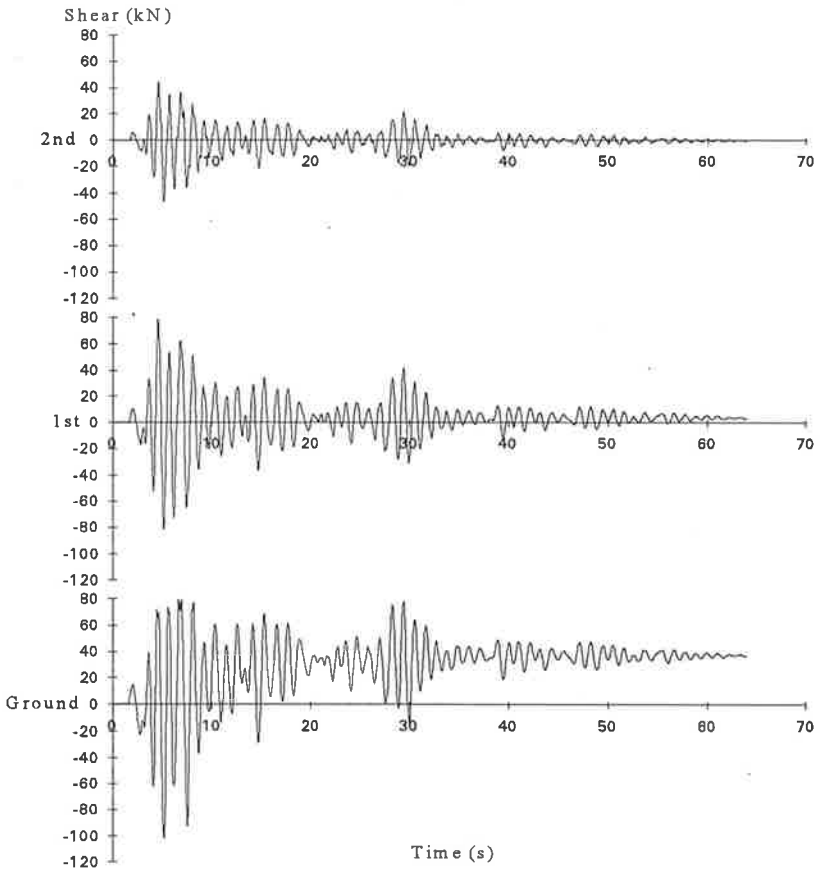

Figure 5.14 - Shear Forces for Exterior Columns for EQ8

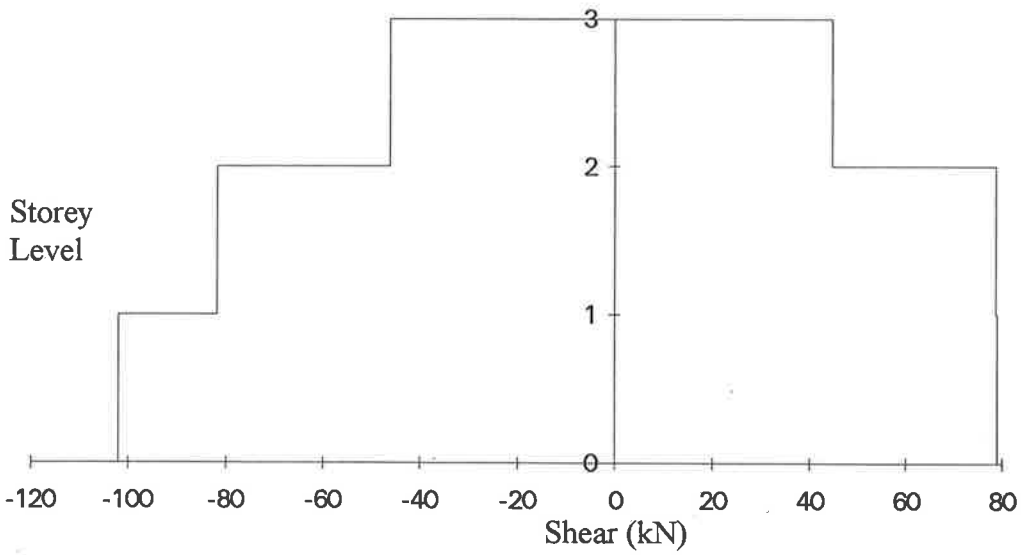

Figure 5.15 - Maximum Shear Profile of Exterior Columns for EQ8

Figure 5.16 shows the exterior column hysteresis behaviour during EQ8. It can be seen that a significant amount of yielding occurred in one direction in the ground storey column. Upon examining member M13 (corresponding member to M1 on the right side of the frame) the column hysteresis showed again inelastic response in only one direction. For member M13 the yielding was in the opposite direction to member M1. The columns on the upper two storeys behaved elastically. Stiffness degradation of the ground storey joint was also observed. It degraded approximately 30% (from 3.8kN/mm to 2.6kN/mm).

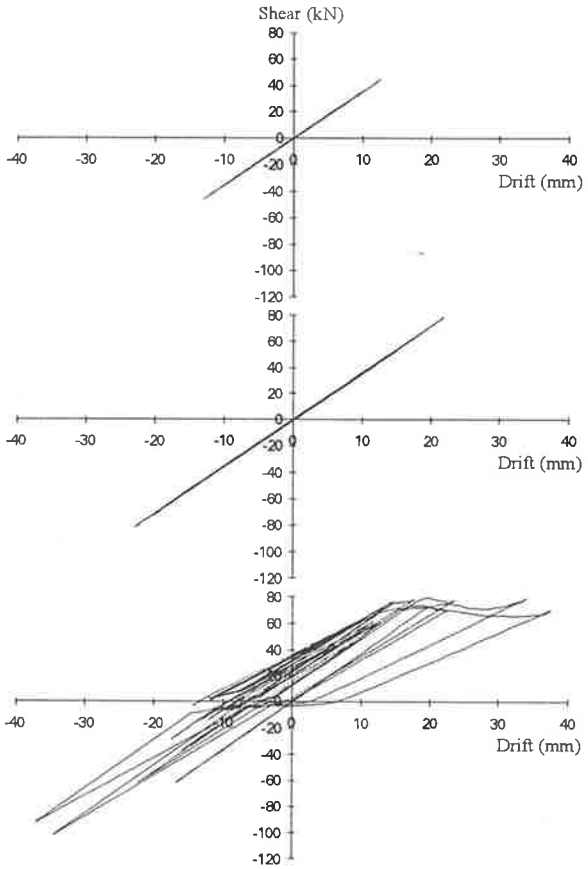

Figure 5.16 - Shear Force Hysteresis for Exterior Columns for EQ8

Interior Columns: Figure 5.17 shows the shear forces for the interior columns during EQ8. The maximum base shear for the interior column (member M7) was 113kN and 106kN in each direction compared to 79kN and 102kN for the exterior column. When compared to the exterior joint forces, here they were larger due to the extra mass being carried by the internal columns.

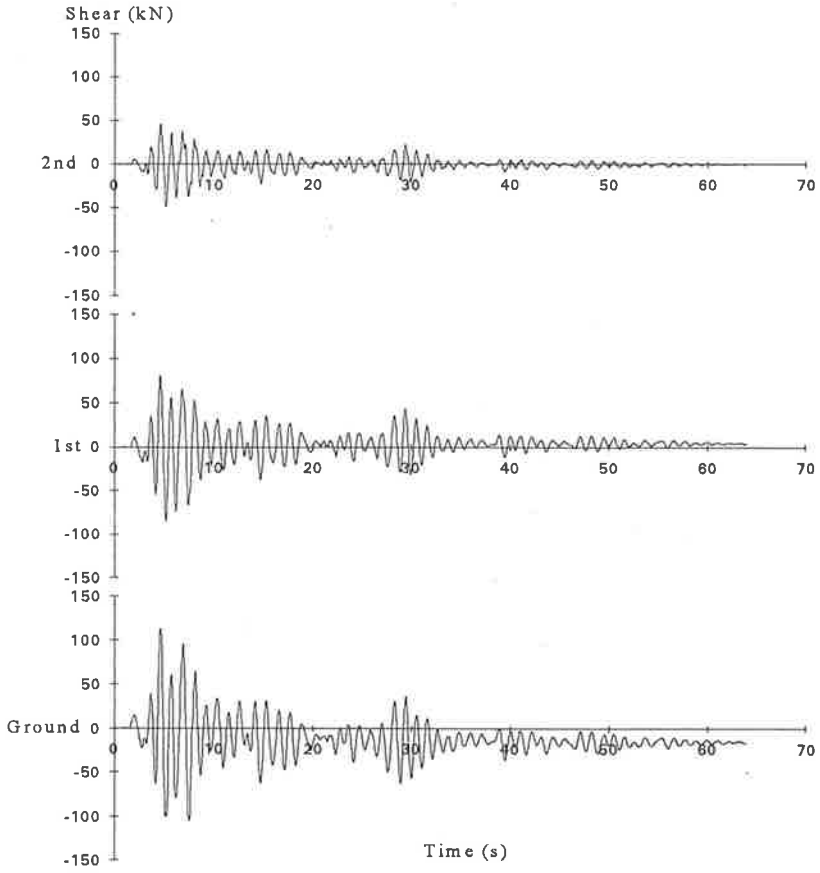

Figure 5.17 - Storey Shear Forces for Interior Columns for EQ8

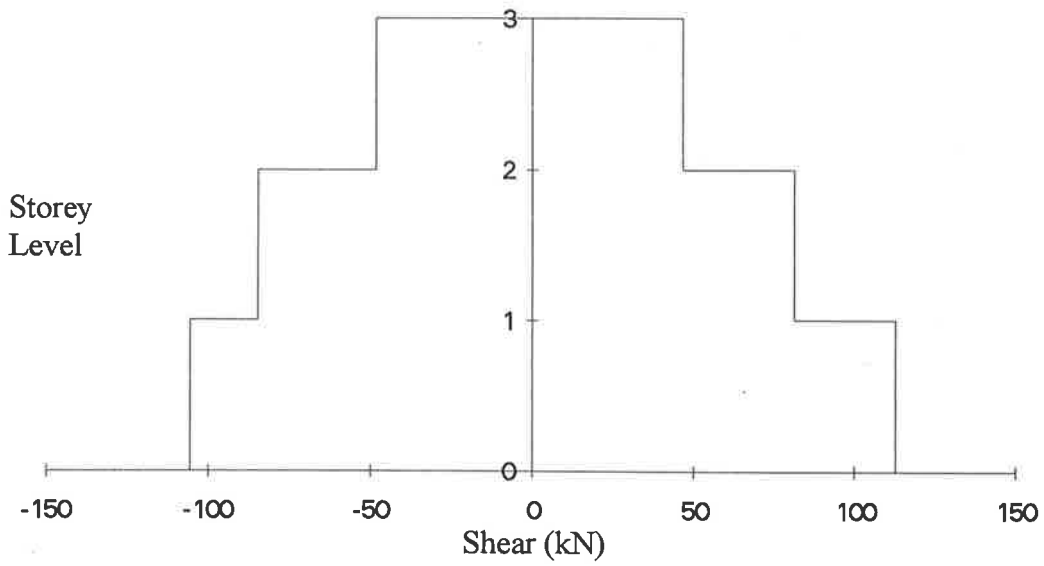

Figure 5.18 - Maximum Shear Profile of Interior Columns for EQ8

When compared to the maximum shear profile of the exterior columns (Figure 5.15), the interior columns profile (Figure 5.18) was much more symmetrical and with uniform increments on both sides, due mainly to the presence of beam members on both sides of the column faces in the direction of loading.

From Figure 5.19, it could be seen that some yielding occurred in the ground storey of the interior column. However, unlike the exterior columns, here yielding occurred in both directions of loading and in a fairly even manner. A slight stiffness degradation was also observed. The extent of the degradation was similar to that recorded for the corresponding exterior column (i.e. from 3.8kN/mm to 2.6kN/mm). The interior columns on the upper levels remained undamaged and behaved elastically through the earthquake as seen with the exterior columns on the corresponding storeys.

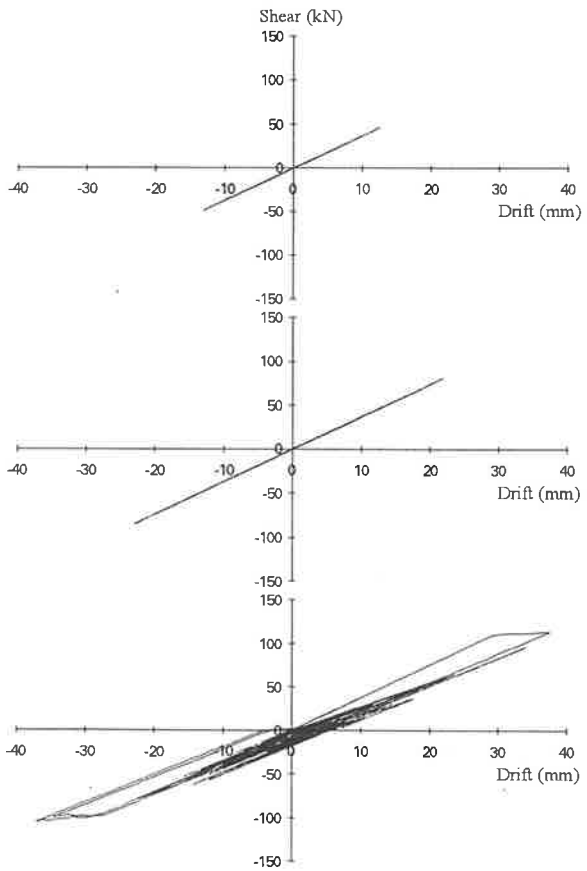

Figure 5.19 - Shear Force Hysteresis for Interior Columns for EQ8

5.3.3 Earthquake Test 10 (EPA=0.105g)

This was the largest magnitude earthquake tested on the prototype structure prior to failure and with an effective peak acceleration of 0.105g, this corresponded to the design magnitude earthquake for cities such as Adelaide and Newcastle (AS 1170.4 [1]).

The maximum roof displacements (Figure 5.20) of the frame were 89mm and 86mm in either direction respectively.

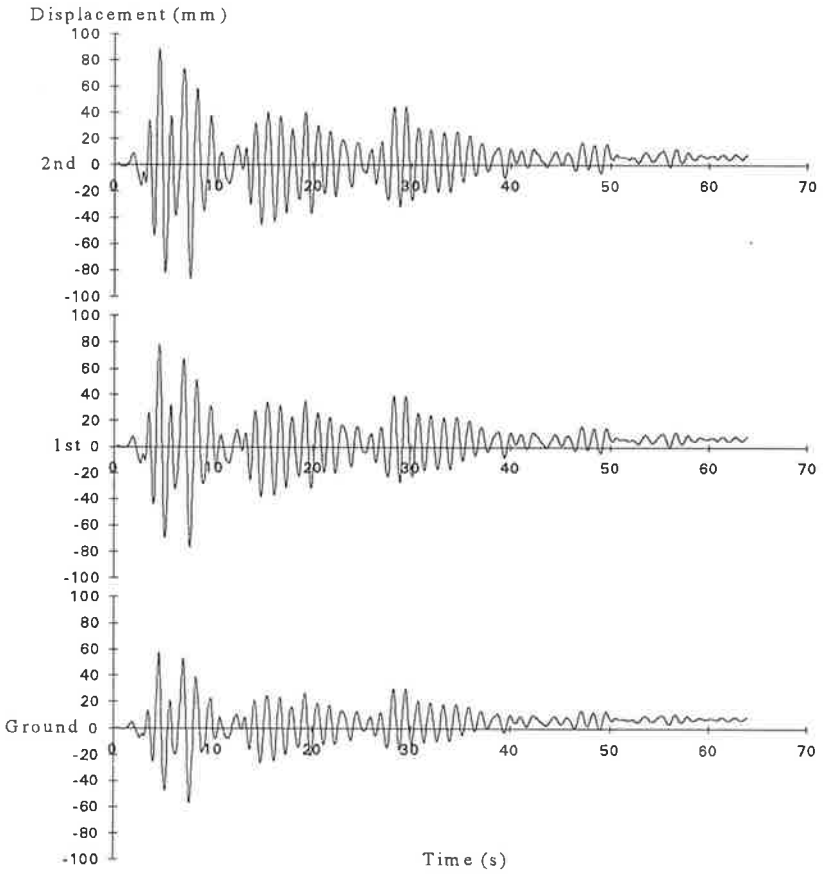

Figure 5.20 - Storey Displacement for EQ10

The maximum displacement profile (Figure 5.21) of the internal frame had a non-linear shape. The non-linearity was even more pronounced (especially at the ground storey) than was observed during EQ5 (Figure 5.5) and EQ8 (Figure 5.13). The majority of deformation was at the ground storey rather than the first storey.

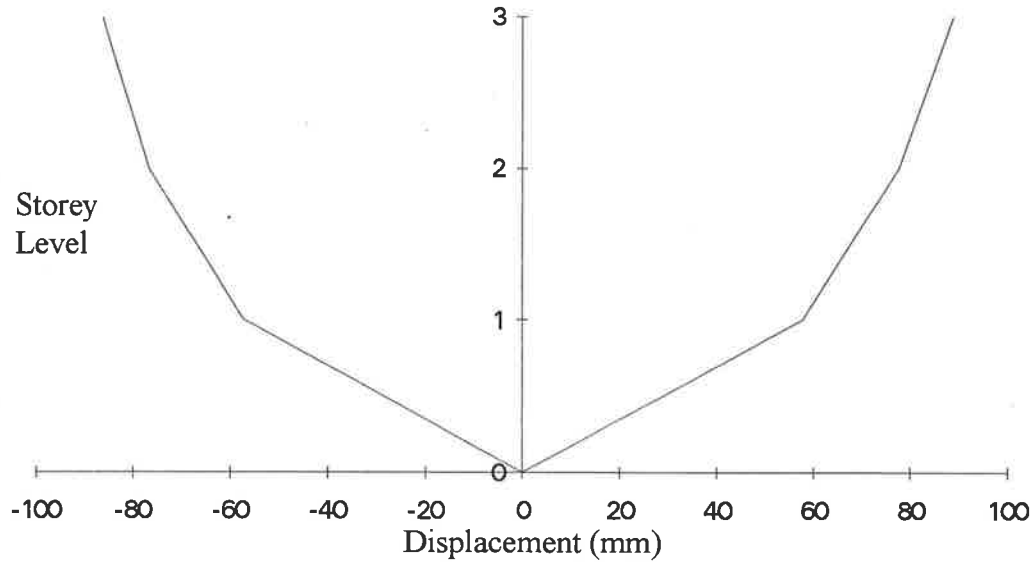

Figure 5.21 - Maximum Displacement Profile for EQ10

Figure 5.22 shows the total base shear force for the internal frame during EQ10. It shows that static equilibrium existed for the structure which is not shown by the shear force time history plots for a single column since some residual shear was left in each column at the end of the shaking due to non-symmetric yield events.

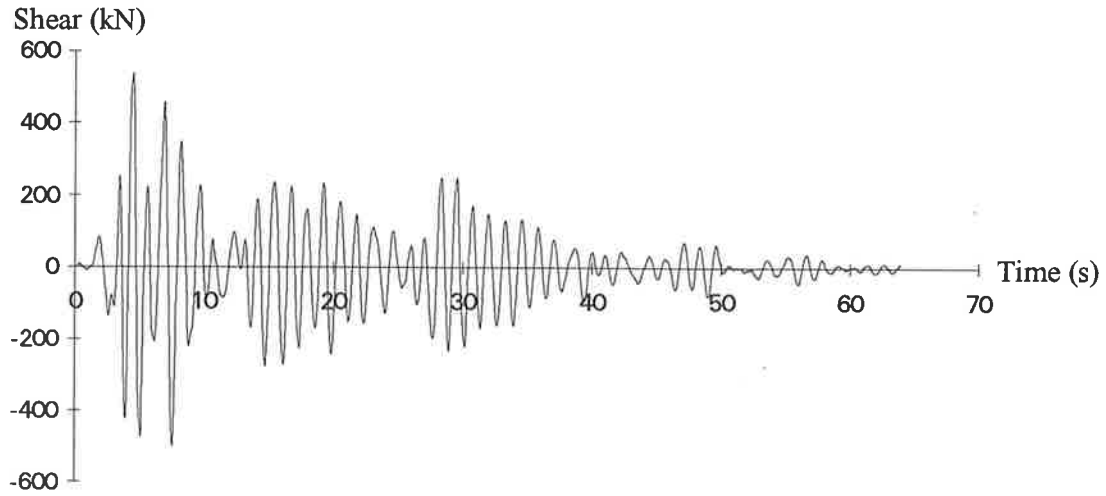

Figure 5.22 - Total Base Shear for EQ10

Figure 5.23 shows the ground storey hysteresis where it can be seen that yielding occurred in both directions. The presence of the loops further indicates energy dissipation in the ground storey columns.

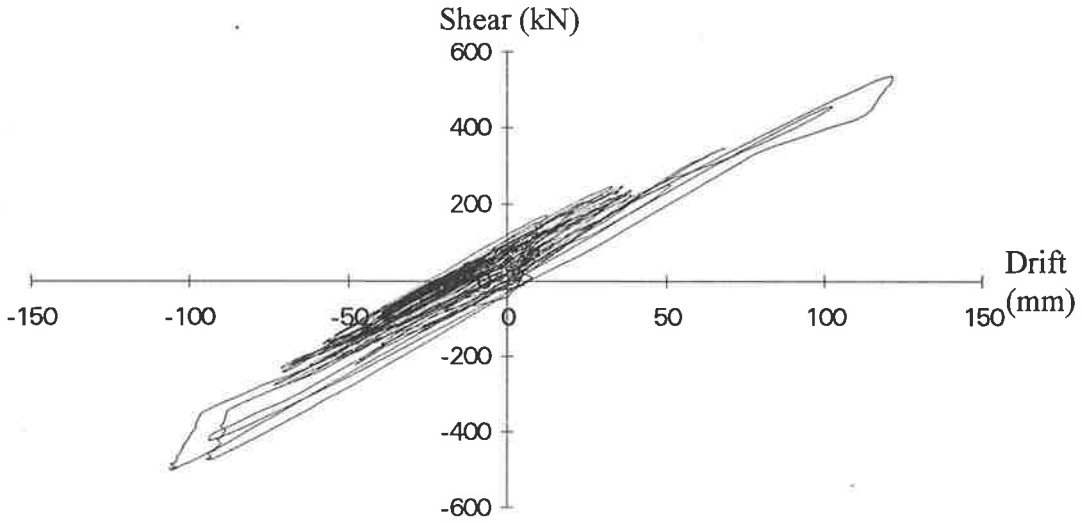

Figure 5.23 - Total Storey Hysteresis at Ground Level for EQ10

Exterior Columns: The maximum base shear recorded for the exterior column was 81kN and 114kN in each direction (Figure 5.24). The maximum shear profile of the exterior column (Figure 5.25) was similar to the maximum shear profile of the same column for EQ8. The unsymmetrical shape of the profile, which was caused by the one-sided shape of the shear force diagram, was again present. The shear force difference between the ground and first storey in one direction was very small due to the limitation of yield strength. This limited yield strength occurred only in one direction which was caused by the presence of an orthogonal beam on only one side of the joint.

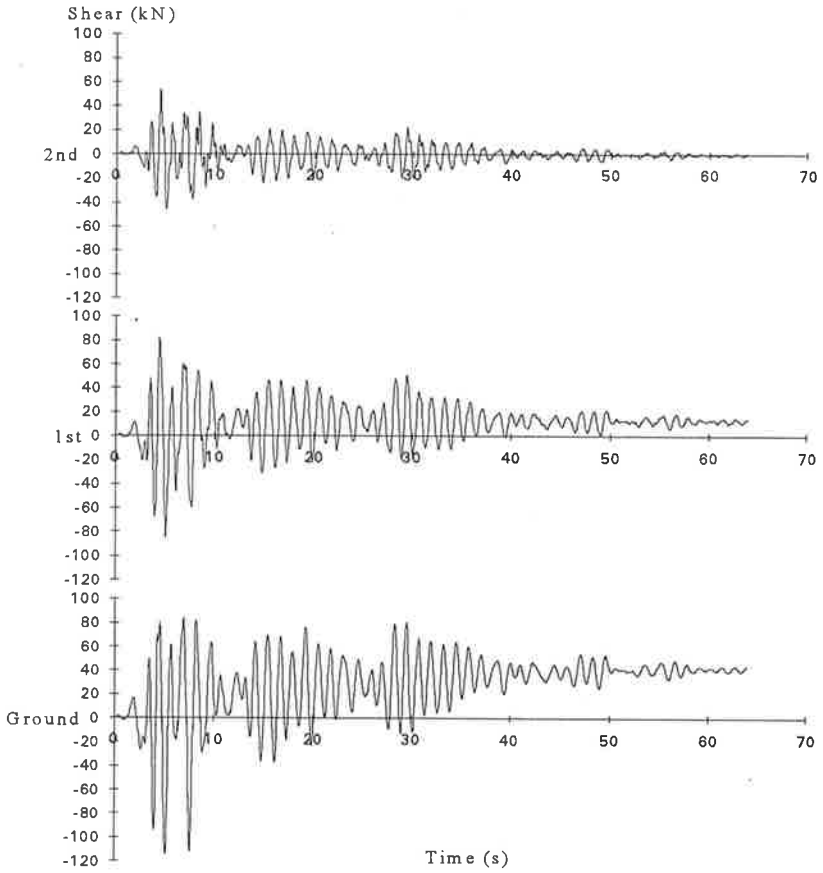

Figure 5.24 - Storey Shear Forces for Exterior Columns for EQ10

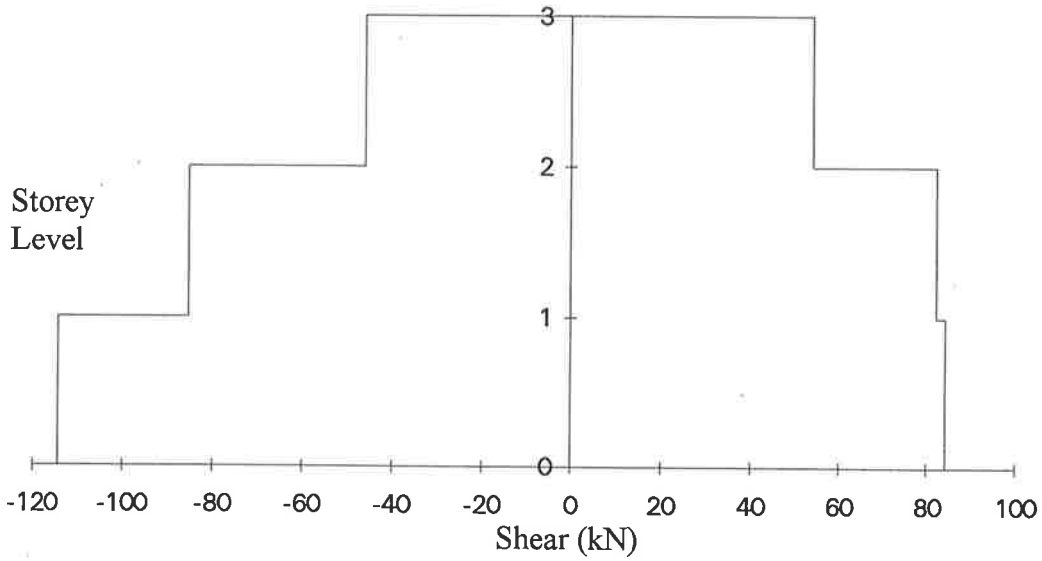

Figure 5.25 - Maximum Shear Profile of Exterior Columns for EQ10

Figure 5.26 shows the exterior column shear hysteresis for the three levels. The ground storey exterior column exhibits yielding in one direction and slight stiffness degradation. The first storey exterior column also exhibited some yielding (for the first time) during this magnitude earthquake. The column at the top remained elastic. Note that the yielding in the first storey column was in the same direction as the ground storey.

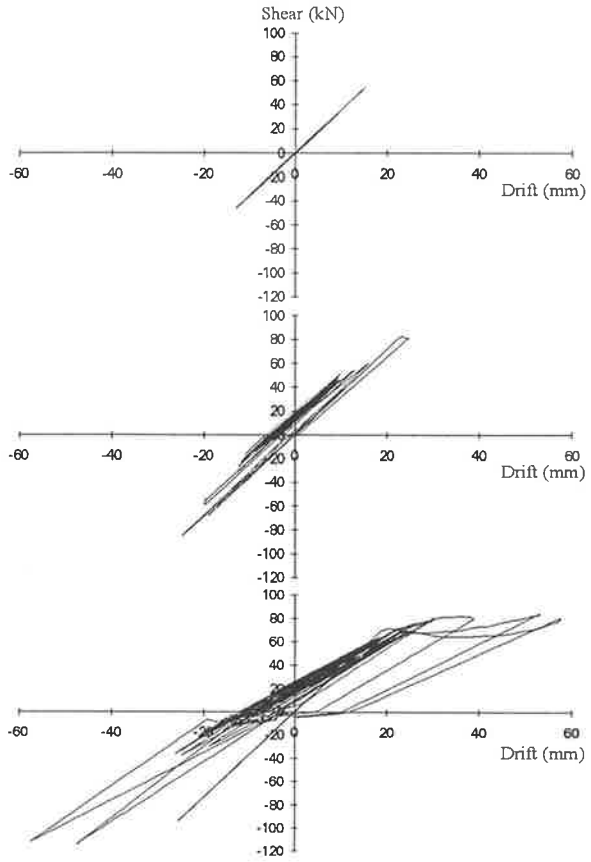

Figure 5.26 - Storey Hysteresis for Exterior Joints for EQ10

Interior Columns: Figure 5.27 shows the shear forces in the interior columns on the three levels. The maximum base shear force experienced by this column were 120kN and 111kN. When compared to the maximum shear profile for the exterior column (Figure 5.25), the one for the interior column (Figure 5.28) was much more symmetrical and the steps were much more uniform.

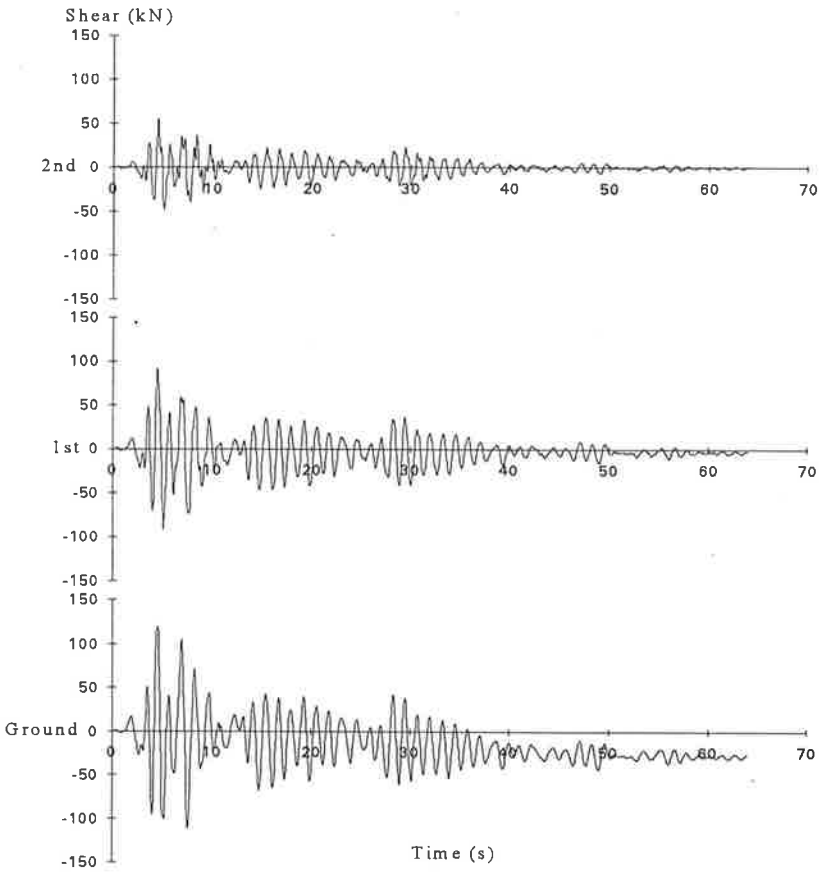

Figure 5.27 - Storey Shear Forces for Interior Columns for EQ10

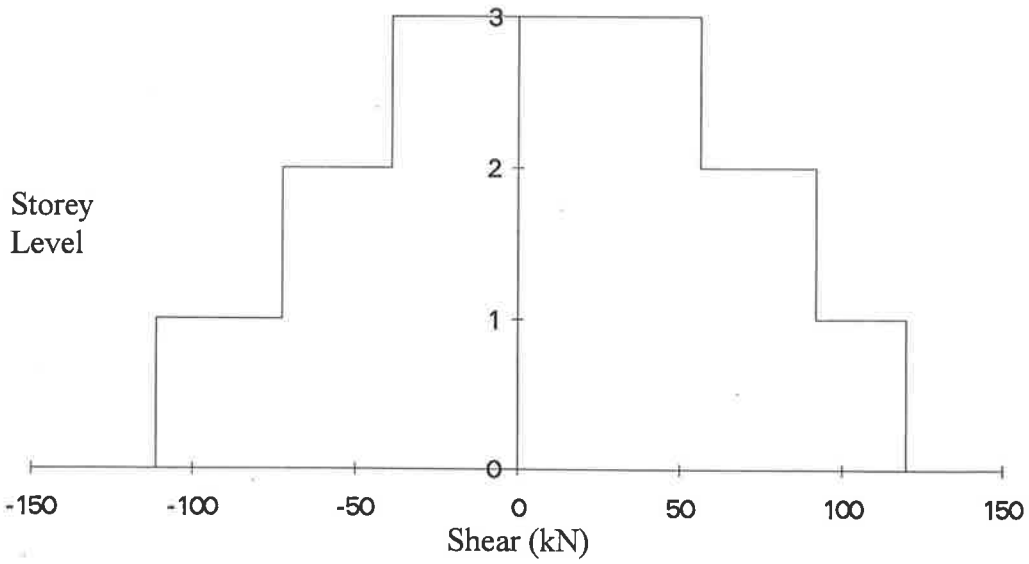

Figure 5.28 - Maximum Shear Profile of Interior Columns for EQ10

The ground storey hysteresis shows (Figure 5.29) that significant yielding has occurred in both directions. There was clearly column stiffness degradation. The large loops indicated energy dissipation by the column. The column hysteresis (Figure 5.29) of the interior columns on the upper storeys showed no sign of yielding during EQ10 whereas the first storey exterior columns of the same frame yielded. (Refer to Figure 5.26)

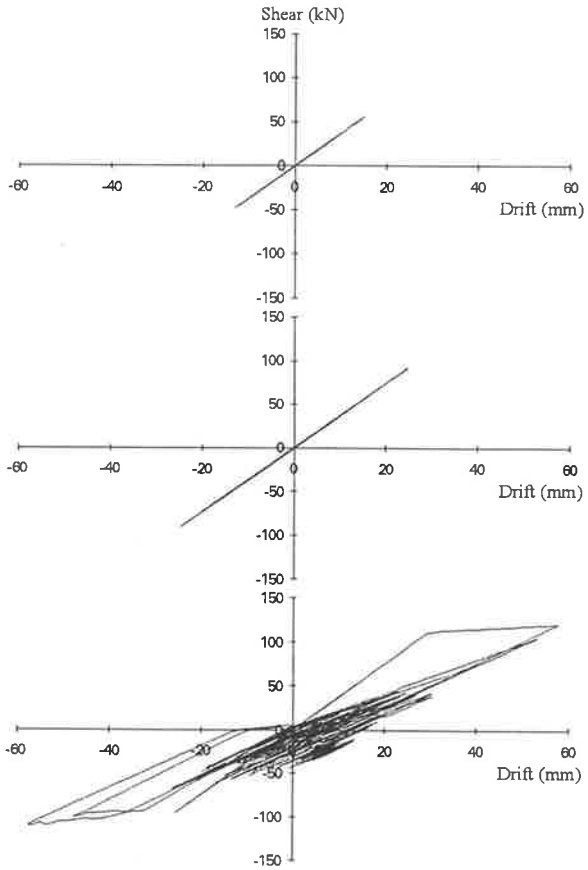

Figure 5.29 - Storey Hysteresis for Interior Joint for EQ10

5.3.4 Prior to Failure

In this section, the prototype structure was loaded with a scaled up version of the acceleration record of earthquake test 10 recorded in the 1/5-scale shake table test performed at the University of Adelaide. The internal frames failed at a 0.15g magnitude earthquake. The results from the computer analysis after failure were erratic and did not show any data which could be used to explain what was happening to the structure. Therefore, it was decided to run the analysis as close to failure as possible without failing the structure. This was done by first finding the largest magnitude earthquake not to cause collapse at which the frames failed at then performing the analysis with a slightly smaller earthquake. It was found that 1.42 times EQ10 would be the largest earthquake load the internal frame could sustain without failing. The maximum roof displacements obtained were 128mm and 96mm in either direction (Figure 5.30). This compared to 89mm and 86mm observed during EQ10. Significant permanent offsets were present at all three levels which indicated that yielding of the structure had occurred.

The shape of the maximum displacement profile for the structure (Figure 5.31) shows that most of the deformations occurred at the ground storey. When compared to the maximum displacement profile of the same frame during EQ10, the non-linearity of the profile was much more obvious. The inter-storey drift was much larger at the ground storey than the upper two storeys, confirming that the displacements were no longer evenly distributed through the three storeys as seen on smaller magnitude earthquakes. This suggested a soft-storey collapse mechanism would occur.

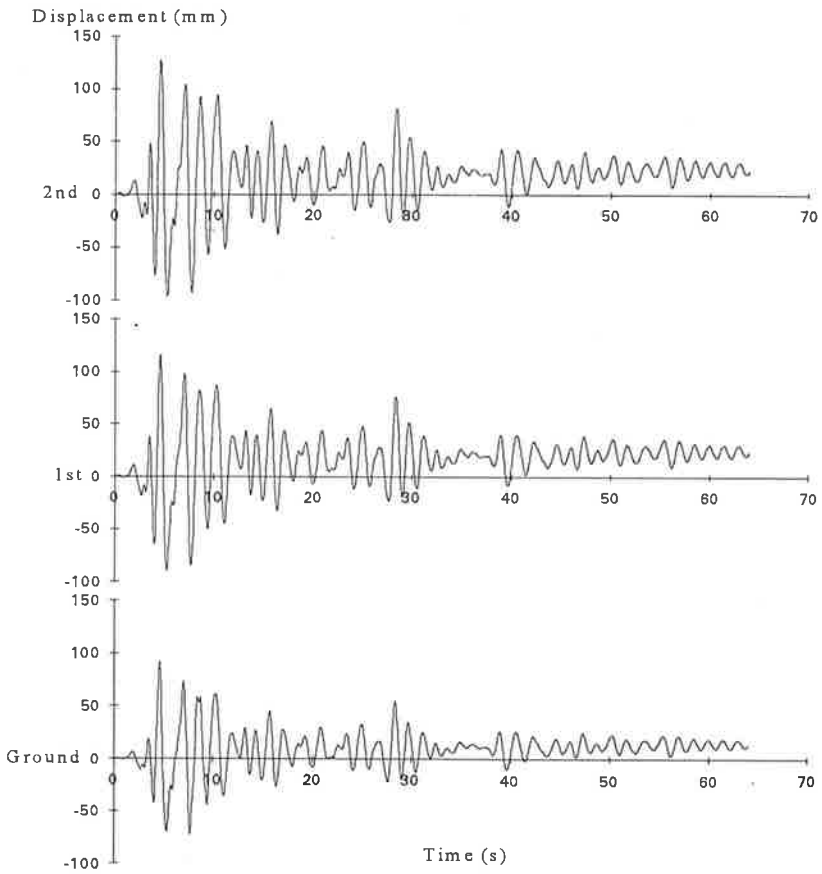

Figure 5.30 - Storey Displacement for 1.42EQ10

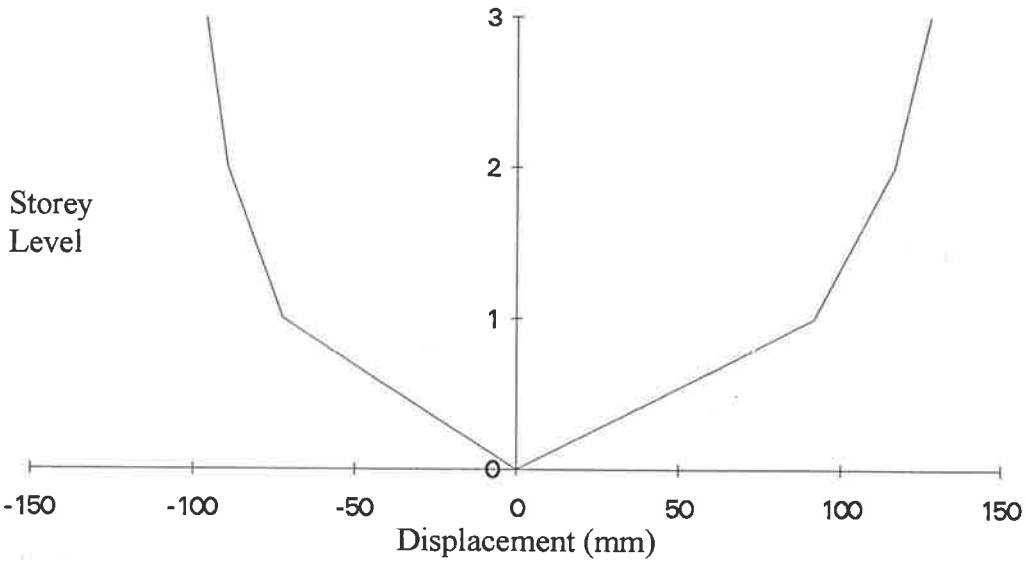

Figure 5.31 - Maximum Displacement Profile for 1.42EQ10

The maximum total base shear of the structure was 592kN and 524kN in the two directions respectively. This compared to the values of 538kN and 502kN correspondingly for EQ10. Note that this graph (Figure 5.32) shows that static equilibrium existed in the frame although the shear force diagram of individual columns had a residual shear force at the end of the earthquake shaking.

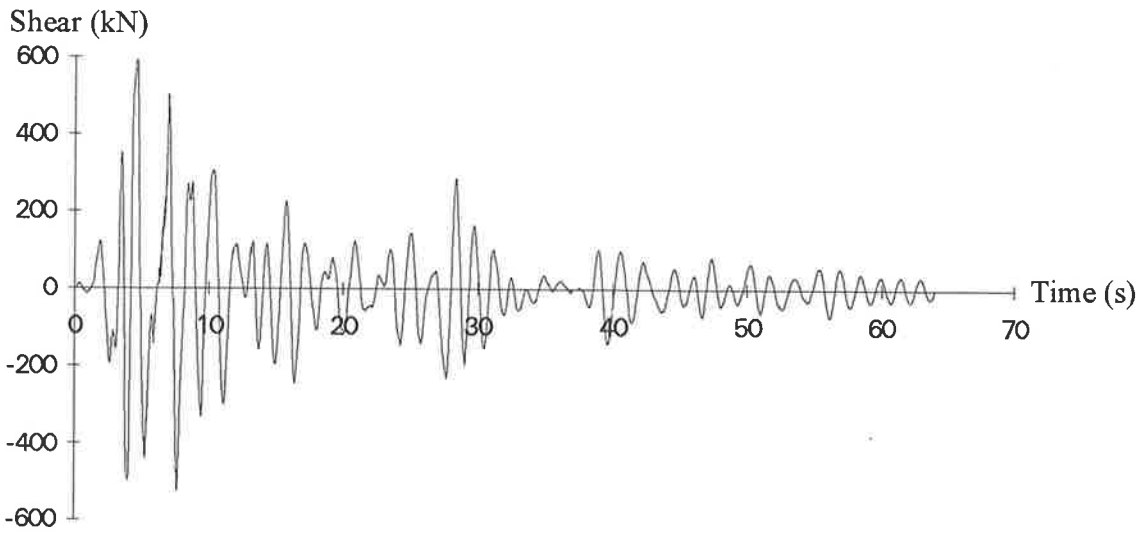

Figure 5.32 - Total Base Shear Force for 1.42EQ10

The storey hysteresis for the ground storey (Figure 5.33) shows that significant yielding occurred. A big open loop indicated that a large amount of energy was dissipated by the structure while the stiffness had in turn reduced by a significant amount. The stiffness degraded from 18.9kN/mm initially to a final stiffness of 5.5kN/mm within a few cycles (approximately 30% of the original stiffness) which indicated that the structure did not exhibit good ductility.

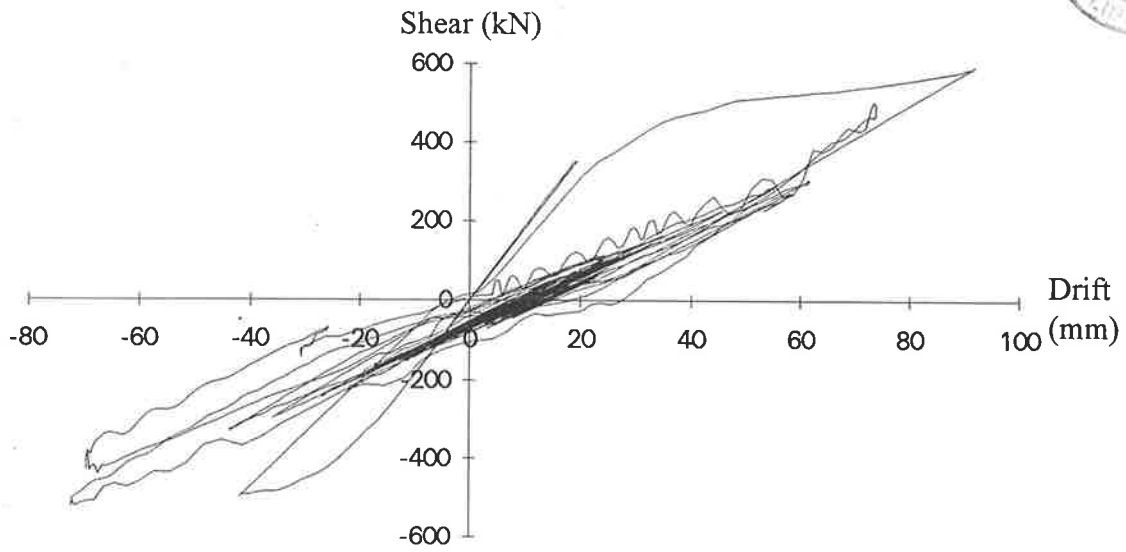

Figure 5.33 - Total Storey Hysteresis at Ground Level for 1.42EQ10

Exterior Columns: The maximum shear force in member M1 was 91kN and 136kN which were much larger than the 81kN and 114kN recorded for EQ10. Once yielding occurred, the shear force in the exterior column was larger in one direction than in the other. This was caused by the opening and closing of the joint with beam member helping confinement in one direction and no additional help for confinement of the joint in the other. There was a large residual shear force in the first storey column (Figure 5.34) which was caused by yielding of the column at that level. The maximum shear force for the ground storey column in one direction was much larger than that in the opposite. This in turn caused the maximum shear profile to be very unsymmetrical in shape (Figure 5.35).

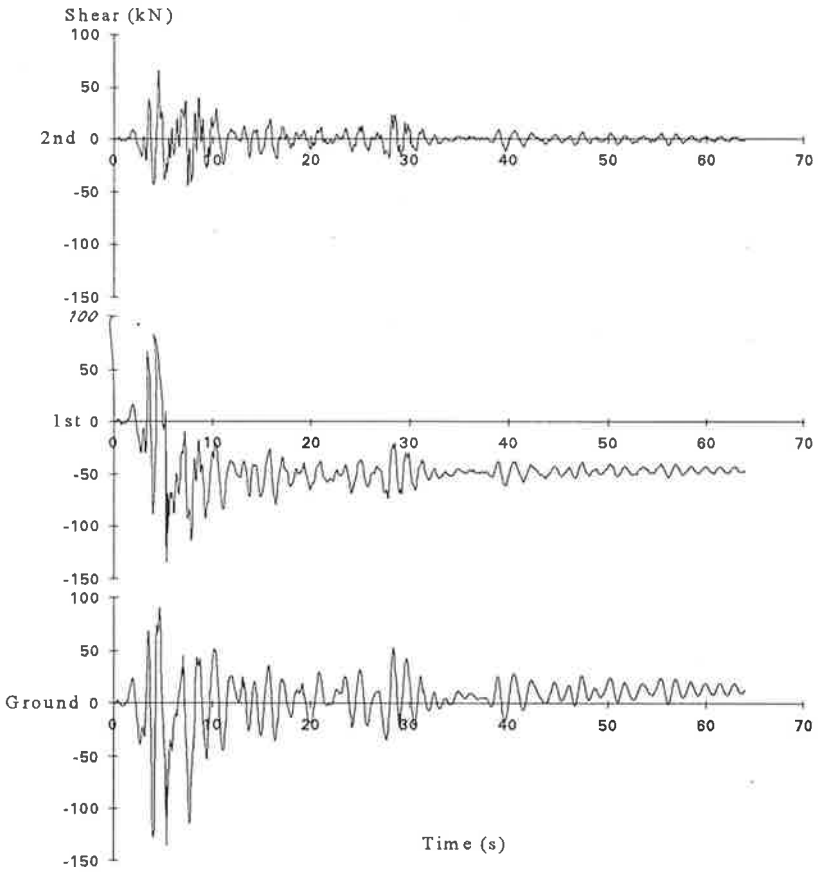

Figure 5.34 - Storey Shear Force for Exterior Columns for 1.42EQ10

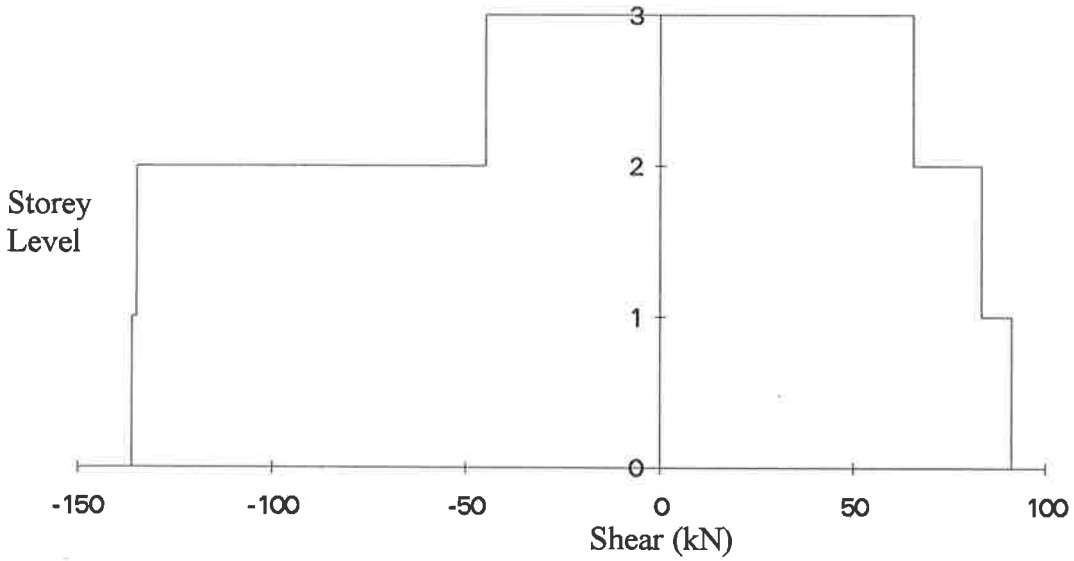

Figure 5.35 - Maximum Shear Profile of Exterior Columns for 1.42EQ10

Figure 5.36 shows the ground storey exterior column hysteresis. Similar to the storey hysteresis, a large amount of yielding occurred and significant member stiffness degradation also occurred. The speed with which the member stiffness degraded indicated that the column was not behaving in a ductile manner. Within a few cycles, the member stiffness had reduced from 3.8kN/mm initially to a final stiffness of 1.1kN/mm (approximately 30%). The shear force hysteresis of the first storey column (Figure 5.36) indicated that yielding had also occurred there. Stiffness degradation was also present at the first storey interior column. It degraded from an initial stiffness of 3.6kN/mm to 2.0kN/mm (approximately 53%). However, on the second storey, the column remained elastic.

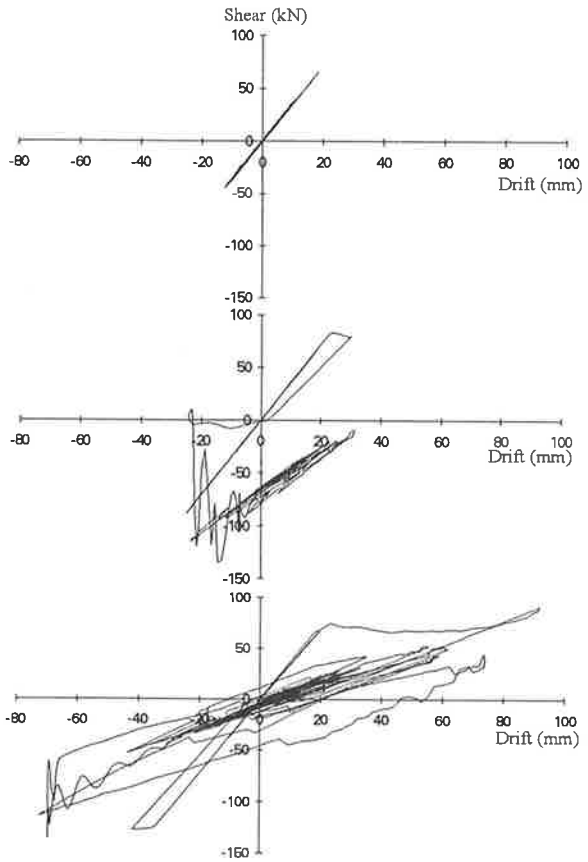

Figure 5.36 - Shear Force Hysteresis for Exterior Columns for 1.42EQ10

The axial-force-bending moment strength interaction diagram for member M1 (Figure 5.37) shows that the ground storey exterior column member was very close to failure as expected. The failure mode was likely to be flexural failure of the member.

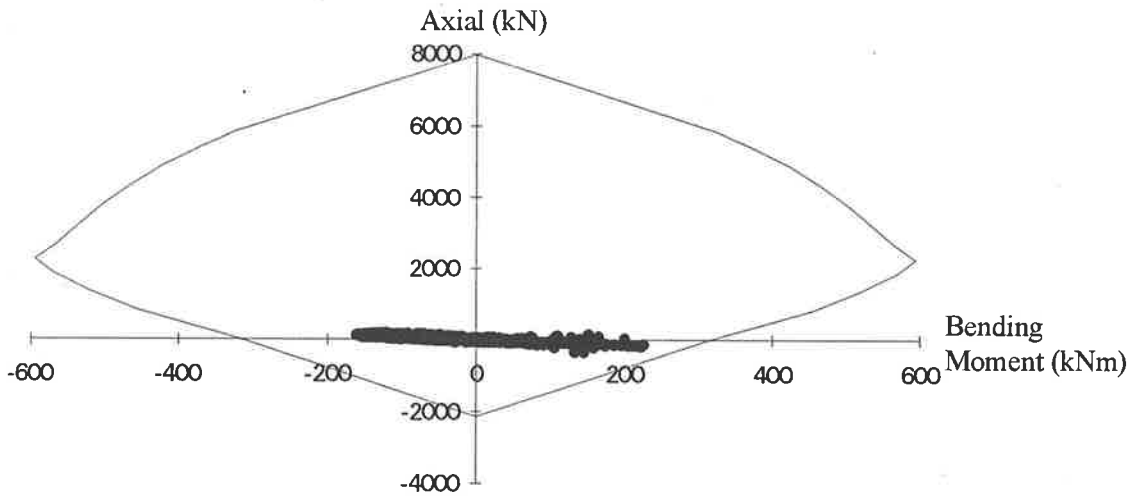

Figure 5.37 - Strength Interaction Diagram for Member M1

Interior Columns: The maximum shear forces for the interior ground storey column (member M7) were 144kN and 103kN. The large residual shear force in the ground storey exterior column was not observed in the corresponding interior column (Figure 5.38). This would imply that significant yielding might not have occurred in this column.

The maximum shear profile for the interior column is shown in Figure 5.39. The most noticeable character of the profile was that the shear forces for the ground and first storey in one direction were very close in magnitude hence giving a much smaller "step" than the corresponding forces in the opposite direction. In general, the shape of the profile is very similar to those found in EQ5, EQ8 and EQ10.

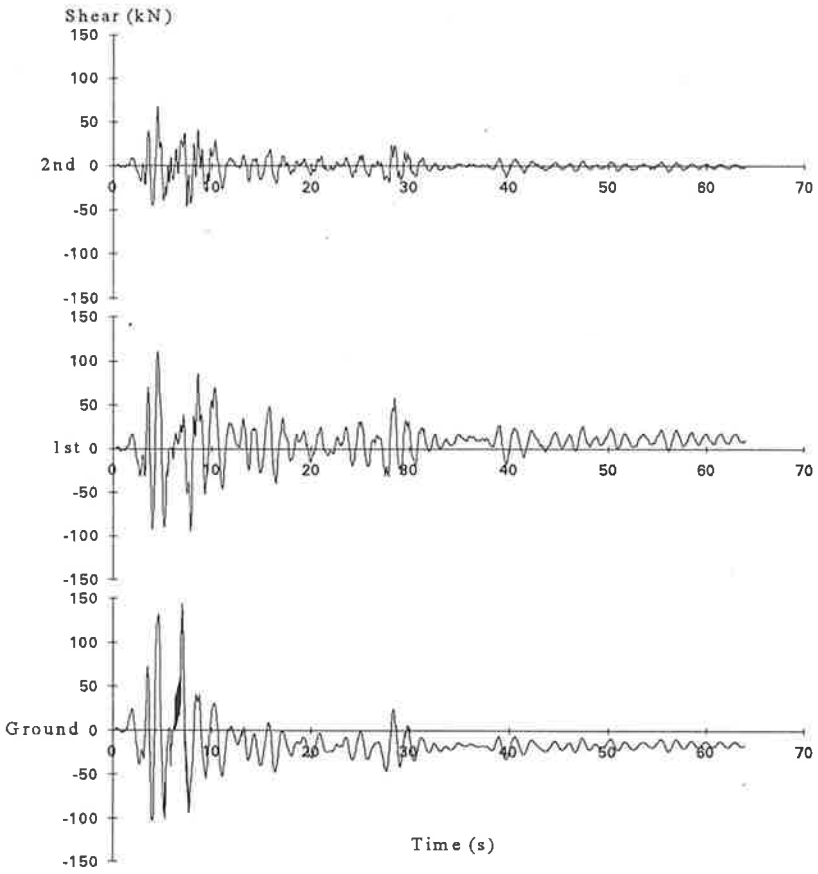

Figure 5.38 - Storey Shear Force for Interior Columns for 1.42EQ10

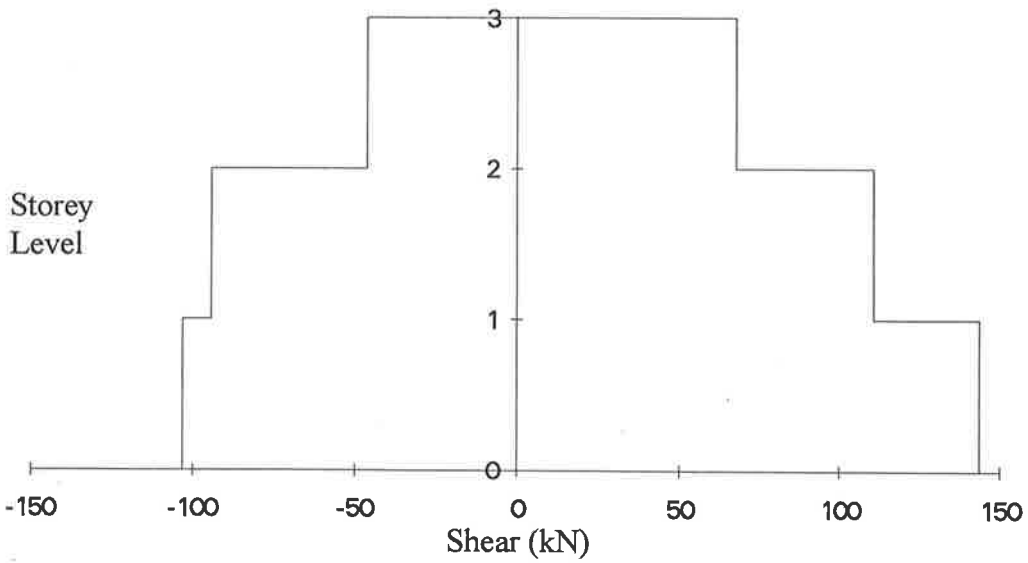

Figure 5.39 - Maximum Shear Profile of Interior Columns for 1.42EQ10

Similar behaviour to the exterior ground storey column was observed in the ground storey interior column (Figure 5.40). Following yielding, the stiffness of the member degraded rapidly showing no ductility. The stiffness dropped from an initial stiffness of 3.9kN/mm to 1.1kN/mm (approximately 30% of the original stiffness). This reduction of stiffness was consistent with the reduction observed in the ground storey exterior column. For the upper two storeys, no significant yielding was observed. As a comparison, no yielding was observed also for these two columns during EQ10.

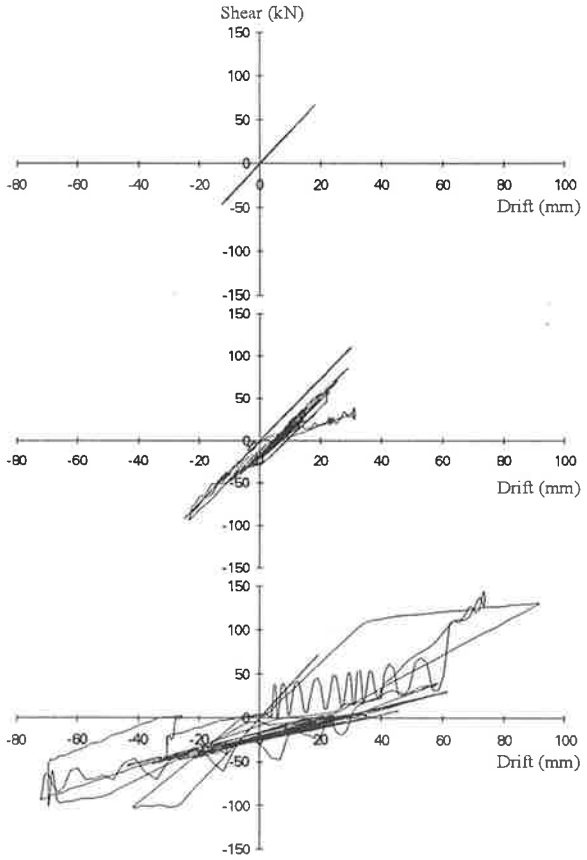

Figure 5.40 - Shear Force Hysteresis for Interior Columns for 1.42 EQ10

Figure 5.41 shows the axial force versus bending moment during the earthquake loading. It was also very close to failure. When compared to (Figure 5.37) member M1, it was concluded that member M7 was critical for the internal frame.

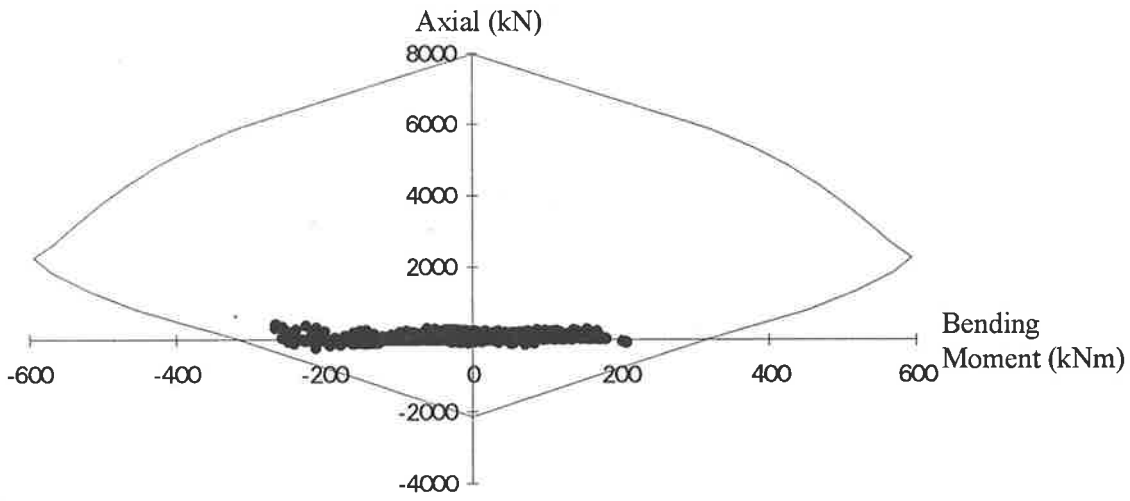

Figure 5.41 - Strength Interaction Diagram for Member M7

5.4 SUMMARY AND CONCLUSION

The interior frame of a prototype structure was subjected to a series of dynamic analyses. The prototype structure was a three storey four bay moment resisting frame in the direction of loading (and three bays in the direction orthogonal to the loading). Three different magnitude earthquakes: EQ5, EQ8 and EQ10 were considered in the series of analyses. The structure was further loaded in an effort to establish what its ultimate capacity was.

For the smallest of the earthquakes (EPA=0.047g), the prototype frame behaved very much in an elastic manner. No stiffness degradation nor yielding was observed in the column members of the internal frame.

The effective peak acceleration 0.078g earthquake test represented the design base earthquake for Melbourne and Sydney. At this level of loading, the maximum displacement profile of the structure showed some non-linearity. Displacements were no longer evenly distributed through the three storeys. Yielding at the base of the exterior columns of the structure was observed for the internal frame. Some member stiffness degradation was also observed, the stiffness dropped in the order of approximately 20%.

This magnitude of degradation was consistently observed in the exterior columns. The interior ground storey columns showed minor yielding when compared to the exterior columns and no noticeable stiffness degradation. All columns on the first and second storey remained elastic.

The third earthquake represented the design base earthquake for Adelaide with EPA=0.105g. The maximum displacement profile showed pronounced non-linear distribution of displacements throughout the three storeys. Significant yielding was observed in the ground storey exterior columns. Although the extent of yielding had increased (especially with the interior ground storey columns), the member stiffness degradation was about the same as was observed for EPA=0.078g. The storey hysteresis for EQ10 (Figure 5.29) showed that the structure exhibited a drift of approximately 1.8% during this magnitude earthquake (the design basis earthquake for Adelaide) thus indicating that failure of the structure is imminent.

The ultimate capacity of the internal frame was found to be 0.15g or approximately 1.42 times EPA=0.105g. The displacement profile was highly non-linear with most deformations occurring in the ground storey. The maximum base shear forces for the internal frame were 592kN and 524kN. The storey hysteresis plots showed that significant yielding had occurred. For the exterior and interior ground storey columns both yielding and stiffness degradation were observed. The exterior column stiffness degraded to 30% of its initial stiffness (3.8kN/mm to 1.1kN/mm). This same degradation was observed for the interior column where it dropped from 3.9kN/mm to 1.1kN/mm. The swift stiffness degradation indicated that minimal ductility were in the columns. The only other column which showed yielding was the exterior first storey column and there was a stiffness degradation of approximately 25%. The magnitude at which the prototype structure failed was approximately 1.5 times EQ10 which correspond to approximately 1.5 times the design basis earthquake. Griffith and Whittaker [78] has shown that the ratio of maximum capable earthquake to design basis earthquake in Australia is approximately 2 to 3 whereas the same ratio in California is approximately 1.2 to 1.5. Therefore, in the event of an earthquake with the magnitude of the maximum capable

earthquake, the prototype structure and other similarly detailed reinforced concrete structure are very likely to fail and/or collapse.

Overall, the prototype building represented a common multi-storey, multiple bay reinforced concrete frame structure with joint detailing corresponding to the ordinary moment resisting frame standard. It was found that yielding occurred to the structure when loaded with an earthquake with EPA=0.078g. With the EPA=0.105g, yielding occurred at the first storey. The interior ground storey columns (M7) of the internal frames were found to be the first members to yield under earthquake loading and the overall mode of failure will be a soft storey collapse. The inadequacy of the joints designed according to AS 3600 [2] as a normal moment resisting frame in resisting earthquake loading is again highlighted here as was concluded by Huang [26] and Corvetti [71].

The Australian earthquake loading code AS1170.4 [1] adopted a similar design philosophy to that used in the United States by incorporating in the seismic design provisions for building structures a force reduction factor expressed as a response modification factor R_f. This factor is also known as R in the National Earthquake Hazards Reduction Program (NEHRP) or a system performance factor, R_w in the Uniform Building Code (UBC) [55]. The force reduction factor is used to reduce the linear elastic response spectra structural base shear to an inelastic design value on the basis that the actual structure will possess some ductility and structural overstrength.

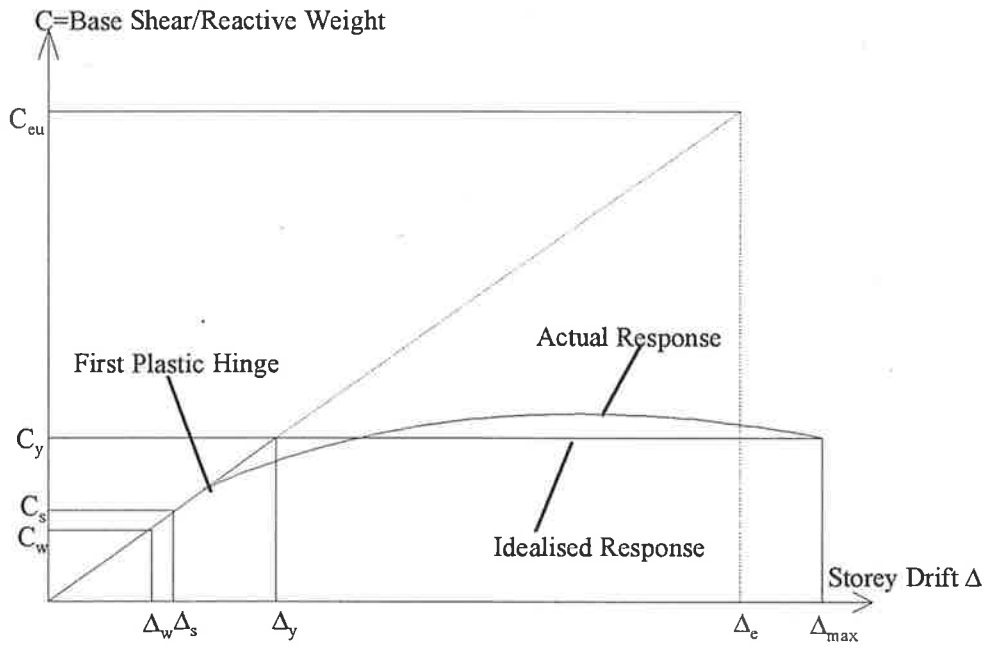

Figure 5.42 General Structural Response

Figure 5.42 shows the required elastic strength expressed in terms of base shear ratio C_{eu},

$$C_{eu} = \frac{V_e}{W} \tag{5.1}$$

where W is the weight of the reactive mass and V_e is the maximum base shear which the structure would develop if it remained in the elastic range. For the design of structures, NEHRP allows the designer to reduce the C_{eu} level to the C_y level for design. This is the force level beyond which the structural response will deviate significantly from the elastic response. The advantage of this method is that designers only need to perform elastic analysis. However, design using elastic procedures mean that the designer will not necessarily know the actual strength of the structure and if the structure overstrength (i.e. reserve strength beyond the design level C_s) is significantly less than that implied in the seismic response modification factor, the structural performance could be inadequate during a severe earthquake. Another problem with using an elastic design procedure is that the maximum inelastic deflections cannot be calculated directly from an elastic

analysis. Uang [79,80] derived a basic formula for establishing the response modification factor R, as the product of a ductility reduction factor (R_μ) and an overstrength factor (Ω) i.e.

$$R = R_\mu \cdot \Omega \tag{5.2}$$

However, the period of the prototype building considered in this study (refer to page 78) is greater than that corresponding to the peak elastic spectral response [77]. As mentioned in Chapter 4, Priestley and Paulay [76] observed that for these structures, the maximum inelastic displacement Δ_{max} is about equal to the elastic response displacement, thus this structure was expected to behave in accordance with the *equal-displacement principle*. Thus Figure 5.42 can be modified to that shown in Figure 5.43.

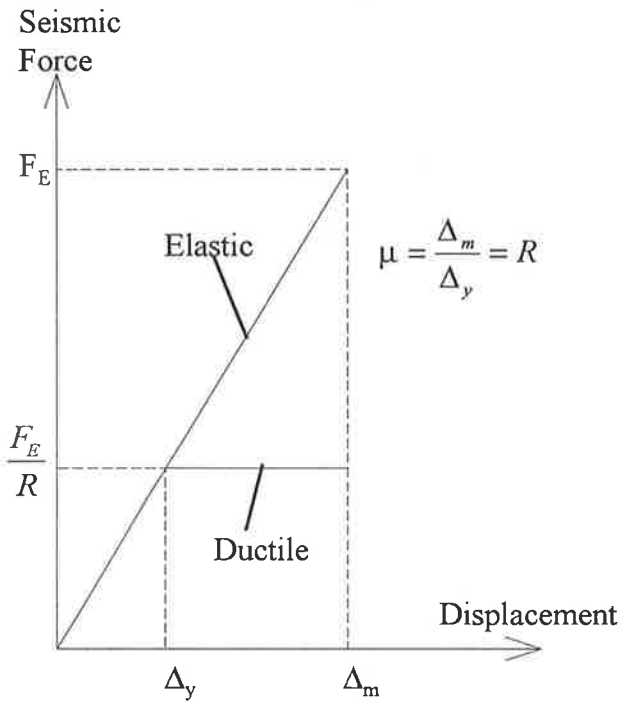

Figure 5.43 - Equal Displacement Principle

This implies that the ductility achieved by the inelastic system should be approximately equal to the force reduction factor, i.e.

From the results obtained for the prototype structure in Figure 5.33,

$$\Delta_{max}= 90mm \text{ and } \Delta_y=30mm$$

thus

$$\mu = 3$$

Therefore this suggests that the proposed value specified by the code will result in an overstrength factor $\Omega \geq 4/3$ which is comparable to value for Ω reported elsewhere.

CHAPTER 6
CONCLUSION

6.1 SUMMARY

This aim of this thesis was to investigate the behaviour of Australian designed reinforced concrete frame structures which had been designed primarily for static and wind loading. A computer model was created which enabled the modelling of the behaviour of a typically Australian designed reinforced concrete frame structure which accounted for joint stiffness and strength degradation under seismic loading through modifications to beam-column element hysteresis models.

Two sets of experimental results were used to calibrate the computer model (1/2 scale joint tests done at the University of Melbourne and 1/5 scale frame test done at the University of Adelaide). An existing non-linear dynamic analysis package Ruaumoko [74] was used as the

analytical tool and a hysteresis rule was chosen based primarily on the experimental data from the 1/2 scale joint tests i.e. the hysteresis rule which gave the closest characteristics such as shape of the curve, the pinching effect and rate of stiffness degradation to the experimentally obtained results when the 1/2 scale joint tests were simulated using the computer analysis package. The Mehran Keshavarzian degrading and pinching rule was chosen based on the aforementioned criteria, however it was interesting to note that this rule was originally developed to better simulate the hysteretic behaviour of wall-frame and/or coupled shear wall structures.

A second model was produced by using the scaled cross sectional properties of the columns and beams used in the 1/5 scaled model directly without calibration. Both computer models were used to simulate the structural behaviour of the full scale equivalent of the 1/5 scale frame tested in Adelaide. The three storey structure was loaded with various magnitudes of the N-S component of the 1940 El-Centro earthquake [77]. The different magnitudes were chosen to represent a good cross section of earthquakes magnitude which affect the area in Australia where most of the population is concentrated, i.e. the capital cities.

When the results from the computer models were compared to the full scaled equivalent of the experimental results form Adelaide, it was found that both computer models were consistently over-estimated the storey stiffness at ground storey. The deformations were shown to be fairly even throughout the three storeys by the computer models while the experiment showed that deformations were concentrated mostly at the ground storey.

The calibrated computer model developed in Chapter 3 was used to predict the structural behaviour of a multiple bay multi-storey prototype building during seismic loading. Due to limitations of the computer program, a two-dimensional internal frame was analysed as a representative of this type of reinforced concrete structures. The structure was loaded with the same three magnitude earthquakes used in Chapter 4 and then the loading was increased until failure was imminent. Column behaviour (external and internal) was monitored so that the behaviour of the structure could be analysed. The stiffness degradation of both interior

and exterior ground storey column was quantified to 30% of the initial column stiffness. There was little ductility shown by the columns as the rate of stiffness degradation was very rapid as expected from a normal moment resisting frame with no special detailing to allow for seismic performance. Upon examining the strength interaction diagram of both the exterior column and interior column, it was concluded that the failure mode would to be a soft storey collapse with member 7 (refer to Figure 5.3), an internal column at the ground level, to fail first.

6.2 CONCLUSION AND RECOMMENDATION

4 main conclusion were drawn from the research presented.

(1) The Response Modification Factor (R or R_f) calculated from the analytical results indicated good correlation with the value specified by AS1170.4[1]. An overstrength factor of greater than or equal to 4/3 is a reasonable value for this type of reinforced concrete structure.

(2) There is an inadequacy in the modelling of the non-linear behaviour of concrete beam-column members in the model used for this research. It clearly showed that the proposed computer model, which is based on a degrading bi-linear model, can not reflect the non-linear behaviour of the concrete members at levels of stress less than the yield stress which was observed during much of the experimental testing.

(3) A conclusion can be drawn from the analytical results with the prototype building that the magnitude for the design basis earthquake specified in AS1170.4[1] is adequate. The structure has exhibited non-linear behaviour under this magnitude earthquake without failure.

(4) However, the fact that the prototype structure failed at a magnitude earthquake only 1.5 times the design basis earthquake specified by the code is a concern especially with the

knowledge that in an area of low seismicity, the maximum capable earthquake can be 2 to 3 times greater than that of the design basis earthquake.

There is a need for better hysteresis models for full non-linear behaviour of concrete members especially at low-to-medium stress levels which was highlighted by this research to be inadequate.

REFERENCES

(1) Standards Association of Australia: SAA Minimum Design Loads on Structures, Part 4: Earthquake Loads AS1170.4 - 1993, Sydney.

(2) Standards Association of Australia: SAA Concrete Structures Code: AS3600 - 1988, Sydney.

(3) Ishibashui, K., Kamimura, T. and Sonobe, Y., "Behaviour of RC Beam Column Connection with Large Size Deformed Bars under Cyclic Loads, " World Conference on Earthquake Engineering, New Delhi 1977, Vol. 3, pp 3251.

(4) Yunfei, H., Chingchang, H. and Yufeng, C., "Further studies on the behaviour of reinforced concrete beam-column joint under reversed cyclic loading, " World Conference on Earthquake Engineering, San Fransico 1984, pp 485-492.

(5) Ehsani, M.R. and Wight, J.K., " Reinforced Concrete Beam-to-Column Connections Subjected to Earthquake-Type Loading, " World Conference on Earthquake Engineering, San Fransico 1984, pp 421-428.

(6) Durrani, A.J. and Wight, J.K., " Experimental Study of Interior Beam to Column Connections Subjected to Reversed Cyclic Loading, " World Conference on Earthquake Engineering, San Fransico 1984, pp 429-436.

(7) Zebre, H.E. and Durrani, A.J., " Seismic Behaviour of Intermediate R/C Beam-Column Connection Subassemblies, " World Conference on Earthquake Engineering, Tokyo 1988, Vol. 4, pp 663-668.

(8) Tang, J. and Xu, X., " Seismic Behaviour of Lightweight Reinforced Concrete Beam-Column Joints, " World Conference on Earthquake Engineering, Tokyo 1988, Vol.4, pp 651-656.

(9) Ehsani, M.R., and Alameddine, F., " Response of High-Strength Concrete Beam-Column Joints Subjected to Pseudo Dynamic Loading, " Proceedings of the Fourth U.S. National Conference on Earthquake Engineering, Palm Springs California 1990, Vol. 2, pp 677-686.

(10) Paulay, T., Park, R. and Priestley, M.J.N., " Reinforced Concrete Beam-Column Joints Under seismic Actions, " American Concrete Institute Structural Journal, 1978, Vol.75 No. 7-12, pp 585-593.

(11) Fenwick, R.C. and Irvine, H.M., " Reinforced Concrete Beam-Column Joints for Seismic Loading, " Bulletin of New Zealand National Society for Earthquake Engineering, 1977, Vol. 10, pp 121-128.

(12) Park, R., Gaerty, L. and Stevenson, E.C., " Tests on an Interior Reinforced Concrete Beam-Column Joint, " Bulletin of New Zealand National Society for Earthquake Engineering, 1981-1982, Vol. 14-15, pp 81-92.

(13) Pessiki, S.P., Conley, C., White, R.N. and Gergely, P., " Seismic Behaviour of the Beam-Column Connection Region in Lightly-Reinforced Concrete Frame Structures, " Proceedings of the Fourth U.S. National Conference on Earthquake Engineering, 1990, Vol. 2, pp 707-716.

(14) Park, R. and Keong, Y.S., " Tests on Structural Concrete Beam-Column Joints with Intermediate Column Bars, " Bulletin of New Zealand National Society for Earthquake Engineering, 1979, Vol. 12 No. 3, pp 189-203.

(15) Alameddine, F., and Ehsani, M.R., " High-Strength RC Connections Subjected to Inelastic Cyclic Loading, " The American Society of Civil Engineers, Journal of the Structural Division, 1991, Vol.117 No.3, pp 829-850.

(16) Paulay, T. and Scarpas, A., " The Behaviour of Exterior Beam-Column Joint, " Bulletin of New Zealand National Society for Earthquake Engineering, 1982, Vol.14-15, pp 131-144.

(17) Megget, L.M. and Park, R., " Reinforced Concrete Exterior Beam-Column Joints under Seismic Loading, " 1971, New Zealand Engineering, Vol.21, pp 341-353.

(18) Lee, D.L.N., Wight, J.K. and Hanson, R.D., " RC Beam-Column Joints under Large Load Reversals, " The American Society of Civil Engineers, Journal of the Structural Division, 1977, Vol.103 ST12, pp 2337-2350.

(19) Bertero V.V., Popov, E.P. and Forzani, B., " Seismic Behaviour of Lightweight Concrete Beam-Column Subassemblages, American Concrete Institute Journal, 1980, Vol.77 No.1, pp 44-52.

(20) Blakeley, R.W.G., Edmonds, F.D., Megget, L.M. and Priestley, M.J.N., " Performance of Large Reinforced Concrete Beam-Column Joint Units under Cyclic Loading, " World Conference on Earthquake Engineering, New Delhi 1977, Vol.3, pp 3095-3100.

(21) Hanson, N.W., " Seismic Resistance of Concrete Frames with grade 60 Reinforcement, " The American Society of Civil Engineers, Journal of the Structural Division, 1971, Vol.97, pp 1685-1700.

(22) Hanson, N.W. and Connor, H.W., " Seismic Resistance of Reinforced Concrete Beam-Column Joints, " The American Society of Civil Engineers, Journal of the Structural Division, 1967, Vol.93 ST5, pp 533-560.

(23) Corvetti, J., Goldsworthy, H. and Mendis, P.A., " Assessment of Reinforced Concrete Exterior Beam-Column Joints as Specified in the New Draft Earthquake Standard, " The 13th Australasian Conference on the Mechanics of Structures and Materials, 1993, Vol.1, pp 225-232.

(24) Park, R. and Paulay, T., " Behaviour of Reinforced Concrete External Beam-Column Joints under Cyclic Loading, " World Conference on Earthquake Engineering, Rome 1973, Vol.2-3, pp 88.

(25) Kitayama, K., Lee, S., Otani, S. and Aoyama, H., " Behaviour of High-Strength R/C Beam-Column Joints, " World Conference on Earthquake Engineering, Spain 1992, Vol.6, pp 3151-3156.

(26) Huang, Y., Mendis, P.A. and Corvetti, J., " Cyclic Behaviour of Reinforced Concrete Beam-Column Joints Designed According to AS3600, " The 13th Australasian Conference on the Mechanics of Structures and Materials, 1993, Vol.1, pp 397-403.

(27) Shin, S.W., Lee, K.S. and Ghosh, S.K., " High-Strength Concrete Beam-Column Joints, " World Conference on Earthquake Engineering, Spain 1992, Vol.6, pp 3145-3150.

(28) Oka, K. and Shiohara, H., " Tests of High-Strength Concrete Interior Beam-Column Joint Subassemblages, " World Conference on Earthquake Engineering, Spain 1992, Vol.6, pp 3211-3217.

(29) Owada, Y., "Seismic Behaviours of Beam-Column Joint of Reinforced Concrete Exterior Frame", World Conference on Earthquake Engineering Spain 1992, Vol. 6, pp 3181-3184.

(30) Raffaelle, G.S., Gentry, T.R. and Wight J.K., " Earthquake Loading on R/C Beam-Column Connections, " World Conference on Earthquake Engineering, Spain 1992, Vol.6, pp 3185-3190.

(31) Bercadino, F. and Spandea, G., " Behaviour of Fibre-Reinforced Concrete Beams under Cyclic Loading, " The American Society of Civil Engineers, Journal of the Structural Division, May 1997, Vol.123 No.5, pp 660.

(32) Kumar, S., Itoh, Y., Saizuka, K. and Usami, T., " Pseudodynamic Testing of Scaled Models, " The American Society of Civil Engineers, Journal of the Structural Division, April 1997, Vol.123 No.4, pp 525.

(33) Higazy, E.M.M., Elnashai, A.S. and Agbabian, M.S., "Behaviour of Beam-Column Connections under Axial Column Tension, " The American Society of Civil Engineers, Journal of the Structural Division, May 1996, Vol.122 No.5, pp 501.

(34) D'Ambris, A. , Filippou, F.C., " Correlations Studies on an RC Frame Shaking-Table Specimen, " Earthquake Engineering and Structural Dynamics, Vol.26 No.10, October 1997, pp 1021-1040.

(35) Miranda, E. and Bertero, V.V., " Seismic Performance of an Instrumented Ten-Storey Reinforced Concrete Building, " Earthquake Engineering and Structural Dynamics, Vol.25 No.10, October 1996, pp 1041-1059.

(36) Institution of Engineers Australia, " Conference on the New Castle Earthquake, " Conference Proceedings 15th-17th February 1990, pp 155.

(37) Institution of Engineers Australia, " Newcastle Earthquake Study, " (Editor R.E. Melchers), June 1990, pp 159.

(38) Alford, J.L. and Housner, G.W., " A Dynamic Test of a Four-Story Reinforced Concrete Building, " U.S. Coast and Geodetic Survey, Special Publication No.21, 1936.

(39) Townsend, W.H. and Hanson, R.D., " Hysteresis Loops for Reinforced Concrete Beam-Column Connections, " World Conference on Earthquake Engineering, Rome 1973, Vol.1, pp 137.

(40) Abad de Aleman, M., Meinheit, D.F. and Jirsa, J.O., " Influence of Lateral Beams on the Behaviour of Beam-Column Joints, " World Conference on Earthquake Engineering, New Delhi 1977, Vol.3, pp 3089-3094.

(41) Leon, R. and Jirsa, J. O., "Bidirectional Loading of Reinforced Concrete Beam-Column Joints", Earthquake Spectra, Vol. 2, No 3, 1986, pp 537.

(42) Beres, A., Pessiki, S.P., White, R.N. and Gergely, P., " Implication of Experiments on the Seismic Behaviour of Gravity Load Designed RC Beam to Column Connections, " Earthquake Spectra, May 1996, Vol.12 No.2, pp 185.

(43) Minowa, C., Hayashida, T., Kitajima, K., Abe, I. and Okada, T., "A Shaking Table Damage Test of Three Storey Actual Size Reinforced Concrete Structure", Pacific Conference on Earthquake Engineering, Australia, 20-22 November 1995, Vol. 2, pp 23.

(44) Kang, Y. J. and Scordelis, C., "Nonlinear Analysis of Prestressed Concrete Frames", The American Society of Civil Engineers, Journal of the Structural Division Vol. 106 No.4, 1990, pp 445-462.

(45) Tsonos, A. G., Tegos, I. A. and Penelis, G. Gr., "Seismic Resistance of Type 2 Exterior Beam-Column Joint Reinforced with Inclined Bars", ACI 89, No 1, 1992, pp 3-12.

(46) Castro, J. J., Imai, H. and Yamaguchi, T., "Seismic Performance of Precast Concrete Beam-Column Joints", World Conference on Earthquake Engineering, Spain 1992, Vol. 6, pp 3131-3137.

(47) Monti, G. and Nuti, C., "Ciclic Tests on Normal and Lightweight Concrete Beam-Column Subassemblages", World Conference on Earthquake Engineering, Spain 1992, Vol. 6, pp 3225-3228.

(48) Noguchi, H. and Kashiwazaki, T., "Experimental Studies on Shear Performances of Reinforced Concrete Interior Column-Beam Joints with High Strength Materials", World Conference on Earthquake Engineering, Spain 1992, Vol. 6, pp 3163-3168.

(49) Clough, W. and Johnston, S. B., "Effect of Stiffness Degradation on Earthquake Ductility Requirements", Second Japan National Conference on Earthquake Engineering 1966, pp 227-232.

(50) Takeda, T., Sozen, M. A. and Nielsen, N. N., "Reinforced Concrete Response to Simulated Earthquakes", The American Society of Civil Engineers, Journal of the Structural Division, 1970, Vol. 96, No 12, pp 2557-2573.

(51) Saiidi, M., "Hysteresis Models for Reinforced Concrete", American Society of Civil Engineers, Journal of the Structural Division 1982, Vol. 89 ST.4, pp 557-579.

(52) Popov, E. P., Bertero, V. V. and Krawinkler, H., "Cyclic Behaviour of Three Reinforced Concrete Flexural Members with High Shear", Earthquake Engineering Research Center, EERC 72-5, University of California, Berkley, California, August 1975.

(53) Imbeault, F. A. and Nielsen, N. N., "Effect of Degrading Stiffness on the Response of Multistorey Frames Subjected to Earthquake", World Conference on Earthquake Engineering 1973, Vol 1, pp 220.

(54) Anderson, J.C. and Townsend, W. H., "Models for Reinforced Concrete Frames with Degrading Stiffness", The American Society of Civil Engineers, Journal of the Structural Division, 1977, Vol. 103 ST12, pp 2361-2376.

(55) Uniform Building Code (UBC), Int. Conference of Building Officials, Whittier, California, 1988.

(56) Saiidi, M. and Sozen, M.A., " Simple and Complex Models for Nonlinear Seismic Response of Reinforced Concrete Structures, " Report UILU-ENG-79-2031, Department of Civil Engineering, Universtiy of Illinois, August, 1979.

(57) Shimazu,T. and Hirai, M., "Strength Degradation of Reinforced Concrete Columns Subjected to Multi-Cycle Reversals of Lateral Load at Given Amplitudes of Post Yielding Deformation", World Conference on Earthquake Engineering 1973, Vol. 1, pp 139.

(58) Keshavarsian, M. and Schnodrich, W. C., "Computed Nonlinear Analysis of Reinforced Concrete Coupled Shear Walls", World Conference on Earthquake Engineering 1984, Vol. 4, pp 695-702.

(59) Sotoudeh, V. and Boissonnade, A., "A Probabilistic Study of the Dynamic Response of A Stiffness-Degrading Single Degree of Freedom Structure Exited by a Strong Ground Motion with Specific Probabilistic Characteristics", World Conference on Earthquake Engineering, 1984, pp 99-106.

(60) Clough, P.W., " Effects of Stiffness Degradation on Earthquake Ductility Requirements, " Structural Engineering Lab., University of California, Berkeley, CA , USA, Report No. 66-16.

(61) Wang, M. L. and Subia, S., "Analysis of Reinforced Concrete Structures Using Nonlinear Hysteresis with Stiffness and Strength Degradation", Pacific Conference on Earthquake Engineering, 1987, pp 153-164.

(62) Sanjayan, G. and Darvall, P., "Dynamic Response of Softening Structures", Proceeding of the 10th Australian Conference on the Mechanics of Structures and Materials, University of Adelaide, 1986, pp 371.

(63) Sanjayan, G. and Darvall, P., "Dynamic Analysis of Reinforced Concrete Frame Structures with Hysteresis and Softening", First National Structural Engineering Conference, 1987, Vol. 1, pp 335-340.

(64) Diaz, O., Mendoza, E. and Esteva, L., "Seismic Ductility Demands Predicted by Alternative Models of Building Frames", Earthquake Spectra, Vol. 10, No 3, 1994, pp 465.

(65) Mosalam, K.M., Gergely, P. and White, R.N., " Three Dimensional Analysis of R/C Frame-Slab Building Systems, " Fifth U.S. National Conference on Earthquake Engineering, July 10-14 1994, Chicago, Illinois, Vol.1, pp 75.

(66) Priestly, M.J.N., "Displacement Based Seismic Assessment of Existing Reinforced Concrete Buildings", Proceedings of the Pacific Conference on Earthquake Engineering, Melbourne, Australia, November 1995, pp 20.

(67) Park, R., "A Static Force-Based Procedure for the Seismic Assessment of Existing Reinforced Concrete Moment Resisting Frames", Proceedings of the 1996 Annual Conference, New Zealand National Society of Earthquake Engineering, New Plymouth, March 1996.

(68) Vukazich, S.M., Mish, K.D. and Romstad, K.M., " Nonlinear Dynamic Response Using Lanczos Modal Analysis, " The American Society of Civil Engineers, Journal of the Structural Division, December 1996, Vol. 122 No. 12, pp 1418.

(69) Spacone, E., Filippou, F.C. and Taucer, F.F., " Fibre Beam-Column Model for Non-Linear Analysis of R/C Frame : Part I Formulation, " Earthquake Engineering and Structural Dynamics, January 1996, Vol. 25 No. 7, pp 711-725.

(70) Spacone, E., Filippou, F.C. and Taucer, F.F., " Fibre Beam-Column Model for Non-Linear Analysis of R/C Frame : Part II Application, " Earthquake Engineering and Structural Dynamics, January 1996, Vol. 25 No. 7, pp 727-742.

(71) Corvetti, G. M., "Assessment of Reinforced Concrete External Beam-Column Joints Designed to the Australian Earthquake Standard", Thesis Submitted for the Degree of Master of Engineering Science, The University of Melbourne, July 1994.

(72) Griffith, M.C. and Heneker, D. G., "Comparison of Dynamic Analysis Technique for Earthquake Loading of Concrete Building, " The 13th Australasian Conference on Mechanics of Structures and Materials, 5-7 July 1993, University of Wollongong.

(73) Mendis, P.A., " Softening of Reinforced Concrete Structures, " Thesis Submitted for the Doctorate of Philosophy in Engineering, Monash University, 1986.

(74) Carr, A., "RUAUMOKO", User's manual, University of Canterbury, 1996.

(75) Muto, K., Ohmori, N., Sugano, T., Miyashita, T. and Shimizu, H., " Non-Linear Analysis of Reinforced Concrete Buildings, " Theory and Practice in Finite Element Structural Analysis, Yamada, Y. and Gallangher, R.H., Eds. University of Tokyo Press, Tokyo, 1973, pp 339-421.

(76) Paulay, T. and Priestley, M.J.N., "Seismic Design of Reinforced Concrete and Masonry Buildings", John Wiley and Sons Publication, New York, 1992.

(77) Earthquake Catalog of California, January 1, 1900 to December 31, 1974, Charles R. Read et al., California Edition of Mines and Geology, Special Publication No. 52, 1st Edition and Cal. Tech. Report No., EERL 80-01, D.M. Lee, P.C. Jennings, G.W. Housner, (January 1980).

(78) Griffith M.C. and Whittaker, A.S., "Base Isolation for the Seismic Protection of Structures in Australia, " Conference Proceedings, Pacific Conference on Earthquake Engineering, University of Melbourne, Melbourne, 1995.

(79) Uang, C. M., "Establishing R (or R_w) and C_d Factors for Building Seismic Provisions", ASCE Structural Division, Vol. 117, No. 1, 1991, pp 19-28.

(80) Uang, C. M., "Comparison of the Seismic Force Reduction Factors Used in U.S.A. and Japan", Earthquake Engineering and Structural Dynamics, Vol. 20, 1991, pp 389-397.

APPENDIX A

```
HALF SCALE MELBOURNE UNI JOINT (Mehran Keshavarzian Model)
2 0 1 1 2 -1 0 2 0
6 5 3 5 1 2 9.81 5.0 5.0 0.01 201.0 1.0
0 1 0 0 1.0 10.0 0.7 0.1
0 0
NODES
1  0.50  0.0  0 1 0  0 0 0  0
2  0.50  1.0  0 0 0  0 0 0  0
3  0.50  2.0  1 1 0  0 0 0  0
4  2.25  1.0  0 1 0  0 0 0  0
5  1.10  1.0  0 0 0  0 0 0  0
6  0.00  0.0  1 1 1  0 0 0  0
ELEMENTS
1  1 1 2  0 0  0
2  1 2 3  0 0  0
3  2 2 5  0 0  0
4  2 5 4  0 0  0
5  3 6 1  0 0  0
PROPS
1 FRAME                                                          !COLUMNS
 2 0 0 20 2 0                                                    !PARAMETERS
 34.7E9 10.4E9 4.0E-2 0.0 22.05E-6 960.0 0.0 0.0 0.0 0.0 0.0  !100% A;30%Ig
 0.25 0.25                                                       !r
 -1211.6E3 -331.3E3 41.7E3 38.4E3 32.2E3 23.8E3 81.71E3 0     !65% N/M
 1.0 20.0 0.005                                                  !DEGRADING HYST
 0.5                                                             !MEHRAN
2 FRAME                                                          !BEAMS
 2 0 0 20 2 0                                                    !PARAMETERS
 34.7E9 10.4E9 7.0E-2 0.0 157.77E-6 1.68E3 0.0 0.0 0.0 0.0     !100% A;30%Ig
 0.25 0.25                                                       !r
 -1859.0E3 -641.9E3 107.8E3 94.84E3 73.26E3 46.5E3 156.0E3 0   !65% N/M
 1.0 20.0 0.005                                                  !DEGRADING HYST
 0.5                                                             !MEHRAN
3 SPRING
 1 0 0 0 2.08E14 2.08E14 1.0E12 1.0 0.25 0.25                    !STIFFNESS
 1.0 -1.0 1.0 -1.0 1.0 -1.0                                      !YIELD
WEIGHTS
1
2
3
4
5
6
LOADS
1
2
3
4
5
```

```
6
SHAPE
1 4.16E11                                   !2mm
2
3
4
5
6
EQUAKE
1 1 0.1 1 -1                                !SINE 10s/CYCLE
```

```
HALF SCALE MELBOURNE UNI JOINT (Muto Degrading Tri-Linear Model)
2 0 1 1 2 -1 0 2 0
6 5 3 5 1 2 9.81 5.0 5.0 0.01 81.0 1.0
0 1 0 0 1.0 10.0 0.7 0.1
0 0
NODES
1  0.50  0.0  0 1 0  0 0 0  0
2  0.50  1.0  0 0 0  0 0 0  0
3  0.50  2.0  1 1 0  0 0 0  0
4  2.25  1.0  0 1 0  0 0 0  0
5  1.10  1.0  0 0 0  0 0 0  0
6  0.00  0.0  1 1 1  0 0 0  0
ELEMENTS
1  1 1 2  0 0  0
2  1 2 3  0 0  0
3  2 2 5  0 0  0
4  2 5 4  0 0  0
5  3 6 1  0 0  0
PROPS
1 FRAME                                                    !COLUMNS
 2 0 0 13 2 0                                              !PARAMETERS
 40.8E9 10.4E9 4.0E-2 0.0 40.89E-6 960.0 0.0 0.0 0.0 0.0 !100% A; Icr
 0.025 0.025                                               !r
 -1864.0E3 -512.5E3 64.1E3 59.0E3 49.6E3 36.6E3 125.7E3 0    !N/M
INTERACTION
 1.0 8.0 0.05                                              !DEGRADING HYST
 0.5 5.25E3 -5.25E3 5.25E3 -5.25E3                         !MUTO
2 FRAME                                                    !BEAMS
 2 0 0 13 2 0                                              !PARAMETERS
 40.8E9 10.4E9 7.0E-2 0.0 290.56E-6 1.68E3 0.0 0.0 0.0 0.0     !100% A; Icr
 0.025 0.025                                               !r
 -2860.0E3 -987.6E3 165.8E3 145.9E3 112.7E3 71.5E3 240.0E3 0   !N/M
INTERACTION
 1.0 8.0 0.05                                              !DEGRADING HYST
 0.5 16.06E3 -16.06E3 16.06E3 -16.06E3                     !MUTO
3 SPRING                                                !TO ENFORCE DISPLACEMENT
 1 0 0 0 2.08E14 2.08E14 1.0E12 1.0 0.25 0.25              !STIFFNESS
 1.0 -1.0 1.0 -1.0 1.0 -1.0                                !YIELD SURFACES
WEIGHTS
1
2
3
4
5
6
LOADS
1
2
3
```

4
5
6
SHAPE
1 6.24E12
2
3
4
5
6
EQUAKE
1 1 0.1 1 -1 !SINE 10s/CYCLE

```
HALF SCALE MELBOURNE UNI JOINT (Q-Hyst Degarding Stiffness Hysteresis)
2 0 1 1 2 -1 0 2 0
6 5 3 5 1 2 9.81 5.0 5.0 0.01 81.0 1.0
0 1 0 0 1.0 10.0 0.7 0.1
0 0
NODES
1  0.50  0.0  0 1 0  0 0 0  0
2  0.50  1.0  0 0 0  0 0 0  0
3  0.50  2.0  1 1 0  0 0 0  0
4  2.25  1.0  0 1 0  0 0 0  0
5  1.10  1.0  0 0 0  0 0 0  0
6  0.00  0.0  1 1 1  0 0 0  0
ELEMENTS
1  1 1 2  0 0  0
2  1 2 3  0 0  0
3  2 2 5  0 0  0
4  2 5 4  0 0  0
5  3 6 1  0 0  0
PROPS
1 FRAME                                                          !COLUMNS
  2 0 0 12 2 0                                                   !PARAMETERS
  40.8E9 10.4E9 3.0E-2 0.0 40.89E-6 960.0 0.0 0.0 0.0 0.0 !75% A; Icr
  0.25 0.25                                                      !r
  -1864.0E3 -512.5E3 64.1E3 59.0E3 49.6E3 36.6E3 125.7E3 0      !N/M
INTERACTION
  1.0 8.0 0.05                                                   !DEGRADING HYST
  0.0                                                            !Q-HYST
2 FRAME                                                          !BEAMS
  2 0 0 12 2 0                                                   !PARAMETERS
  40.8E9 10.4E9 5.25E-2 0.0 290.56E-6 1.68E3 0.0 0.0 0.0 0.0    !75% A; Icr
  0.25 0.25                                                      !r
  -2860.0E3 -987.6E3 165.8E3 145.9E3 112.7E3 71.5E3 240.0E3 0   !N/M
INTERACTION
  1.0 8.0 0.05                                                   !DEGRADING HYST
  0.0                                                            !Q-HYST
3 SPRING                                          !TO ENFORCE DISPLACEMENT
  1 0 0 0 2.08E14 2.08E14 1.0E12 1.0 0.25 0.25                   !STIFFNESS
  1.0 -1.0 1.0 -1.0 1.0 -1.0                                     !YIELD SURFACES
WEIGHTS
1
2
3
4
5
6
LOADS
1
2
3
```

4
5
6
SHAPE
1 6.24E12
2
3
4
5
6
EQUAKE
1 1 0.1 1 -1 !SINE 10s/CYCLE

```
HALF SCALE MELBOURNE UNI JOINT (Calibrated Joint Model)
2 0 1 1 2 -1 0 2 0
6 5 3 5 1 2 9.81 5.0 5.0 0.01 81.0 1.0
0 1 0 0 1.0 10.0 0.7 0.1
0 0
NODES
1  0.50  0.0  0 1 0  0 0 0  0
2  0.50  1.0  0 0 0  0 0 0  0
3  0.50  2.0  1 1 0  0 0 0  0
4  2.25  1.0  0 1 0  0 0 0  0
5  1.10  1.0  0 0 0  0 0 0  0
6  0.00  0.0  1 1 1  0 0 0  0
ELEMENTS
1  1 1 2  0 0  0
2  1 2 3  0 0  0
3  2 2 5  0 0  0
4  2 5 4  0 0  0
5  3 6 1  0 0  0
PROPS
1 FRAME                                                          !COLUMNS
  2 0 0 20 2 0                                                   !PARAMETERS
  34.7E9 10.4E9 3.0E-2 0.0 40.89E-6 960.0 0.0 0.0 0.0 0.0 !75% A;Icr
  0.25 0.25                                                      !r
  -1864.0E3 -512.5E3 64.1E3 59.0E3 49.6E3 36.6E3 125.7E3 0     !100N/M
  1.0 8.0 0.1                                                    !DEGRADING HYST
  0.3                                                            !MEHRAN
2 FRAME                                                          !BEAMS
  2 0 0 20 2 0                                                   !PARAMETERS
  34.7E9 10.4E9 5.25E-2 0.0 290.56E-6 1.68E3 0.0 0.0 0.0 0.0   !75% A;Icr
  0.25 0.25                                                      !r
  -2860.0E3 -987.6E3 165.8E3 145.9E3 112.7E3 71.5E3 240.0E3 0  !100N/M
  1.0 8.0 0.1                                                    !DEGRADING HYST
  0.3                                                            !MEHRAN
3 SPRING
  1 0 0 0 2.08E14 2.08E14 1.0E12 1.0 0.25 0.25                   !STIFFNESS
  1.0 -1.0 1.0 -1.0 1.0 -1.0                                     !YIELD
WEIGHTS
1
2
3
4
5
6
LOADS
1
2
3
4
5
```

```
6
SHAPE
1 6.24E12                                   !30mm
2
3
4
5
6
EQUAKE
1 1 0.1 1 -1                                !SINE 10s/CYCLE
```

APPENDIX B

```
UNI ADELAIDE FRAME MODEL - FULLSCALE (WITH CALIBRATED
PROPERTIES)0.5FLOORMASS
1 0 1 1 2 0 0 2 0                                   !ANALYSIS OPTIONS
8 9 2 5 1 2 9.81 3.0 3.0 0.01 64.0 1.0              !EQ5 ACTUAL ACCEL
0 1 0 0 1.0 10.0 0.7 0.1                            !OUTPUT/PLOTTING
0 0
NODES                        !CORRECTED E & Icr TO MATCHED FREQ
1  0.0 0.00  1 1 1  0 0 0  0
2  0.0 3.50  0 0 0  0 0 0  0
3  0.0 7.00  0 0 0  0 0 0  0
4  0.0 10.5  0 0 0  0 0 0  0
5  6.0 0.00  1 1 1  0 0 0  0
6  6.0 3.50  0 0 0  0 0 0  0
7  6.0 7.00  0 0 0  0 0 0  0
8  6.0 10.5  0 0 0  0 0 0  0
ELEMENTS
1  1 1 2  0 0  0                                   !COLUMNS
2  1 2 3  0 0  0                                   !  "
3  1 3 4  0 0  0                                   !  "
4  1 5 6  0 0  0                                   !  "
5  1 6 7  0 0  0                                   !  "
6  1 7 8  0 0  0                                   !  "
7  2 2 6  0 0  0                                   !BEAMS
8  2 3 7  0 0  0                                   !  "
9  2 4 8  0 0  0                                   !  "
PROPS
1 FRAME                                             !COLUMN
  2 0 0 20 3 0                                      !BASIC PROPS
  34.7E9 10.4E9 16.0E-2 0.0 392.54E-6 3.84E3 0.0 0.0 0.0 0.0    !0.6Icr
  0.25 0.25                                         !r
  -4.85E6 -1.325E6 333.6E3 307.2E3 257.6E3 190.4E3 326.8E3 0    !N/M
INTERACTION
  1.0 7.0 0.1                                       !DEGRAD PARAMS
  0.5                                               !ALFA
2 FRAME                                             !BEAM
  2 0 0 20 3 0                                      !BASIC PROPS
  34.7E9 10.4E9 36.4E-2 0.0 15.39E-3 25.088E3 0.0 0.0 0.0 0.0   !0.6Icr&0.5floor
  0.25 0.25                                         !r
  -7.436E6 -2.568E6 862.4E3 758.72E3 586.08E3 372.0E3 624.0E3 0 !N/M
INTERACTION
  1.0 7.0 0.1                                       !DEGRAD PARAMS
  0.5                                               !ALFA
WEIGHTS
1
2
3
4
5
6
```

7
8
LOADS
1
2
3
4
5
6
7
8
EQUAKE
1 1 0.0112 1.0 -1